Faculty of Sciences

Relative positioning with Galileo E5 AltBOC code measurements

Cécile Deprez

Dissertation submitted to the University of Liège in partial requirements for the degree of Master of Geomatics and Geometrology.

Dissertation advisor: R. Warnant
Examiners: R. Billen, A. Demoulin

Academic year 2014-2015

I would like to express my deepest gratitude and appreciation to my dissertation advisor, R. Warnant, *who has been a constant source of knowledge and a valuable aid during the analysis and the writing of this dissertation.*

I also thank in advance my examiners, R. Billen and A. Demoulin, *for their proofreading.*

I am grateful to L. Gollogly and C. Gruslin *for their participation in the review of the text.*

I wish to thank all my family and friends for their continued support.

Contents

Symbols

In order of appearance in the text:

t_{ref}: time in the reference time system of the GNSS considered
t^s: time of emission of the signal in the satellite time system
δt^s: satellite clock bias
t_r: time of reception of the signal in the receiver time system
δt_r: receiver clock bias
Δt: interval of time between the emission and the reception of the signal
t^s_{ref}: time of emission of the signal in the reference time system of the considered GNSS
$t_{r,ref}$: time of reception of the signal in the reference time system of the considered GNSS
R^s_r: geometric distance between satellite and receiver
$c = 299,792,498 m/s$: speed of light in a vacuum
τ^s_r: signal time of travel from satellite to receiver
$\Delta\delta t$: difference between satellite and receiver clock bias
$\overrightarrow{\Delta^s_r}$: vector of satellite-to-receiver distance
$\overrightarrow{r^s}$: vector of instantaneous satellite position
$\overrightarrow{r_r}$: vector of instantaneous receiver position
$P^s_{r,k}(t)$: code pseudorange measurement as a function of time
D^s_r: distance between a satellite s and a receiver r
T^s_r: tropospheric delay
$I^s_{r,k}$: ionospheric delay
$M^s_{r,k,m}$: multipath delay
$d_{r,k,m}$: receiver hardware delay
$d^s_{k,m}$: satellite hardware delay
$\epsilon^s_{r,k,m}$: observation noise
$\Phi^s_{r,k}(t)$: phase pseudorange measurement as a function of time
λ: signal wavelength
$N^s_{r,k}$: the initial ambiguity
e^s_r: receiver inertial noise
h^s_r: external to receiver noise
C/N_0: carrier-to-noise ratio
X_r: X component of the receiver position
Y_r: Y component of the receiver position
Z_r: X component of the receiver position
$T^s_{r,mod}$: modeled tropospheric delay
$I^s_{r,k,mod}$: modeled ionospheric delay
$\delta t^s(t^s_{ref,mod})$: modeled satellite clock bias
X^s: X component of the satellite position
Y^s: Y component of the satellite position
Z^s: X component of the satellite position
$X_{r,0}$: *a priori* X component of the receiver position
$Y_{r,0}$: *a priori* Y component of the receiver position
$Z_{r,0}$: *a priori* X component of the receiver position

ΔX_r: the difference between estimated X component of a position and its *a prior* value
ΔY_r: the difference between estimated Y component of a position and its *a prior* value
ΔZ_r: the difference between estimated Z component of a position and its *a prior* value
$D^s_{r,0}$: *a priori* distance between a satellite s and a receiver r
$P^s_{r,k,0}$: *a priori* and modeled terms of the code pseudorange equation
$\underline{W}$: the vector containing the observations
$\underline{\eta}$: the vector of residuals
A: the matrix containing the partial derivatives resulting from Taylor linearization
$\underline{x}$: the vector of unknowns
Σy: the variance-covariance matrix of the unknowns
Σz: the variance-covariance matrix of the observations
J: the *Jacobian*
σ^2: the variance
$\sigma.\sigma$: the covariance
$\frac{\delta f_u}{\delta x_n}$: the partial derivatives terms
σ_{pos}: the precision of the positioning
σ_{obs}: the precision of the observations
$Q_{\underline{\hat{x}}}$: the cofactor matrix
$\underline{X_B}$: vector of unknown position
$\underline{X_A}$: vector of known position
$\underline{b_{AB}}$: baseline vector
$P^i_{12,k}$: the single difference of code pseudoranges
D^i_{12}: the single difference distance term
T^i_{12}: the single difference tropospheric term
$I^i_{12,k}$: the single difference ionospheric term
$M^i_{12,k,m}$: the single difference multipath term
$d_{12,k,m}$: the single difference receiver hardware delay
$\epsilon^i_{12,k,m}$: the single difference observation noise
$P^{ij}_{12,k}$: the double difference of code pseudoranges
D^{ij}_{12}: the double difference distance term
T^{ij}_{12}: the double difference tropospheric term
$I^{ij}_{12,k}$: the double difference ionospheric term
$M^{ij}_{12,k,m}$: the double difference multipath term
$\epsilon^{ij}_{12,k,m}$: the double difference observation noise
σ_{SD}: the precision of the single difference
σ_{SD}: the precision of the double difference
$P(t)$: the weight or correlation matrix

Abreviations

In alphabetical order:

AltBOC: Alternative Binary Offset Carrier
BOC: Binary Offset Carrier
BPSK: Binary Phase-Shifted Key
C/A: Coarse/Acquisition
CBOC: Composite Binary Offset Carrier
CS: Commercial Service
DOP: Dilution of Precision
DOY: Day of Year
ESA: European Space Agency
FOC: Full Operational Capability
GDOP: Geometric Dilution of Precision
GIOVE: Galileo In Orbit Validation Element
GLONASS: Global Navigation Satellite System
GNSS: Global Navigation Satellite System
GPS: Global Positioning System
GST: Galileo System Time
HDOP: Horizontal Dilution of Precision
IAT: Internation Atomic Time
IGS: International GNSS Service
INS: International Navigation System
IOV: In Orbit Validation
LSA: Least Squares Adjustment
MBOC: Multiplexed Binary Offset Carrier
Mcps: Megachips per second
MEO: Medium Earth Orbit
MRSE: Mean Radial Spherical Error
OS: OpenService
P: Precision
PDOP: Position Dilution of Precision
PPP: Precise Point Positioning
PRN: PseudoRandom Noise
PRS: Public Regulated Service
QPSK: Quadrature Phase-Shifted Key
QZSS: Quasi-Zenith Satellite System
RINEX: receiver independent exchange format
RTK: Real Time Kinematic
SAR: Search and Rescue
SoL: Safety of Life
TDOP: Time Dilution of Precision
TEC: Total Electron Content
TECU: Total Electron Content Unit
TID: Travelling Ionospheric Disturbances
VDOP: Vertical Dilution of Precision

Chapter 1

Introduction

On the 27th of March 2015, two state-of-the-art spacecrafts joined the European Galileo satellite constellation. This recent system is still in test phase but already available for measurements, including atmosphere parameters' evaluation and positions' estimation.

This master's thesis focuses on the opportunity given by Galileo to measure improved positions using different types of modulated signals.

This chapter sets the basis of satellite-based positioning, its advantages and the major issues that have to be considered as far as precise positioning is concerned. It also describes the two *Global Navigation Satellite Systems* (GNSS) on which this dissertation relies, namely Galileo and *Global Positioning System* (GPS), and the particularities of the modulation techniques, which play an important role in the context of this dissertation.

1.1 GNSS

This section describes the GPS and Galileo satellite systems, their signals and orbits definition but also the similarities that make them compatible. The other GNSS such as GLONASS, the Russian system, QZSS, the Japanese system, or even BeiDou, the Chinese system are not considered in this dissertation as they are not presently interoperable with the two former ones[1].

1.1.1 Interoperability and compatibility

When comparing GNSS, two essential notions need to be distinguished: *compatibility* and *interoperability*. As explained in the two hereunder paragraphs, compatibility does not automatically imply systems interoperability [Avila-Rodriguez et al., 2007].

According to [ICGNSS & UNOOSA, 2010], compatibility and interoperability can be defined as following:

Compatibility: the ability of space-based positioning, navigation and timing services to be used separately or together without interfering with each individual service or signal.

Interoperability: the ability of civil space-based positioning, navigation and timing services to be used together to provide the user with better capabilities than would be achieved by relying solely on one service or signal.

[1] BeiDou will soon be equipped with new modulations compatible with GPS and Galileo but it is still in development.

1.1.2 GPS

Since June 1995, the American Global Positioning System (GPS) is fully operational. Initially designed with a constellation of 24 satellites in a medium Earth orbit (MEO) at an altitude of 20 200 km, this system is nowadays evolving. The satellites are distributed into 6 equally-spaced planes surrounding the Earth, each plane containing 4 satellites.They orbit the Earth in 12 sidereal hours.This leads to a complete coverage of the Earth, ensuring at least 4 satellites visible everywhere from the ground. Nevertheless, 31 satellites are permanently available in case of malfunction or decommissioning of satellites belonging to the core constellation. In June 2011, the achievement of the "Expandable 24" operation lead to an improvement of GPS geometry and accuracy. This program included the movement of 3 satellites in order to rearrange satellites-slots for a better coverage of the Earth [GPS-SSI, 2015].

GPS has long functioned only with two pseudorandom noise codes (PRN codes, see section 1.2), a civil one and a military one, still modulated on carrier frequencies today. Firstly, the coarse/acquisition-code (C/A-code), the civil code, with a wavelength of approximatively 300 meters, is modulated on L1 carrier frequency only. Its duration is approximatively 1 millisecond during which the 1023 chips composing the code are broadcast at a frequency of 1.023 Megachips per second (Mcps). Secondly, the precision code (P code) which is modulated both on L1 and L2 carrier frequencies and reserved for military operations[2]. Its wavelength is 10 times smaller than the C/A-code for a frequency 10 times bigger. The number of chips that compose it total $2.354 \cdot 10^{14}$ and it is partitioned into 37 unique code segments of approximatively 7 days' length.

In 1998, the White House announced a GPS modernisation program that should be completed by the launch of satellites of GPS III Block generation over the coming years [GPS-SSI, 2015]. This program includes the construction of new satellites:

- a first Block IIR(M): "Modernized", launched in 2005-2009
- a second Block IIF: "Follow-on", launched since 2010
- finally, GPS III Block, the launch of which will begin in 2017

Furthermore, a new carrier and new civil signals complete each of these spacecraft generations:

- on Block IIR(M): addition of a second civil signal on L2 frequency, the L2C code
- on Block IIF: addition of a new frequency, L5 frequency, and addition of a new civil code on this frequency, the L5C code
- on GPS III Block: a fourth civil signal, the L1C code, will be modulated soon on the L1 frequency

As a result, on April 21st 2015, the GPS constellation was composed of 29 active satellites, including 9 Block IIF satellites, allowing positioning with the new L5C signal.

Table 1.1 shows the characteristics of these signals.

Signal	Factor($.f_0$)	Frequency[MHz]	Wavelength[cm]
L1	154	1,575.420	19.0
L2	120	1,227.600	24.4
L5	115	1,176.450	25.5

Table 1.1: GPS frequency bands. Source: [Hofmann-Wellenhof et al., 2008], p. 329

[2]This code is encrypted in an anti-spoofing mode under the name of Y-code.

The GPS system relies on a fundamental frequency f_0 of 10.23 MHz produced by highly accurate atomic clocks. Each of the signals described above results from the multiplication of this fundamental frequency by a given factor. In Block IIF and GPS III generations of satellites, advanced atomic clocks onboard improve accuracy.

Carrier	PRN Code	PRN code length [chip]	Code rate [Mcps]	Bandwith [MHz]	Modulation type	Access
L1	C/A	1023	1.023	2.046	BPSK	Civil
	P	∼7 days	10.23	20.46	BPSK	Military
	L1C	10,230	1.023	4.092	BOC	Civil
L2	P	∼7 days	10.23	20.46	BPSK	Military
	L2C	10,230	1.023	2.046	BPSK	Civil
L5	L5C (L5I	10,230·10	10.23	20.46	BPSK	Civil
	L5Q)	10,230·20	10.23	20.46	BPSK	Civil

Table 1.2: GPS ranging signals. Source: [Hofmann-Wellenhof et al., 2008]

As shown Table 1.2, the new signal L5C, available with the Block IIF satellites generation, has two components: L5I and L5Q. The -I component carries data and ranging code whereas -Q, the quadrature component, carries another ranging code but no data. Both are BSPK modulated (see section 1.2) onto the carrier which confers to the signal better resistance to interferences as well as better tracking performance [ESA, 2013]. The characteristics of the modulation of the carrier frequencies will play an essential role in this dissertation and will be detailed in section 1.2.

Fig. 1.1 illustrates the evolution of the GPS signals.

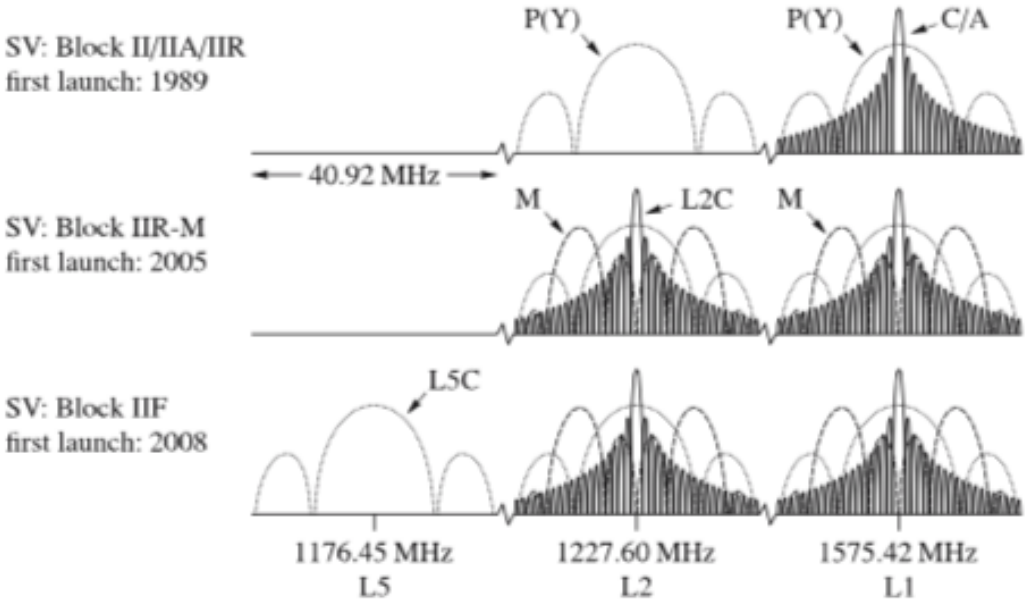

Figure 1.1: GPS signals evolution. Source: [Hofmann-Wellenhof et al., 2008]

1.1.3 Galileo

Only very recently, Europe has started to develop a European satellite system. Initiated in 1999, the Galileo project finally materialized a few years ago. The European Space Agency (ESA) reckons on a constellation of 30 satellites (27 operational and 3 others in case of malfunction) spread

over 3 circular orbits inclined 56° to the equator. Those satellites will be positioned at an altitude of above 23 222 kilometers above WGS84 reference ellipsoid, which should enable a constant cover of all regions of the Earth by at least 4 satellites. They broadcast 10 navigation signals modulated on four carrier frequencies: E5a, E5b, E6 and E1. The first prototypes, GIOVE-A and GIOVE-B were launched respectively in 2005 and 2008 and were decommissioned in 2012.

Since October 2012, 4 *In Orbit Validation* phase (IOV) satellites orbit around the Earth, enabling the first signal measurement and position determination in March 2013. At the time of writing, 4 other satellites, from the *Full Operational Capability* (FOC) phase joined the initial constellation mentioned above. The present constellation is described in Table 1.3:

Satellite	Launched	Operational	Status	PRN	Constellation
GIOVE-A	12-28-05		Decommissioned		Test prototypes
GIOVE-B	4-27-08		Decommissioned		Test prototypes
GSAT0101	10-21-11	12-10-11	Available	E11	IOV
GSAT0102	10-21-11	1-16-12	Available	E12	IOV
GSAT0103	10-12-12	12-1-12	Available	E19	IOV
GSAT0104	10-12-12	12-12-12	Not Available	E20	IOV
GSAT0202	08-22-14		Under commisionning	E18	FOC
GSAT0201	08-22-14		Under commisionning	E14	FOC
GSAT0203	03-27-15		Under commisionning	E26	FOC
GSAT0204	03-27-15		Under commisionning	E22	FOC

Table 1.3: Almanac of the Galileo constellation

Among the IOV satellites, anomalies on E20 became apparent in May 2014 when the satellite stopped broadcasting the E5a+b signals. Later, the emissions on Galileo E5a, E5b and E5a+b signals were turned off and are still unavailable at time of writing. Furthermore, the E14 and E18 satellites experienced technical problems. When launched, they were sent to a wrong orbit and, only after many maneuvers, were able to be exploited. Still, they encounter many orbit calculation problems, particularly E14, that will be detailed in chapter 6. The satellite E26 started emitting in June 2015. Therefore, positions estimated in this dissertation only rely on the availability of 6 satellites: E11, E12, E12, E14, E18 and E26.

The ranging code and carrier frequencies available on Galileo are described in Table 1.4 and Table 1.5. As in GPS case, those frequencies are all multiples of the fundamental frequency f_0.

Signal	Factor ($.f_0$)	Frequency[MHz]	Wavelength[cm]
E1	154	1575.420	19.0
E5a	115	1176.450	25.5
E5b	118	11207.140	24.8
E5 or E5a+b	116.5	1,191.795	25.2
E6	125	1278.750	23.4

Table 1.4: Galileo frequency bands. Source: [Hofmann-Wellenhof et al., 2008], p. 384

Carrier	PRN code	Code rate [Mcps]	Modulation type	Acess
E1	E1A	2.5575	BOC	Authorized users only (PRS)
	E1B	1.023	MBOC	All users (OS)
	E1C	1.023	MBOC	All users (OS)
E6	E1A	5.115	BOC	Authorized users only (PRS)
	E1B	5.115	BPSK	Commercial access (CS)
	E1C	5.115	BPSK	Commercial access (CS)
E5	E5a-I	10.23	BPSK } AltBOC	All users (OS)
	E5a-Q	10.23	BPSK } AltBOC	All users (OS)
	E5b-I	10.23	BPSK } AltBOC	All users (OS)
	E5b-Q	10.23	BPSK } AltBOC	All users (OS)

Table 1.5: Galileo ranging signals. Source: [Hofmann-Wellenhof et al., 2008]

As shown in Table 1.5, the E5a and E5b frequencies are components of the E5 or E5a+b or even the E5 AltBOC[3] frequency. They are both composed of a data channel and a pilot channel, respectively E5a-I, E5b-I and E5a-Q, E5b-Q. Modulated together thanks to the AltBOC modulation onto the E5 frequency, this particular signal shows low multipath errors and high code tracking accuracy [Silva et al., 2012]. This particularity is quite interesting and represents the core of this dissertation.

E1 and E6 signals are composed of three components: an encrypted one (-A component) and two commercial ones (-B and -C components) corresponding respectively to a data channel and a pilot channel, similarly to-I and -Q components of E5a and E5b signals.

Fig. 1.2 illustrates the Galileo signals.

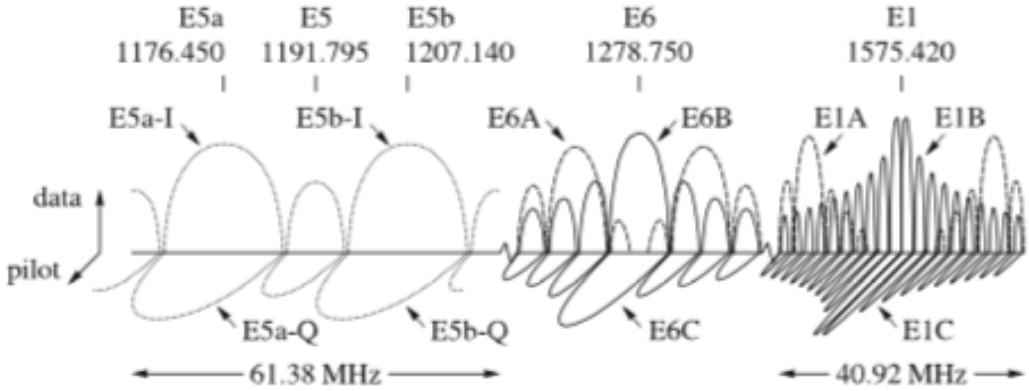

Figure 1.2: Galileo signals. Source: Hofmann-Wellenhof, 2008

The Galileo signals will provide users with the services described below [Avila-Rodriguez et al., 2007]:

- Open Service (OS): this single frequency service will be provided by the three signals E1, E5a and E5b. This service will offer free access for all users. Moreover, both GPS and Galileo will be combined to enable their use in severe environments such as urban canyons [ESA, 2014].

[3]Galileo E5 AltBOC, Galileo E5a+b and Galileo E5 notations will be all three used to define this signal in the further chapters.

- Commercial Service (CS): gives access to two additional encrypted signals. This service will be available on E6 (B and C) and can be combined with the OS signals (E1, E5a and E5b) for an improved performance [Avila-Rodriguez et al., 2007].
- Safety of Life (SoL): this service is already available for aviation thanks to EGNOS[4] and will soon be improved by Galileo. It will be provided by E5b and E1 (B and C).
- Search And Rescue (SAR): this service will facilitate location of distress signals.
- Public Regulated Service (PRS): this service is dedicated for authorities (police, military, etc.) who require encrypted specific signals. The E1-A and E6-A signals will be used to broadcast those encrypted signals.

Table 1.6 summarizes the signals associated with each services.

ID	OS	SoL	CS	PRS
E5a	x		x	
E5b	x	x	x	
E6A				x
E6BC			x	
E1A				x
E1BC	x	x	x	

Table 1.6: Signals and services association

Aware of the importance of interoperability with other GNSS signals, Galileo's carrier frequencies were designed to be interoperable with the diverse existing GNSS carrier frequencies. Thus, E5a is compatible and interoperable with the L5 signal of GPS system and E1 coincides with GPS L1.

Originally developed to allow interoperability between civil signals on GPS and Galileo, L1 will soon be adopted as a new standard of interoperability by satellite systems such as BeiDou in China (BeiDou B1) or QZSS in Japan. In a similar way, BeiDou and GLONASS both adapt their signals to create a new interoperability with the L5 band (BeiDou B2a and GLONASS L5) [Subarina et al., 2013].

Table 1.7 illustrates the interoperability existing between GPS and Galileo signals.

GPS	Galileo	Frequency[Mhz]	Wavelength[cm]
L1	E1	1575.420	19.0
L5	E5a	1176.450	25.5

Table 1.7: Signal interoperability between GPS and Galileo

1.2 Modulation

The modulation of codes on a carrier wave is at the very basis of satellite navigation. Firstly, a data message from the satellite usually containing information about satellite health, orbits and clocks is added to a ranging code using modulo two addition (see Fig. 1.3). This ranging code appears as a rectangular signal consisting in a sequence of pulses whose value is either logic 0 or

[4]EGNOS (*European Geostationary Navigation Overlay Service*) is a satellite-based augmentation system developed by the ESA, the European Commission and EUROCONTROL

logic 1. Such a code is also known as *PseudoRandom Noise* noise (PRN). The resulting signal is then modulated on the carrier frequency.

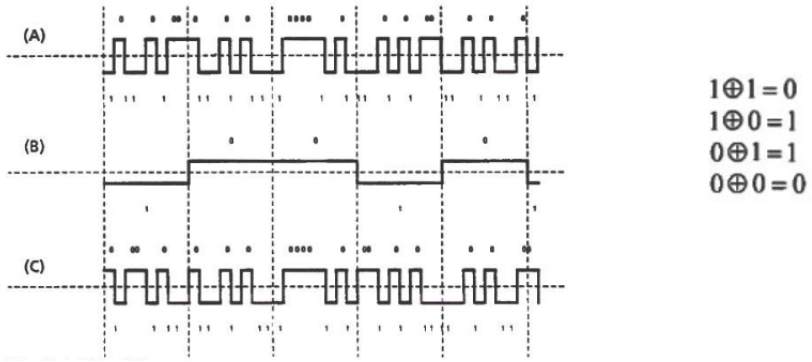

Figure 1.3: Data message added to ranging codes, (A) Ranging code, (B) Data message, (C) Chips sequence resulting of the modulation by modulo two. Source: [Warnant, 2013]

Signal strength, which characterizes satellite tracking, as well as multipath and noise influence (see section 1.4) are dependent on modulation of the PRN codes on the carrier frequencies [Silva et al., 2012]. As shown in Figure 1.4, several approaches exist in order to modulate a code on a carrier, notably using amplitude, frequency or phase modulation.

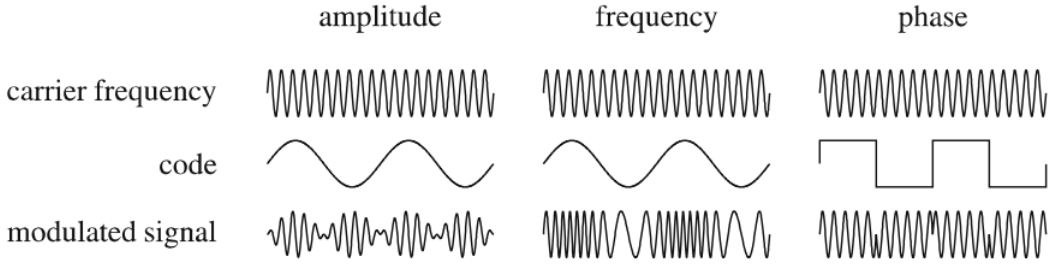

Figure 1.4: Modulation methods. Source: [Hofmann-Wellenhof et al., 2008]

The GNSS modulation techniques are all based on phase modulation.

1.2.1 PSK modulation

A simple phase modulation consists in adding a code on a phase by shifting the phase of π each time the chips sequence of the PRN code changes its state from logic 0 to logic 1 and conversely. The phase is thus multiplied by 1 each time the code pulse corresponds to logic 0 and multiplied by -1 when the ranging code value is logic 1. This modulation is known as *Binary Phase-Shifted Key* (BPSK) as only two states of the phase can exist. This method is the simplest one as it only transmits one bit per step but, thanks to this characteristic, it is less likely to be subject to interference and bit errors.

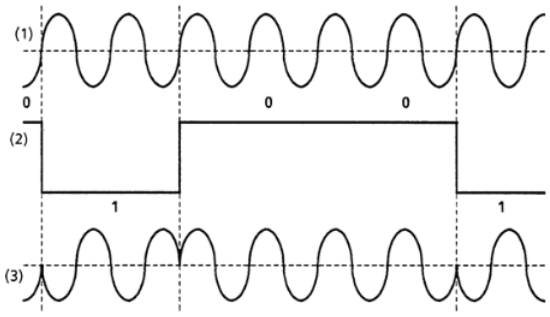

Figure 1.5: BPSK Modulation scheme: (1) Carrier frequency, (2) PRN code, (3) Phase modulation on the carrier frequency. Source: [Warnant, 2013]

When more than one ranging code is broadcast by the carrier, which is often the case, one generally refers to QPSK where Q stands for *Quadrature*. This modulation modifies the carrier signal in two ways: codes being broadcast on the I channel shift once; the carrier and codes on the Q channel shift it twice. Therefore, as four different $\pi/2$ shiftings exist, the *quadrature* adjective replaces *binary*.

1.2.2 BOC modulation

BOC modulation (*Binary Offset Carrier modulation*) consists in modulating the PRN code previously shaped by a rectangular subcarrier (Fig. 1.6). This first modulation provides energy to the code, which results in an improved tracking performance.

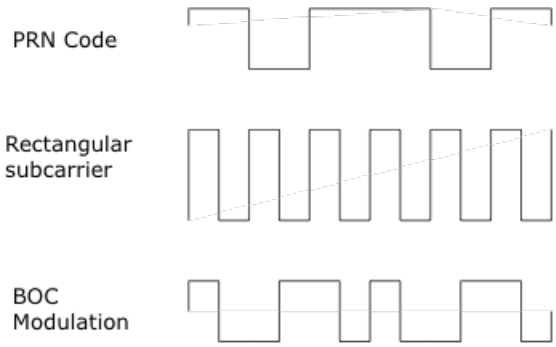

Figure 1.6: BOC Modulation Scheme

1.2.3 AltBOC modulation

The AltBOC modulation is the reason why Galileo E5 a+b signal, also referred to as E5 Alt-BOC, is expected to be revolutionary. This modulation is based on the BOC modulation, that can be generated by two BPSK modulated signals. In the case where those two BPSK signals would broadcast different PRN codes, the modulation is called AltBOC modulation (*Alternative* BOC modulation).

This particularity authorizes a single independent sideband process. Indeed, the term *eight-phase modulation* is also employed when talking of AltBOC modulation. It refers to the fact that an AltBOC modulation can be considered as a double sideband carrier resulting from the modulation of two other carriers. Because these sub-carriers can be modulated independently, each of them can be considered as the result of a Quadrature PSK modulation. Therefore, the AltBOC modulation can also be considered as an eight-BPSK signal [Shivaramaiah & Dempster, 2009].

Fig. 1.7 illustrates the eight-phase modulation of Galileo E5 a+b signal with the F/NAV and I/NAV navigation messages broadcast by Galileo E5a and Galileo E5b frequencies.

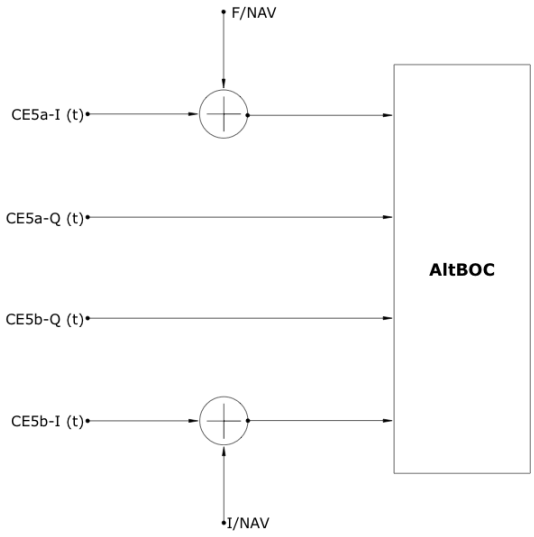

Figure 1.7: E5 AltBOC Modulation

The challenge with this new modulation technique resides in the fact that the demodulation is much more complicated than a simple BPSK or BOC demodulation for reasons given above. Actually, two demodulation schemes are conceivable: a demodulation considering the AltBOC modulation as unique signal, very powerful and wide, or a demodulation based on the characteristic that AltBOC is an eight-BPSK signal and thus, can be demodulated as a set of BPSK modulated signals.

According to [Tawk et al., 2012], tracking Galileo E5 a+b as an AltBOC modulation is more suitable for highly sensitive or robust applications.

Nonetheless, this modulation technique is expected to be the most important contribution of Galileo new signals [Silva et al., 2012] and [Diessongo et al., 2012].

1.2.4 MBOC modulation

A MBOC modulation (*Multiplexed* BOC modulation) has also been implemented since multiple BOC signals can be modulated on the carrier, amplifying power on the higher frequencies and consequently increasing the interference stability. The Galileo E1 signal uses a particular implementation of the MBOC modulation called the CBOC (*Composite* Binary Offset carrier) [Avila-Rodriguez et al., 2007].

1.3 Positioning

Satellites supply a large panel of services, from the collection of meteorological data to telecommunication management. In the early 60's, at their very beginning, they were used by geodesists in order to determine Earth's dimensions. This task required, amongst other things, the estimation of a reference system based on a mathematical surface mapping of the physical shape of the Earth. Such a reference system was required to precisely determine ground station positions and hence, to calculate positions.

This section will focus on positioning techniques and on the errors that may alter the result.

1.3.1 Principle

As discussed in sections 1.1 and 1.2, satellites are designed to send messages to receivers located on the ground through modulated radio signals. Satellite-based positioning is therefore logically based on measurement of the propagation time of those signals between the satellite and the receiver. In this section, three different scales of time are considered.

Firstly, the reference time of the specific GNSS. Each GNSS is based on a time of reference, generated by an atomic clock of reference, and on which every reference device or measurements are based. The *Galileo system time* (GST) is based on the *international atomic time* (IAT), to which a certain offset (integer number of seconds) is added. Similarly, the time system of GPS is based on the IAT, and its offset is 90 seconds. In the following sections, this time will be noted t_{ref}.

Secondly, the satellite time system, which is supposed to be perfectly synchronized with the reference time but is, in practice, slightly different as produced by another atomic clock aboard the spaceship. Indeed, two atomic clocks produce two different scales of time. This time will be noted t^s and its deviation from the reference time δt^s.

Eventually, a last time system is considered when positioning is mentioned: the receiver time system (t_r). Once again, this time should be entirely consistent with the reference time and its offset is noted δt_r.

Therefore, the signal travel time is given by:

$$\Delta t = t_r(t_{r,ref}) - t^s(t^s_{ref}) \tag{1.1}$$

where $t_r(t_{r,ref})$ represents the time of reception measured by the receiver clock at the time $t_{r,ref}$ in the reference time system, $t^s(t^s_{ref})$ stands for the time of emission measured by the satellite clock at the t^s_{ref} in the reference time system and Δt is the interval of time between emission and reception of the signal.

Neglecting errors related to signal propagation and clock biases, the distance between receivers and satellites, also expressed as pseudorange R, can be easily determined:

$$R^s_r = \Delta t.c \tag{1.2}$$

with c, the velocity of light in a vacuum.

Accordingly, neglecting clock error synchronization and propagation delays, if three satellites are visible from a ground receiver position, the location of this receiver can be determined at the intersection of three spheres centered on those three satellites, the radius of each sphere corresponding to the respective satellite-to-receiver distance(see Fig. 1.8). The three unknowns of the receiver position (X_r, Y_r and Z_r coordinates) can be calculated using this method.

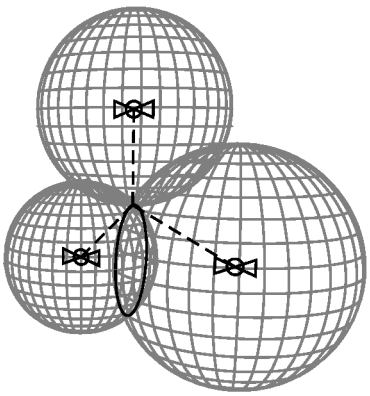

Figure 1.8: Position of the receiver at the intersection of three spheres. Source: Royal Observatory of Belgium

Unfortunately, positioning is subject to lots of biases, neglected up to this part, but that must be considered as far as precise positioning is considered. One of these biases, already aborded in the first paragraphs of this section and which leads to important errors if not taken into account while estimating a position, is the clock error synchronization ($c.\Delta\delta t$).
In the previous equations, one assumes that receiver and satellite clocks are perfectly synchronized with the reference time scale. However, this is never the case in practice.
Furthermore, the very precise atomic clocks aboard satellites produce their own time scale while those in receiver devices also produce their own.
These differences of synchronization can lead to important errors in the positioning and thus, must be considered:

$$t_{r,ref} = t_r(t_{r,ref}) + \delta t_r(t_{r,ref}) \tag{1.3}$$

$$t^s_{ref} = t^s(t^s_{ref}) + \delta t^s(t^s_{ref}) \tag{1.4}$$

with $\delta t^s(t^s_{ref})$ the satellite clock bias at time t^s_{ref} and $\delta t_r(t_{r,ref})$ the receiver clock bias at time $t_{r,ref}$.

The satellite clock bias $\delta t^s(t^s_{ref})$ can be estimated and modeled. It is sent by satellites in their navigation messages (also called ephemerides). Therefore, only the receiver clock bias $\delta t_r(t_{r,ref})$ remains unknown. And thus, four unknowns need to be determined, needing a fourth satellite to resolve the positioning equation.

Finally, the equation of positioning is:

$$R^s_r = c.(t_{r,ref} - t^s_{ref}) + c.(\delta t^s(t^s_{ref}) - \delta t_r(t_{r,ref})) \tag{1.5}$$

And then, τ^s_r can be associated with the time of travel:

$$\tau^s_r = t_{r,ref} - t^s_{ref} \tag{1.6}$$

and the equation (1.5) can be written as:

$$R^s_r = c.\tau^s_r + c.(\delta t^s(t^s_{ref}) - \delta t_r(t_{r,ref})) \tag{1.7}$$

This last equation is also known as:

$$R^s_r = D^s_r + c.\Delta\delta t \tag{1.8}$$

with D^s_r the geometric range between satellite and receiver and $c.\Delta\delta t$ the clock error synchronization.

1.3.2 Observables

In order to measure the time taken by the signal to travel from satellite to receiver, observables are needed. Usually, two types of observables are available with regard to positioning but, no matter which observable is used, the principle is the same. This principle, exposed in the previous section (1.3.1), is summarized in Fig. 1.9 from which the following equation arises:

$$\overrightarrow{\Delta_r^s} = \overrightarrow{r^s} - \overrightarrow{r_r} \tag{1.9}$$

where $\overrightarrow{\Delta_r^s}$ expresses the satellite-to-receiver distance, $\overrightarrow{r^s}$ instantaneous satellite position and $\overrightarrow{r_r}$ the instantaneous receiver position.

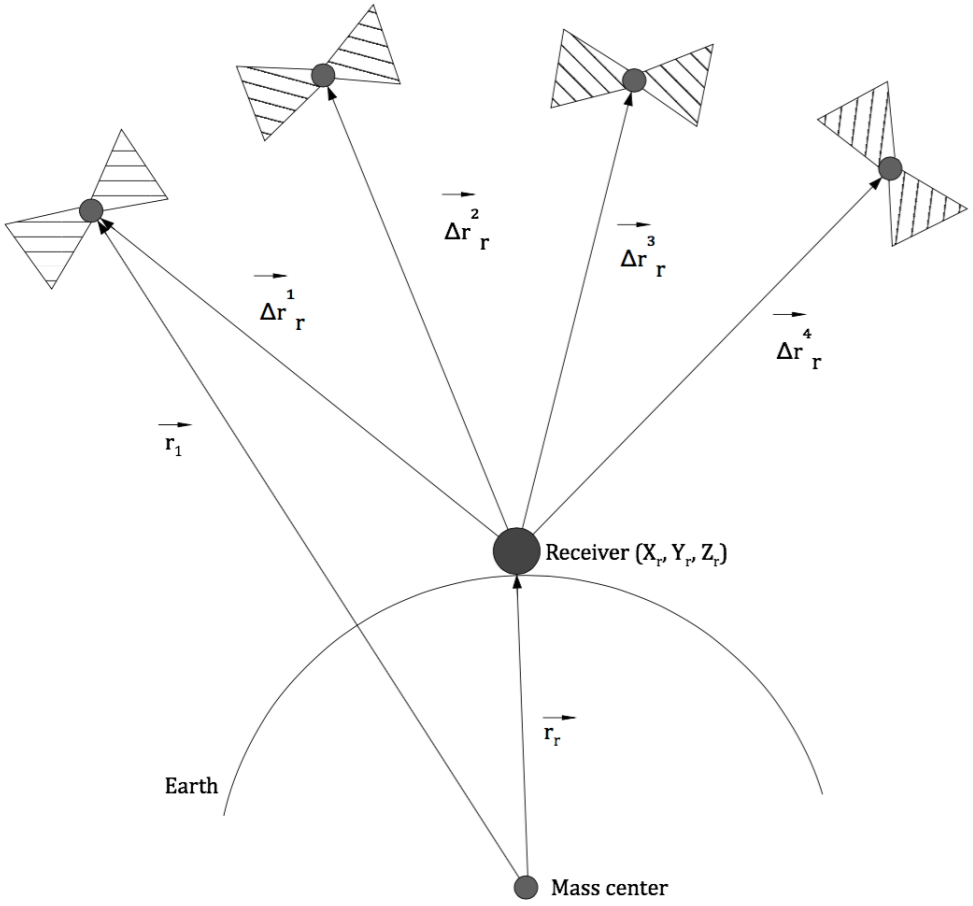

Figure 1.9: Satellite positioning principle with four satellites

Observables are the following:

- code pseudorange measurements
- phase pseudorange measurements

1.3.3 Code pseudorange positioning

Determining a position on the Earth's surface by means of code pseudorange measurements requires the use of a specific part of the signal, namely the code.

An identical code is generated by both satellite and receiver, that would be perfectly synchronized in absence of clock error (see section 1.3.1). Therefore, when a signal is broadcast by a satellite to a ground user, the code modulated on this signal will be offset, at time of reception, from a replica generated by the receiver. Indeed, the code generated by the satellite has travelled the distance from satellite to receiver and thus, an offset exists in comparison with the receiver replica. By measuring precisely this offset, the distance between the satellite and the receiver is given by the formula (1.2) and shown in Fig. 1.10.

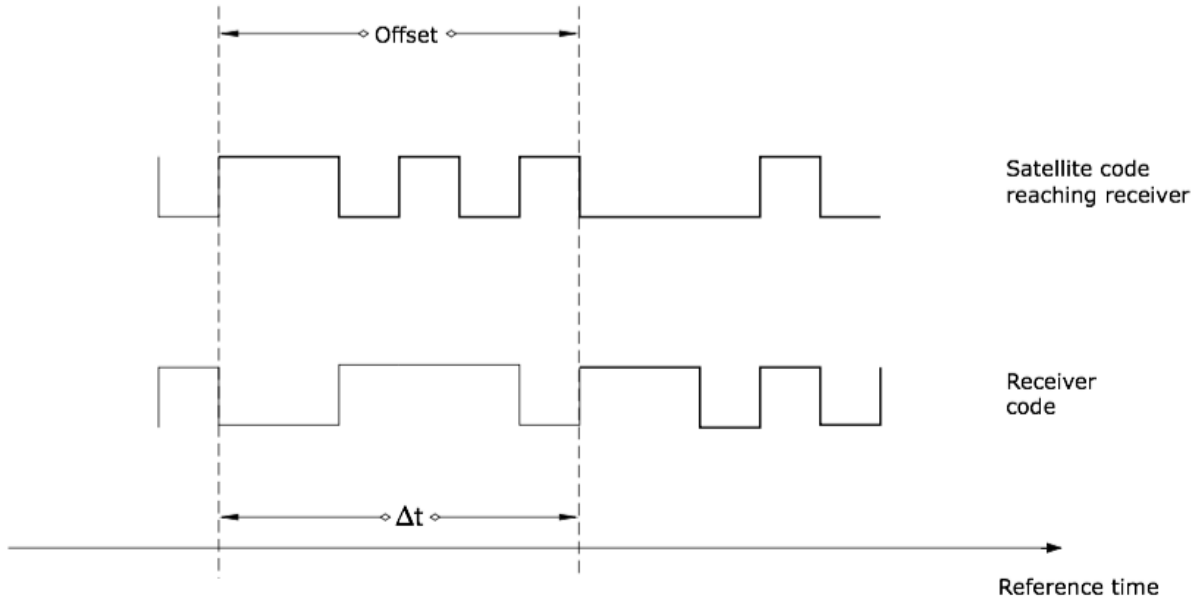

Figure 1.10: Offset between the code emitted by the satellite and its replica generated by the receiver at time of reception

In order to estimate this offset, a cross-correlation operation, as a function of time, is applied to the signals until the maximum correlation is found between the two signals. This correlation consists of a multiplication of both signals and the integration of the result over a given duration.

For further applications, the code pseudorange equation will be noted:

$$P^s_{r,k}(t) = D^s_r + T^s_r + I^s_{r,k} + M^s_{r,k,m} + c.(\delta t^s(t^s_{ref}) - \delta t_r(t_{r,ref})) + d_{r,k,m} + d^s_{k,m} + \epsilon^s_{r,k,m} \qquad (1.10)$$

with $P^s_{r,k}(t)$ denoting the code pseudorange measurement in function of the time, T^s_r the tropospheric delay, $I^s_{r,k}$ the ionospheric delay, $M^s_{r,k,m}$ the multipath delay, $d_{r,k,m}$ and $d^s_{k,m}$ the hardware delays of the receiver and the satellite, respectively, and $\epsilon^s_{r,k,m}$ the observation noise which encompasses unmodeled errors. The indexes k and m stand for "function of the frequency"and "function of the modulation", respectively.

This equation does not consider every possible source of errors that could alter the signal. Biases such as antenna phase center variation or orbital errors will not be explained in this dissertation since their impact on position is less significant than the biases detailed in section 1.4.

1.3.4 Phase pseudorange positioning

The phase pseudorange positioning is based on a different part of the signal: the carrier frequency. This carrier wave is used to broadcast the code on the signal thanks to the modulation techniques covered in section 1.2 . Initially not built for positioning, phase measurements proved to be very precise, much more than code measurements.

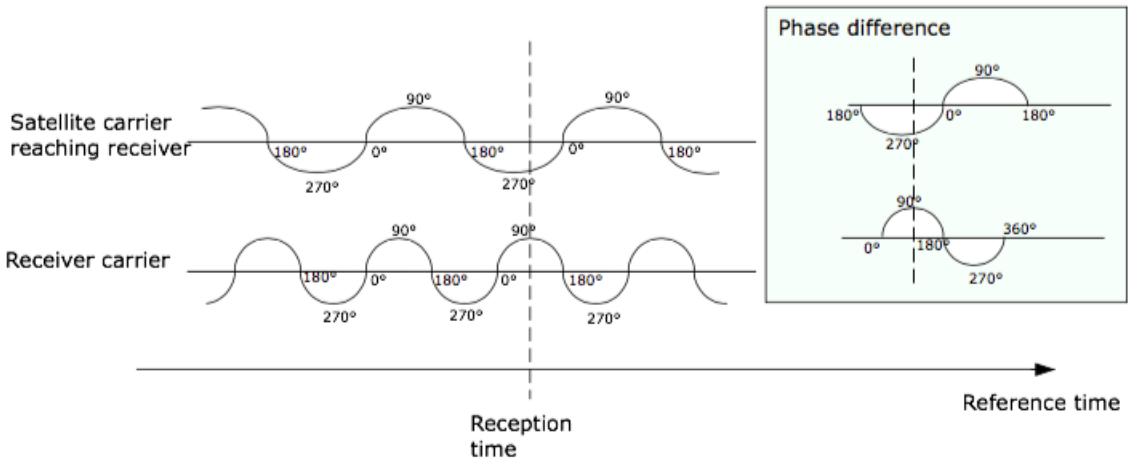

Figure 1.11: Phase difference

Similarly to code pseudorange measurements, the receiver generates a replica of the carrier wave emitted by the satellite. In the absence of synchronization errors, both signals are in phase. The so-called phase observable is obtained by measuring the phase difference between the carrier wave emitted by the satellite and arriving at the receiver. However, contrary to code, the phase wave remains similar at each cycle (Fig. 1.11). Thus, as phase measurements are always ambiguous, the phase difference contains an integer number of cycles which is related to the first measurement epoch. It is referred to as the *initial ambiguity* ($N^s_{r,k}$) and its determination is the major issue of phase pseudorange measurements. This ambiguity must be solved in order to compute precise positions.

Phase pseudorange equations are written as follows:

$$\Phi^s_{r,k}(t) = D^s_r + T^s_r - I^s_{r,k} + M^s_{r,k,\phi} + c.(\delta t^s(t^s_{ref}) - \delta t_r(t_{r,ref})) + d_{r,k,\phi} + d^s_{k,\phi} + \lambda.N^s_{r,k} + \epsilon^s_{r,k,\phi} \quad (1.11)$$

with $\Phi^s_{r,k}(t)$ the phase pseudorange measurement in function of the time, λ the wavelength of the signal, $N^s_{r,k}$ the initial ambiguity, the index ϕ meaning "function of the phase"and the other error sources remaining the same as in the code pseudorange equation (1.10).

In the formulas above, only four parameters are frequency independent: D^s_r, T^s_r, $\delta t_r(t_{r,ref})$ and $\delta t^s(t^s_{ref})$. Additionally, it is worth noticing that all the variables shown in this equation are time dependent except for the initial ambiguity $N^s_{r,k}$ which is supposed to remain constant over the time (unless cycle slips[5] occur).

As in the precedent equation, only a few major biases are considered in these equations, as explained in section 1.3.3.

[5]Cycle slip: momentary loss of signal due to atmospheric perturbations.

1.3.5 Observables comparison

Between those two observables, phase measurements emerge as very precise. As can be seen in Table 1.8, their *range biases* (or *observation noise*) are much smaller than the code ones [Warnant, 2013]. However, the initial ambiguity may require a long time to be solved and thus, code measurements, even if less accurate, are often used in real time application. Furthermore, the complexity of ambiguity resolution equations encourage a code pseudorange solution.

Table 1.8 illustrates the typical magnitude of range biases for the GPS system [Hofmann-Wellenhof et al., 2008]($\epsilon^s_{r,k}$):

Range	Bias [mm]
Code range (coarse code C/A)	1000 - 3000
Code range (precise code P)	100 - 300
Phase range	0.2 - 5

Table 1.8: Phase and code ranges biases

Such important differences in terms of biases are linked to the way code and phase pseudoranges are affected by error sources mentioned in the next section. This observation noise is considered as an accidental error and is closely related to the wavelength of the signal as it is generally accepted that its value corresponds to one-hundredth of the signal wavelength. Or at least before new GPS and Galileo signals arrive (see chapter 2). Indeed, the Galileo E5 AltBOC signal should reduce code range bias to the centimeter level thanks to its particular AltBOC modulation and its very wide bandwidth (51.150 Mhz) [Diessongo et al., 2014]. This hypothesis will be further explored in chapter 2.

1.4 Error sources

In addition to clock errors, many parameters affect the signal while traveling through the atmosphere or when emitted and received. Those alterations must be taken into account to reach an acceptable precision on the calculated positions. The positioning equations (1.10) and (1.11) can not directly be used but need to be corrected from these errors.

This section details the effects and the sources of these biases. They can be divided in three categories: the receiver-based biases, the satellite-based biases and the propagation biases. Some systematic biases are easily modeled and then eliminated or reduced. By contrast, some are very unpredictable and code or/and phase combinations are necessary to partly or entirely get rid of them. These combinations depend on the nature of the error that need to be eliminated. If this error belongs to the satellite-based biases category, then a combination of observations from two different receivers on the same satellite should remove them. Analogously, a receiver-based error will be removed by combining two measurements from the same receiver on two satellites [Hofmann-Wellenhof et al., 2008].

Table 1.9 shows the orders of magnitude on code pseudorange measurements of the errors described below:

Error Source	Precision (Standard deviation σ)
Satellite-based errors:	
- orbital errors	1- 2 m
- clock biases	1 - 2 m
Receiver-based errors:	
- hardware delays	dm - m
- observation noise	0.2 - 1 m
- antenna phase center variation	mm-cm
Propagation errors:	
- tropospheric delays	dm
- ionospheric delays	cm - 50 m
- multipath delays	1-2 m

Table 1.9: Magnitude of code ranges error sources. Source: [Warnant, 2013]

In this table, some errors have already been addressed, such as clock biases and observation noise. The upcoming sections describe the propagation errors: tropospheric delays, ionospheric delays and multipath delays, but also the hardware delays.

The atmospheric errors affect the signal in three different ways [Warnant, 2013]:

- the signal amplitude is reduced
- the signal is deviated
- the velocity of the signal is modified

These propagation errors are highly dependent on elevation as a lower satellite elevation conducts to a longer path to reach the receiver. As far as satellite-based positioning is concerned, it is the third point that presents the greater impact on the solutions as code and phase show different propagation velocities (approximated in the Formulas (1.10) and (1.11) by the speed of light c).

1.4.1 Tropospheric delays

The troposphere is a layer of the atmosphere located in the neutral atmosphere or non-ionized atmosphere. The signal is mainly affected, regardless of the observables chosen, by the water vapor present in this medium, the pressure and the temperature. It is very common to consider the tropospheric effect (T_r^s) as composed of a wet effect (water vapor dependent) and a dry effect. The dry part of this bias is the most important but also the most easily modeled. By contrast, the wet part, essentially a function of the water vapor, affects the signal to a lesser proportion but is widely varying over time and space, rendering it difficult to predict and hence, to model.

Frequency independent, the effects of tropospheric delays can be modeled whatever the signal considered in the measurement. The most generic tropospheric models were proposed by Hopfield(1969) and Saastamoinen (1975). It is Saastamoinen's model that has been chosen in the RTP format used in this dissertation (see section 5.2.3) to be automatically calculated for each observation recorded by the receiver. This model is based on the gas law and the assumption of hydrostatic equilibrium of the atmosphere.

Model application reduces tropospheric effects from approximatively 2.50 m of error to 10 cm. In particular configurations, this error may even be erased (see chapter 4).

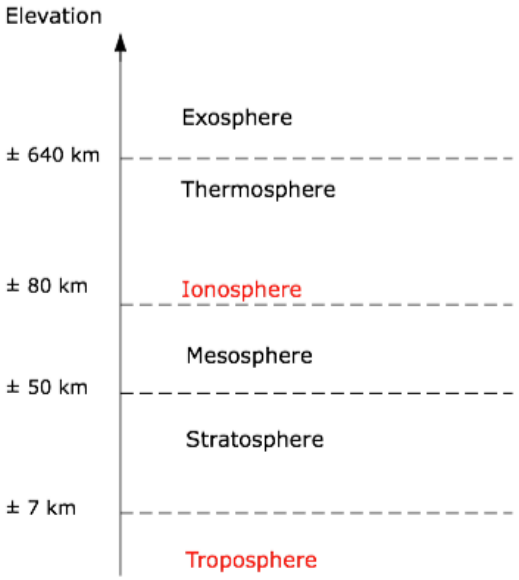

Figure 1.12: Atmospheric layers

1.4.2 Ionospheric delays

The ionosphere, a higher layer in the atmosphere, is, contrary to the troposphere, an ionized medium. Electrons perturb the signal to a varying extent which generates more difficulties in modeling the effects of ionosphere delays ($I^s_{r,k}$) and thus correcting for these effects. The variable used to measure the electron concentration is named TEC (*Total Electron Content*). The TEC differs from one place to another being mainly dependent on solar activity. It can be locally affected by unpredictable phenomena such as scintillations or TID's (*Travelling Ionospheric Disturbances*).

Besides, this part of the atmosphere is sensitive to frequencies and therefore, affects the various signals differently. Furthermore, as the ionosphere is a dispersive medium, code and phase observables are also differently affected due to their velocity differences. Therefore, code and phases are, in absolute value, similarly affected by the ionosphere but the sign of the effect is opposed. As a consequence, phase pseudoranges measured are too short while code pseudoranges are too long.

Ionospheric delays are function of the elevation of the observed satellite but also of the latitude of observation. In middle latitude, no important troubles are detected. On the other hand, in polar latitude or equatorial latitude, the TEC varies considerably and it can reach higher values than those in middle latitude.

As earlier explained, the ionospheric delay can not be easily modeled. In a location without elements encouraging multipath, it is the main error source that affects a signal.

Table 1.10 illustrates the order of magnitude of the TEC values frequently encountered on the Earth's surface measured in TECU (1 TECU = $10^{16} e^- m^{-2}$) and the associated correction in meters to the GPS L1 and L2 signals:

TEC values	Description	Correction on GPS L1[m]	Correction on GPS L2 [m]
1 TECU	The minimal value that can be observed on Earth	0.16	0.27
20 TECU	Regularly observed value in middle latitudes	3.25	5.35
100 TECU	Frequent value reached in equatorial latitudes Maximum value in Brussels	16.24	26.74
220 TECU	The maximal value than can be observed on Earth	36	59

Table 1.10: Frequent TEC values and corrections associated on GPS L1 and L2. Source: [Warnant, 2013]

Models that pattern ionospheric effect exist but the local nature of this bias makes it difficult to predict. These models are either physical or empirical models. The physical models, very poorly adapted to regional TEC variation, are not recommended. On the other hand, empirical models, based on observation, represent the mean effect of these delays but are not useful in case of strong solar activity or geomagnetic storms. Among the models proposed in the literature, the Klobuchar model, an empirical one, is the default model used to correct ionospheric delays in the single point positioning approach (see chapter 4). The precision resulting from both Klobuchar for ionosphere and Staastamoinen for troposphere modeling is around 10 to 30 centimeters. Such a precision level is sufficient for present code pseudorange positioning. But if new signals, such as Galileo E5, brought greatest precision, a more precise model should be used. Similarly, for precise positioning at the centimeter or even millimeter level, this model would not be sufficient. This model correction is precalculated in the RTP format files used for the computation.

1.4.3 Multipath

The signal arriving from the satellite might encounter obstructions on its path to the receiver antenna. The obstacles reflect the signal in such a way that instead of following a direct path, the signal is deviated, creating an offset in the measure of pseudorange as the signal runs a longer path. This error is referred to as *multipath* ($M^s_{r,k}$) and shows a different effect on code or phase ranges. Thus, on carrier phase measurements, its effect can be cancelled by averaging multipath on a long duration whereas in code measurements, multipath can not be suppressed.

As any reflecting surface can engender this error, the multipath on a particular receiver depends on its direct environment. Hence, no generic model of this effect can be estimated.

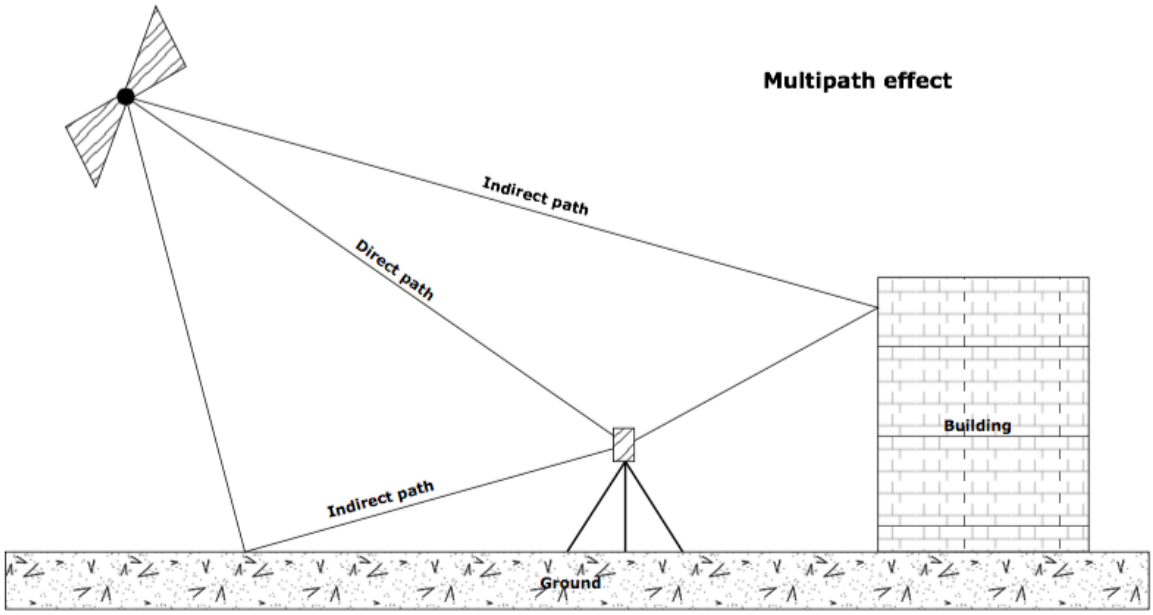

Figure 1.13: Multipath effect

Additionally, multipath presents a periodic effect on measurements as it is function of the geometry of the satellite-receiver direction. Therefore, the same effect is observed at each satellite crossing. The multipath periodicity shows higher values when reflecting objects are located close to the receiver. On the contrary, when the reflection happens far away, the periodicity is reduced. Moreover, the frequency of the signal also has an influence on the importance of multipath.

Similarly to the two previous atmospheric effects, multipath is sensitive to satellite elevation. This is due to the fact that the signal may encounter more reflecting surfaces when the satellite observed is close to the horizon [Hofmann-Wellenhof et al., 2008].

The multipath has meter scale effect on code measurement, and of the centimeter for phase measurements. The E5 AltBOC Galileo signal shows remarkable characteristics in terms of multipath. The multipath effect is very small on this signal in comparison with other GPS and Galileo signals [Caelen, 2014]. Thanks to this property, positioning with this signal is assumed to be very accurate.

As no correction models are available in this case, many techniques can be used to reduce or even eliminate this error:

- location of the receiver choice
- dual-frequency code and carrier phase measurement combination
- day after day correlation (as multipath shows periodicity)
- averaging carrier phases ranges along a certain time duration
- antenna choice
- receiver choice

1.4.4 Observation noise

In his article, [Langley, 1997] gave the following definition of observation noise: "*Any unwanted disturbances, superimposed on a signal, that tend to obscure a signal's usefulness of information content*". Still according to [Langley, 1997], in radio-based communication systems, such as satellite systems, the signal is affected by a certain noise (ϵ_r^s) that originates from diverse sources: the equipment in itself, electronic devices such as radio transmitters, engines or microwave ovens, and natural terrestrial and extraterrestrial sources. It is traditionally divided in two parts: the noise generated by the receiver (e_r^s) and the noise which occurs just before the receiver (h_r^s) (comprising sky and ground noise) [Tiberius et al., 2009]. Noise equation is given by:

$$\epsilon_r^s = e_r^s + h_r^s \tag{1.12}$$

As an example, a well-known internal receiver noise (e_r^s) is called the *thermal noise*. This observation noise component is induced by the movement of electrons in conductor elements present in the receiver. Another component of this thermal noise is introduced by losses from cables inside the receiver.

Regarding noise just before the receiver (h_r^s), two main components can also be distinguished: the sky noise, composed of cosmic noise caused by electromagnetic radiation mainly emitted by the sun and the Milky Way galaxy, and of atmospheric noise in the form of radiation, and the ground noise which includes radiation emitted by the ground itself and the objects surrounding of the antenna.

This observation noise has already been mentioned in section 1.3.5 where orders of magnitude were given.

1.4.5 Hardware delays

As with every hardware, satellites and receivers may engender so-called *hardware delays* (d_k^s and $d_{r,k}$, respectively). These delays include propagation time into internal cables or intrinsic obstacles. They are a function of the frequency of the signal. Moreover, they take different values on code or carrier ranges but do not vary a lot. The encountered variations may come from cable dilatation in case of temperature changes.

[Tiberius et al., 2009] specifies that in general, as hardware delays depend on observation type and signal frequency, a particular hardware value is associated with each modulation and each frequency and considered as unvarying. But it seems that hardware delays for a particular modulation at a certain frequency differ in function of the occupied spectral bandwidth, even if the modulations concerned share an identical bandwidth.

The hardware delays, under normal circumstances, might reach less than 1 decimeter per hour values.

1.5 Conclusion

This first chapter introduced the basic concepts of satellite-based positioning.

Firstly, the main positioning systems used in this dissertation, Galileo and GPS, were discussed. Their orbital characteristics as well as the satellites generation were mentioned. The signals broadcasted by their satellites were briefly described and their main characteristics were given. The Galileo E5 signal expected abilities were addressed.

Secondly, the signal different modulation techniques have been explained. The crucial contribution of the AltBOC modulation to tracking improvement of the signal was mentioned.

Thirdly, position principles were explained. The necessity of observing simultanenously four satellites was specified and receiver clock issue was addressed. Then, the code and phase pseudoranges equations were provide and explained. They set the basis of the error sources analysis that followed. The problematic of the initial ambiguity term present in the carrier phase pseudoranges was discussed.

Finally, satellite-based biases, receiver-based biases, as well as atmospheric errors, multipath and observation noise impacts on the received signals were discussed. The problematic of modeling the ionospheric errors was noted. Multipath and observation noise impacts were described and order of magnitudes were given for each of the mentioned error sources. The ionosphere was identified as the source of the highest errors on the signal.

Chapter 2

State of the art

High precision satellite-based positioning is mainly executed thanks to carrier phase pseudoranges. This observable type shows very low observation noise, low multipath effect and therefore, makes it possible to reach a millimeter accuracy on position determination [Silva et al., 2012]. Nevertheless, carrier phase pseudoranges also present inconveniences. The major drawback of this observable is the initial ambiguity, an integer number of cycles, that must be determined in order to calculate a position.

The code pseudoranges, on the other hand, are widely used because of their simplicity, robustness and the fact that no ambiguity resolution is needed to obtain a position. But in the meantime, the precision of code pseudoranges is in the order of the meter or decimeter. Hence, very precise positioning with these code pseudoranges is not possible.

And yet, some GNSS applications require a few decimeters precision, better than the meter precision of code pseudoranges but less than the millimeter accuracy proposed by expensive carrier phase receivers. This precision could be reached with new GPS and Galileo signals, and particularly with the new Galileo E5 AltBOC signal. Indeed, the E1, E5a and E5b OS signals of Galileo and GPS L5 and L1C should bring significant improvements to satellite-based positioning and related topics such as ionospheric delay estimation, ambiguity resolution performances, tropospheric delay estimation and availability of additional frequencies [Julien et al., 2015]. All the new signals are characterized by low multipath susceptibility, low observation noise and an enhanced resistance to interferences. These properties should lead to more robust and accurate code and phase pseudorange measurements.

This chapter will introduce results of previous studies on the Galileo E5 AltBOC modulation characteristics, the positioning techniques and the first positioning results using the Galileo satellite system.

2.1 Galileo E5 AltBOC

The Galileo E5 AltBOC signal is expected to be revolutionary [Diessongo et al., 2014]. It should theoretically reach a centimeter precision with code pseudoranges even in challenging environments such as urban environments. This exceptional accuracy should lead to high precision positioning with codes pseudoranges only, avoiding complex ambiguity resolutions.
[Junker et al., 2011] even argued that code and phase pseudoranges could soon be comparable in terms of accuracy.

In order to introduce theoretical orders of magnitude, [Silva et al., 2012] expected obser-

vation precision[1] with Galileo E5 AltBOC code pseudoranges ranging from 0.02 meters of accuracy in "open sky" scenarios and 0.08 meters in urban scenarios. In comparison, those errors with Galileo E1 CBOC should range between 0.25 meters and 2.00 meters. These results of a centimeter level for Galileo E5 derive from a better mitigation of the multipath, reducing usual code pseudoranges multipath effect from few decimeters to a couple of centimeters.

2.1.1 Details of the AltBOC modulation

Galileo E5 signal's particular modulation, the AltBOC modulation, is in major part responsible for the highly improved performances of this signal. Composed of two sub-carriers E5a and E5b, the E5 a+b band has a central frequency of 1191.795 MHz. Each of these sub-carriers are transmitted in different frequency bands [Julien et al., 2015]:

- The E5a signal has a central frequency of 1176.450 MHz but its frequency band range from 1164 MHz to 1191.795 MHz.
- The E5b signal is transmitted in a frequency band which ranges from 1191.795 MHz to 1215 MHz, centered on 1207.14 MHz.

Therefore, the E5 band ranges from 1164 MHz to 1215 MHz. In other words, E5 a+b has a reference bandwidth of at least 51.150 MHz, the largest Radio Navigation Satellite System band [EuropeanUnion, 2010]. Moreover, the signal sent from the satellite is transmitted over a bandwidth of some 90 MHz. This wide bandwidth and its AltBOC modulation lead to a low observation noise on E5 a+b code measurements [Diessongo et al., 2014].

The signal is composed of four PRN codes ($E5a-I$, $E5a-Q$, $E5b-I$, $E5b-Q$) and two navigation messages that are modulated onto a complex subcarrier. This subcarrier signal splits the spectrum into two symmetric side lobes E5a and E5b. This property allows demodulation of the signal as a BSPK modulated signal if a bandwidth filter of less than 51.150 MHz centered on the E5a or E5b central frequency is applied (Fig. 2.1).

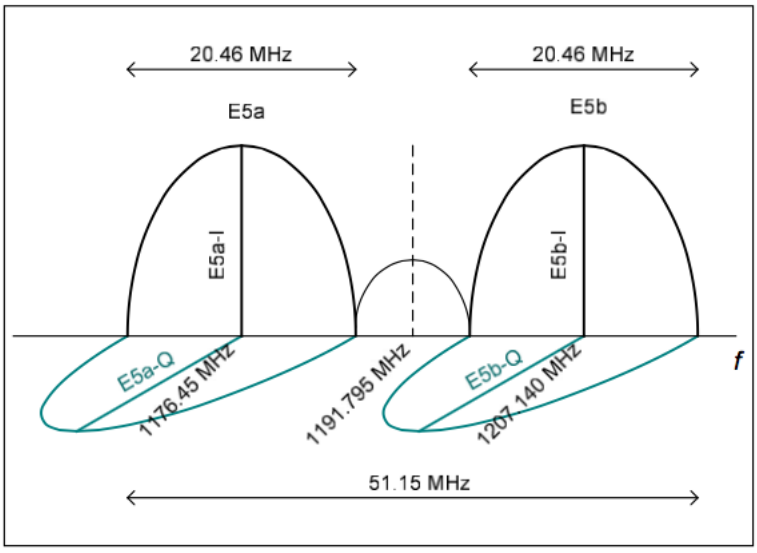

Figure 2.1: E5 AltBOC split spectrum around center frequency. Source: [Shivaramaiah & Dempster, 2009]

[1]The observation precision refers to the quality of the pseudoranges extracted from the signals at their arrival to the receiver.

Galileo E5 AltBOC is supposed to combine three different services: the Open Service (OS), the Commercial Service (CS) and the Safety of Life Service (SoL) into two BOC signals: E5a (OS and SoL services) and E5b (OS, CS and SoL services). Therefore, the AltBOC modulation has been modified from initial non-constant envelope modulation to a constant envelope modulation. The non-constant envelope would have lead to zero values in the baseband signal, which would have resulted in no energy transmitted and would have distorted the broadcast signal. In addition, this modulation would not have split the signal in a lower and an upper band but the signal spectrum would just have been shifted from higher to lower frequencies and conversely [Rebeyrol et al., 2007]. Consequently, the sub-carrier waveforms have been modified to obtain a constant envelope. This envelope requires a small portion of overall power to remain constant but offers the possibility to demodulate the signal in many different ways:

- a simple receiver has the possibility to demodulate the signal as a single wide-band QPSK on E5a or E5b (this demodulation leads to a loss of AltBOC properties)
- the signal can also be demodulated as a double wide-band on both E5a and E5b which allows dual-frequency measurements (this demodulation leads to a loss of AltBOC properties)
- as an AltBOC modulation reduced to its main lobes (this demodulation leads to a loss of AltBOC properties)
- as an AltBOC modulation for the entire bandwidth

Each sideband (E5a and E5b) comprises two code pseudoranges: the in-phase data channel component ($E5a - I$, $E5b - I$) and the quadrature phase pilot channel component ($E5a - Q$, $E5b - Q$) (see section 1.1.3). This innovation, also included in the new GPS L5 signal, should contribute to this code pseudorange precision improvement [Julien et al., 2015]. Indeed, pilot tracking is necessary when weak signals are tracked. Moreover, as they do not carry data bits, they allow a long integration time that improves the accuracy as a more robust tracking is obtained [Tawk et al., 2012] and [Silva et al., 2010].

In addition to this wide bandwidth, the AltBOC modulation is characterized by a sharp autocorrelation function. According to [Silva et al., 2012], observation noise and multipath robustness are closely linked to the autocorrelation function shape. The mean peak, but also the secondary peaks have their importance. A steep mean peak indicates low observation noise and high multipath robustness. The existence of secondary peaks also indicates an improvement in robustness against multipath. However, these secondary peaks require specific techniques to be discriminated from the main peak in the tracked signal. The Fig. 2.2 illustrates the autocorrelation functions of well known modulations.

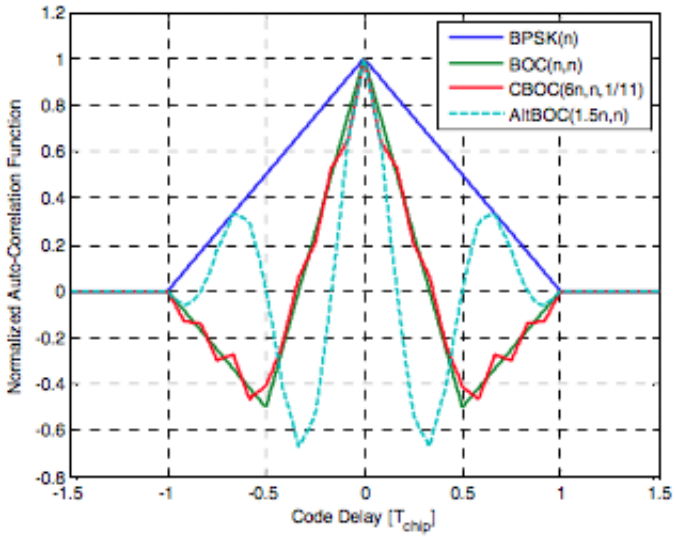

Figure 2.2: Normalized autocorrelation functions for different modulations: BPSK of GPS L1, BOC of Galileo E1 with simplified demodulation[4], CBOC of Galileo E1 and AltBOC of Galileo E5 signals[5]. Source: [Silva et al., 2012]

Fig. 2.2 clearly shows AltBOC superiority to other modulation techniques according to autocorrelation shape parameters. Its peak is much steeper than other signals. Furthermore, it is the only signal that shows secondary peaks.

Fig. 2.3 illustrates the fact that even with a 50 MHz front end filter, more common than 90 MHz filter, the autocorrelation function keeps its original shape. This is due to the fact that the energy present in the main lobes is still captured with this bandwidth [Shivaramaiah & Dempster, 2009]. Therefore, the use of cheapest front-end filter does not affect Galileo E5 signal properties. Still, with reduced front-end filter, the amplitude of the main peak is reduced and rounded.

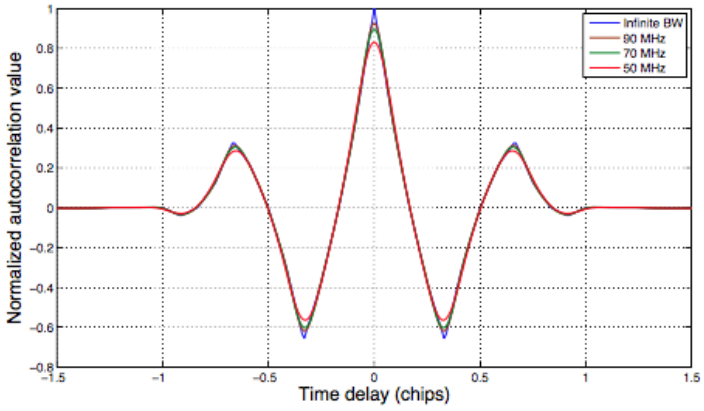

Figure 2.3: Autocorrelation of the GIOVE-A Wideband E5 signal. Source: [Shivaramaiah & Dempster, 2009]

[5]Galileo E1 modulation is a particular MBOC modulation, the CBOC modulation (see section 1.2.4). Only few receivers can use this modulation and thus, the others reduce Galileo E1 to a simple BOC modulation.

[5]The expressions in brackets on the modulations indicate the sub-carrier frequency and the code rate, respectively. They both must be interpreted as multiplied by the fundamental frequency f_0 of 10.23 MHz. This is the classical modulation notation and it will reappear in other figures. It will not be further commented.

Finally, the noise tracking and multipath effect on Galileo E5 AltBOC are illustrated in the last two figures (Fig. 2.4 and Fig. 2.5) in comparison with usual modulation types.

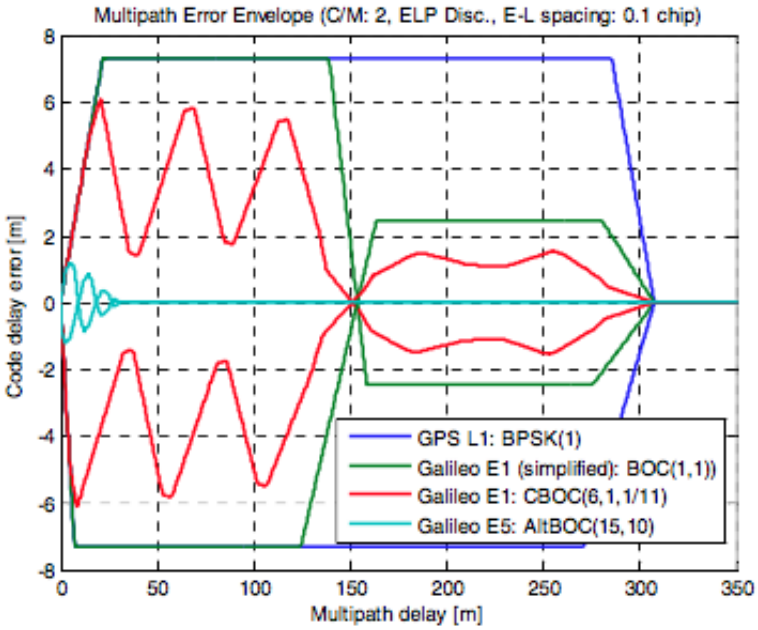

Figure 2.4: Multipath error envelopes for GPS L1 , Galileo E1 and Galileo E5 signals. Source: [Silva et al., 2012]

As already seen in section 1.4.3, the multipath introduces reflected signals that arrive at the receiver at the same time as non-reflected ones. In addition to this, a reflected signal may be altered, and its autocorrelation function may be distorted, leading to positioning errors. The usual representation of the multipath is the one presented in Fig. 2.4. Error envelopes depicting the maximum error on code observation resulting from one reflected signal illustrate the impact of multipath on a certain signal in terms of multipath delay [m]. This multipath delay, represented in meters, is a function of the distance of the obstacles encountered by the signal. The code delay error characterizes the error engendered by the multipath delays on the code pseudorange measurements.

From this figure, it appears clearly that Galileo E5 AltBOC shows a better resistance over short and long multipath delays than all the other signals. Both E1 and E5 signals show better multipath mitigation performance than GPS L1 which is the worse signal in terms of multipath mitigation. Indeed, one can notice that envelope's shapes change mostly along the X axis. This is due to fact that multipath mitigation is a phenomenon that mainly accounts for longer delays (longer than 150 meters for GPS L1 and Galileo E1 for instance). These delay values depend on the location of the antenna receiver [Simsky et al., 2008a] and hence, certain sites with low-range multipath delays will not really be affected by better multipath mitigation of Galileo's new signals apart from E5 which shows important capacity for multipath suppression for both short and long range multipath delays.

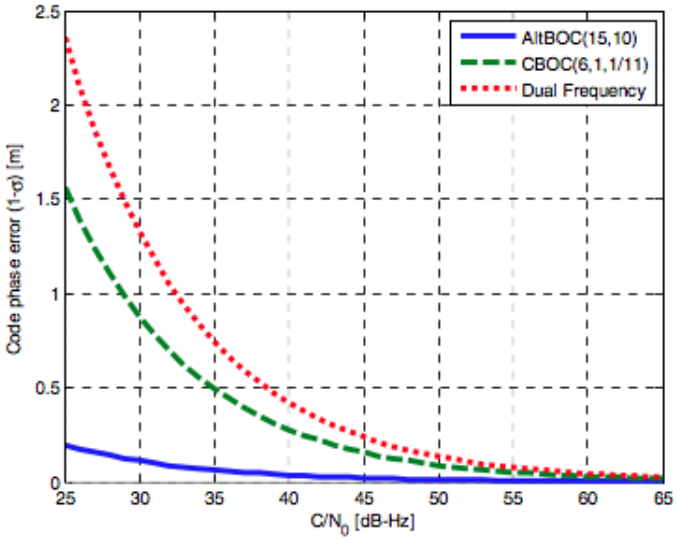

Figure 2.5: Theoretical code measurements noise comparison between Galileo E1 CBOC, Galileo E5 AltBOC and their dual-frequency combination (ionosphere-free). Source: [Silva et al., 2012]

This last figure (Fig. 2.5) represents the noise range error in function of the C/N_0 ratio, the *carrier-to-noise ratio*. This ratio derives from the *signal-to-noise ratio* (S/N) which expresses the quality of the information broadcast by the signal in [dB]. In other words, the ratio between the amount of information and the observation noise present on the signal. When this S/N ratio is divided by the bandwidth, one obtains the C/N_0 ratio. The main benefit of this parameter is that the quality of the signal measured is independent of the tracking algorithms used by the receiver. It is formulated in [dB Hz] [Joseph, 2010].

Going back to Fig. 2.5, one can observe that the dual-frequency combination of BOC and AltBOC signals does not benefit from the AltBOC ow noise characteristic. On the same figure, [Tawk et al., 2012] applied different front-end filters (90 MHz, 75 MHz, 51.15 MHz) to the receiver and deduced that bandwidth and observation noise are negatively correlated: when the bandwidth decreases, the code noise increases. From this graph, AltBOC clearly shows a reduced code observation noise.

A last point about this signal concerns the PRN codes modulated on its sub-carrier. Their high rate chip (10.23 Mhz) also increases multipath mitigation on long delays and lower code noise error [Tawk et al., 2012].

All these characteristics will result in increasingly complex modulation and demodulation structures that will confer robustness and accuracy to this signal.

Yet, Galileo E5 AtlBOC presents some drawbacks. Among them, its wide bandwidth requires a large front-end filter which needs a powerful processor consuming more power to process the signal. This is the reason why some other demodulation processes have been tested to keep benefiting from AltBOC great properties without processing the complete bandwidth (see upper paragraphs in this section).

2.2 Positioning techniques

Many satellite-based positioning techniques exists and an introduction is needed to place further results in context.

2.2.1 Distinction

Among the positioning techniques, differentiation can be made on the basis of:

- the observable chosen (code or phase pseudorange)
- the instantaneity or not of the positioning (real time or post-processing)
- the number of receivers used to determine a position (absolute positioning versus relative positioning)
- the static or kinematic character of the measurements.

Furthermore, considering two or more frequencies in a position calculation may lead to ionospheric first order bias elimination (ionospheric-free combination). This technique is very often used on long baselines were the atmospheric errors are more important. Many authors of the upcoming section based their research on this technique.

The advantages or drawbacks of these techniques are as follows.

Code and phase pseudorange

As seen in chapter 1, phase pseudoranges are more precise than code pseudoranges but they are ambiguous. Positioning with phases is therefore more precise but need a complex algorithm to solve the initial ambiguity.

Real time and post-processing

Concerning the instantaneity of the positioning, methods using post-processing solutions will be able to add corrections to the raw observables. This will lead to more precise results.

Absolute and relative or differential positioning

The absolute positioning is the estimation of a position on the basis of one receiver observations. When two receivers are used to estimate a position, one can differentiate the relative positioning and the differential positioning. The latter consists in applying corrections provided by a reference station on raw observables observed by another receiver in post-treatment. The former is based on baseline computation between two receivers. The position of one of these receivers must be known and the determination of the baseline between them allows an estimation of the position of the second one. The observations made by both receivers are combined together in order to do so, in real-time or post-processing. The precision of the observations is a function of the distance between the receivers. When receivers are close to each other, most of the atmospheric error can be removed because it affects observations tracked by both receivers to a similar extent. With the distance increasing, the common part of the atmospheric biases decreases and the observations are more altered.

Static or Kinematic

Measurements may be static or kinematic. In the first case, the position of the receiver is fixed over the time while in the second case, the receiver is moving.

2.2.2 Position and observation precisions

A clear distinction must be made between both position and observation precisions concepts. Observation precision should not be confused with the position precision. On one hand, the observation precision characterizes the quality of the signal. It depends on the errors affecting the signal,

such as atmospheric errors, satellite-based biases or receiver-based biases, multipath and observation noise. On the other hand, the positioning precision is an indicator of the precision obtained on the estimated position and depends on the geometry of the constellation (DOP, see section. 4.2.2, the number of available satellites and the redundancy of observations (see section. 4.2.1).

2.2.3 Orders of magnitude

This section specifies results with Galileo E5. However, using different methods to compute a position leads to results with different precision values. The following paragraphs give an insight to these methods and the precision they might reach.

Phase positioning

In order to achieve precise positioning, the PPP (*Precise Point Positioning*) is a well validated method. The use of precise GPS orbits coupled with clock data with a centimeter accuracy allows a significantly reduction of two of the most important error sources in GPS positioning [Gao et al., 2006]. In addition, the dual-frequency GPS receivers use enables ionospheric first order effect to be removed. With reduced ionospheric biases, clock and orbits errors, a precision from centimeter to decimeter level is obtained.

The *Real Time Kinematic method* (RTK), is a kinematic method of positioning. This implies that one receiver is moving while the second one is a fixed reference station. This reference station provides real-time corrections or raw data to the moving one. In one case, the positioning is called *differential* as corrections are added to the measure in post-treatment. When raw data are sent, the positioning method is called *relative positioning* as both receiver observations are combined to estimate a position. The observables used in this method are the carrier phases. Centimeter-level precisions can be expected with this technique.

The differential positioning in static mode with carrier phases in post-processing is currently the most precise positioning technique. Millimeter-level precision is expected with such method.

Code positioning

By contrast, real time code absolute positioning in static mode reaches precision values of 10 meters. The best values of precision presently expected on code positioning are of a few decimeters level. The challenge of the new GPS and Galileo code pseudoranges is to outperform these values and reach the centimeter level of precision.

Reference values

In order to clarify the future results, centimeter to millimeter level precision on positioning will be regarded as precise positioning. Such a precision level is only expected with phase carrier pseudoranges. Decimeter to meter level precision on positioning is therefore not considered as precise positioning. These are the common precision values of code pseudorange positioning.

Concerning the observation precisions, decimeters to centimeters level of precision is expected with the new GPS and Galileo code pseudoranges. With the carrier phase observable, millimeter precision on the observations is reached.

2.3 Galileo first results

Until the launch of the first two IOV satellites in October 2011, only two experimental satellites (GIOVE A and GIOVE B) were available. Therefore, before October 2011, it was impossible to

compute a position based only on Galileo real data as a minimum of four satellites are necessary. Hence, in many cases, simulated data were used to assess the superiority of the new Galileo signals (E1 and E5) in terms of accuracy.

2.3.1 Simulated data

This is particularly the case for [Colomina et al., 2012] which simulated Galileo E1 and E5 data in order to test them in kinematic or static mode, with or without tree cover. His results validate the centimeter-level code pseudoranges measurements precision of Galileo E5 AltBOC. [Silva et al., 2012] carried out the same study but, instead of considering a full Galileo constellation, he generated a partial constellation in order to make the model more realistic. The order of magnitude obtained from this paper also predicted centimeter-level accuracies on code pseudorange measurements.

In the same year, [Lopes et al., 2012] used GNSS-INS integration[6] in order to test Galileo E5 AltBOC signal in environments presenting low or high multipath. In order to use Galileo E5 as a calibration for low-cost sensors found in the GNSS-INS integration simulator structure, many tests on different sensors concluded that contrary to GPS L1, Galileo E5 easily reaches centimeter-level code pseudorange positioning accuracies even in a multipath environment with low-cost sensors.

Other simulated data results were established by [Diessongo et al., 2012], [Diessongo et al., 2014] and [Junker et al., 2011]. They operated over long distances with a combination eliminating the ionospheric delays using both code and carrier phases pseudorange measurements. This combination, the *Code-plus-Carrier* combination, includes both code and phase observables. The addition of those observables remove the ionospheric biases from the observations allowing more precise positioning over long distances. Galileo E5 AltBOC showed very impressive results (2 to 3 centimeters of precision) for single-frequency positioning. In comparison, GPS L1 reached 10 to 20 centimeters precision and GPS L5 3 to 6 centimeters on a position determination.

2.3.2 Real data

In 2008, [Simsky et al., 2008a] tried to characterize multipath of the first GIOVE-A and GIOVE-B signals received. According to his multipath results, he classified Galileo signals in three groups:

- the best signals: Galileo E5 AltBOC (OS), E1A (PRS) and E6A (PRS)
- the medium signals: Galileo E5a (OS), E5b (OS) and E6BC (CS)
- the low performance signals: Galileo E1BC (OS)

This classification corresponds to theoretical estimations but in particular cases, E5b and E6BC show performances similar to low performance signals, in the order of E1BC, and E6A sometimes shows medium signal values instead of best signal values. Still, it is important to keep in mind that multipath depends on the location of the user, and therefore, this classification might not be always right.

[6]Integration of GNSS and INS (*Inertial Navigation Systems*) is a conceptual advance that allows measurements of both systems and gathers them in order to improve the final navigation solution [Soloviev & Gibbons, 2012].

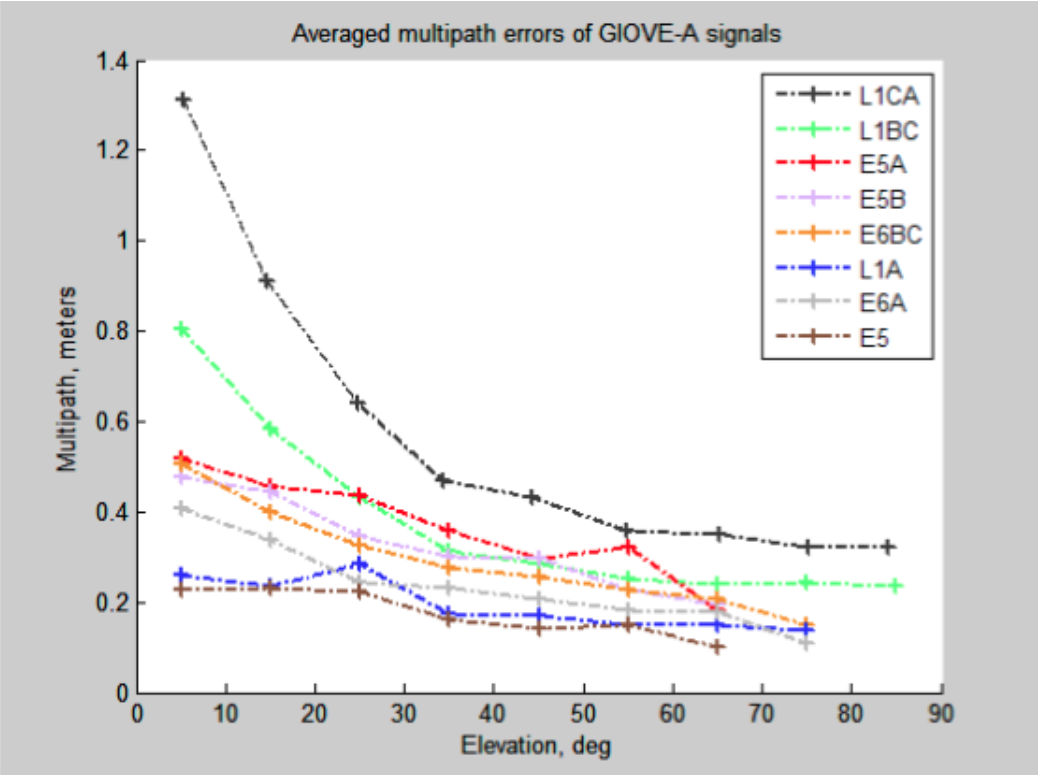

Figure 2.6: Standard deviation of code multipath for Galileo signals in comparison to GPS C/A in Leuven. Source: [Simsky et al., 2008a]

Galileo E5 AltBOC presents very low multipath values (between 25 centimeters at very low elevation to less than 10 centimeters at higher elevation) which should be viewed as a direct consequence of its high chip rate and its complex modulation structure. By contrast, Galileo E5a shows important variations in short-range multipath environments, which was not expected in theory (see section 2.1.1).

In 2009, [de Bakker et al., 2009] (confirmed in [de Bakker et al., 2012]) and [Tiberius et al., 2009] used combinations of GIOVE first broadcast signals and combinations of GPS signals to assess the performances of new Galileo and GPS signals (see details in the next paragraphs). It turns out that both Galileo E5a and GPS L5 show very low observation noise (in the order of 5 to 6 centimeters compared with 10 to 20 centimeters with GPS L1 and Galileo E1). On the contrary, E5a carrier phase observation noise is higher than E1 carrier noise probably due to a C/N_0 ratio lower on E5a band. Nonetheless, strong multipath effects on both Galileo E5a and GPS L5 were detected. According to the authors, these results could be due to the equipment used in the study or to the environment of the experiment.

Later, [Langley et al., 2012] obtained the very first positioning results with four Galileo spacecrafts available. On May 17 2012, just before GIOVE-A and GIOBE-B decommissioning June 30^{th}, four satellites were observed for a period of two and a half hours. Single point positioning ionospheric-free combinations were formed, in order to eliminate ionospheric delays, and tropospheric delays were modeled. These first results with real data lead to meter-level errors with code positioning, decimeter-level errors for code and phase combination positioning and centimeter-level errors for carrier phase positioning. It is important to highlight the fact that GIOVE-A and GIOVE-B were not fully operational satellites. Also, the limited number of satellites did not give redundancy and the geometry conditions were not ideal (see section 4.2.2).

In 2013, [Springer et al., 2013] presented a paper at the AGU meeting of San Fransisco concerning the observation precision (in terms of least squares residuals) associated with each signal of each constellation. Figures 2.7 and 2.8 illustrate his results.

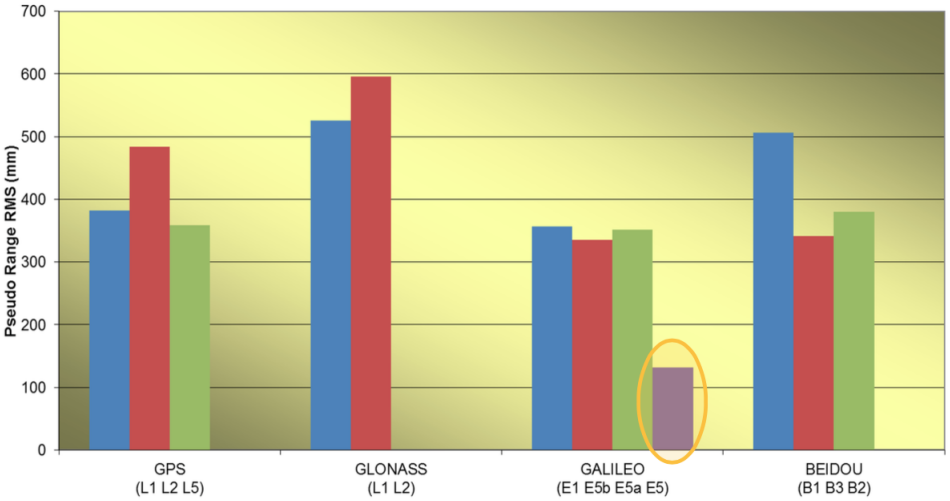

Figure 2.7: Code pseudorange precision. Source: [Springer et al., 2013]

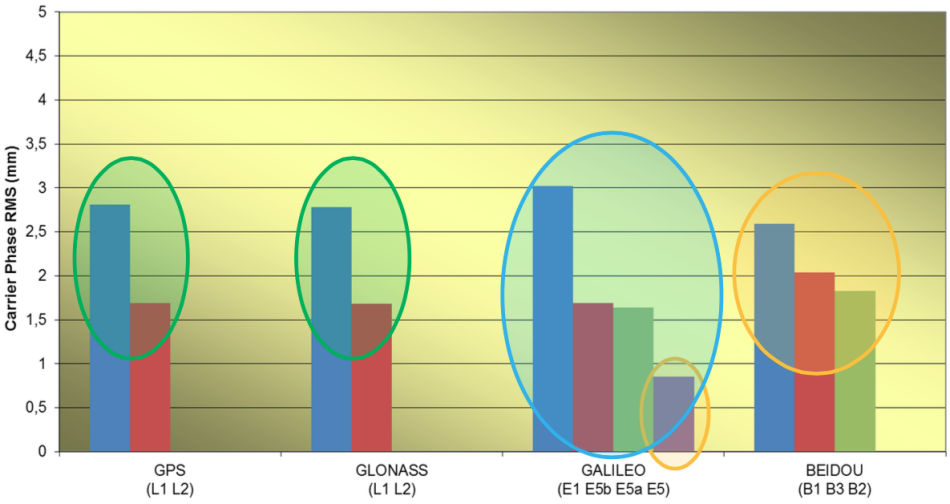

Figure 2.8: Carrier phase precision. Source: [Springer et al., 2013]

These values (Fig. 2.7 and Fig. 2.8) will serve as a reference in the next chapters of this dissertation.

[Steigneberger et al., 2013] found completely different results with regards to carrier measurements. Instead of E5 AltBOC showing great performance, a kinematic-style[7] experiment in relative positioning comparing each Galileo and GPS phase carrier signals from the four IOV satellites led to the following results : the E1 signal clearly out-performs all the Galileo signals, followed by E5a and E5b and then only E5 AltBOC. Compared with a GPS constellation reduced to four satellites, GPS L1 carrier seems to be even better than Galileo E1 signal in kinematic-style po-

[7]The baseline is not constrained to be unchanging and relative-position solution is computed for each epoch of measurement.

sitioning. Concerning code pseudorange positioning, the authors estimated a position with a 3D position error of less than 1.5 meters using an ionospheric-free single point positioning combination based on E1 and E5a frequencies.

In February 2014, [ESA, 2014] declared reaching a positioning accuracy of 8 meters horizontal and 9 meters vertical with a dual-frequency combination (E1-E5a) using only the four available IOV satellites 95 percent of the time.

In 2014, while the first Galileo real data positioning measurements started to be available, [Caelen, 2014] at the Université de Liège assessed the quality of the new GPS and Galileo code pseudorange signals. He based his research on [Tiberius et al., 2009] and [de Bakker et al., 2009]'s methods (which had only been tested mainly using GIOVE-A and GIOVE-B satellite data to evaluate Galileo E1 and E5a and GPS L1 and L5) including two different combinations: a multipath combination and a geometric-free combination. The former one highlights multipath influence while the second shows observation noise effects. In terms of observation noise, his results can be summarized as follows:

- GPS L5 is not clearly less noisy than GPS L1
- GPS L5 and Galileo E5a performances vary a lot due to the fact that their observation noise is less dependent on their C/N_0 ratio
- Galileo E1 and E5a show better results than GPS L1 and L5
- Galileo E5 presents very low observation noise

In the context of this dissertation, the last point is by far the most interesting.[Caelen, 2014] gives orders of magnitude to assess these observations on Galileo E5 AltBOC that can be summarized by saying that AltBOC shows an observation noise from two to ten times lower than GPS L1. The following figure (Fig. 2.9) compares the observation noise of Galileo E5 (C8Q) and Galileo E1 (C1C) measured at the Brussels receiver in 2014:

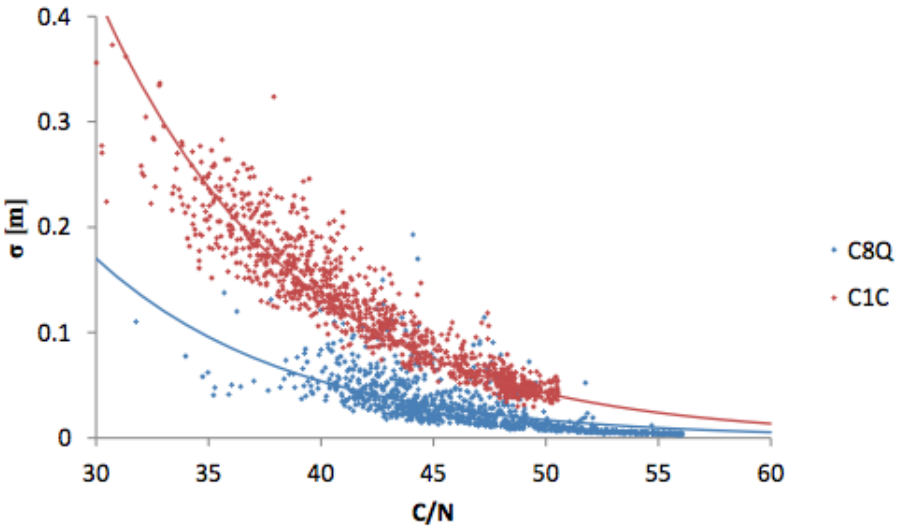

Figure 2.9: Galileo E1 (C1C) vs Galileo E5 (C8Q). Source: [Caelen, 2014]

Galileo E5 AltBOC clearly shows low noise amplitude and less dispersion than Galileo E1. The measure is given in terms of σ which represents the standard deviation of the observations.

Concerning the multipath analysis, [Caelen, 2014]'s results are:

- GPS L5 does not show patent improvements when compared with GPS L1
- Galileo E5 is less affected by multipath than Galileo E1 and Galileo E5a
- Galileo E5a often performs worse than Galileo E1

Moreover, [Caelen, 2014] shows that the maximum multipath variations observed on Galileo E5 AltBOC do not exceed 0.5 meters (which corresponds to GPS L5 usual observation noise). In comparison, GPS L5 and Galileo E5a present maximum multipath variations of the order of 2 meters.

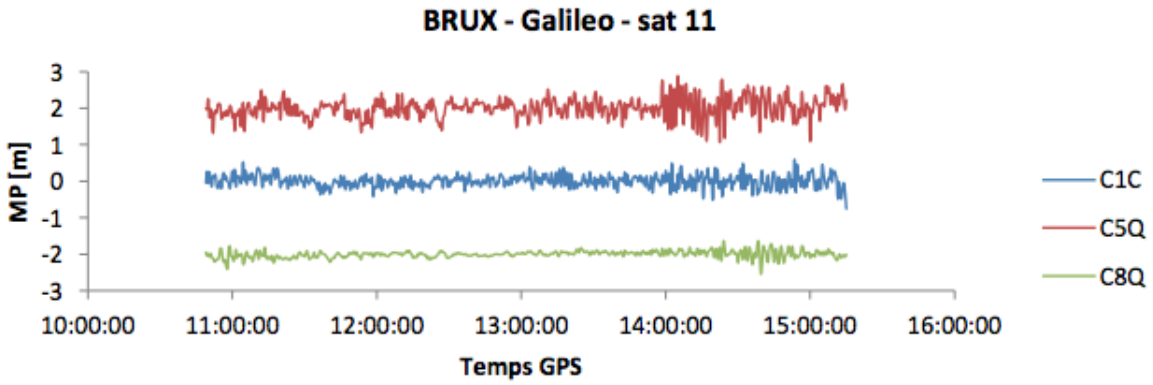

Figure 2.10: Example of multipath on Galileo E1 (C1C), Galileo E5a (C5Q) and Galileo E5 (C8Q). Source: [Caelen, 2014]

Fig. 2.10 illustrates the effect of the multipath on the different code pseudoranges of Galileo. The results have been obtained for the same Brussels receiver as in Fig. 2.9. Moreover, an observation of the multipath variance leads to the conclusion that Galileo E5 AltBOC, in addition to showing low multipath noise, presents a non-dispersive shape multipath measurements. Fig. 2.11 exemplifies this observation on the Brussels station:

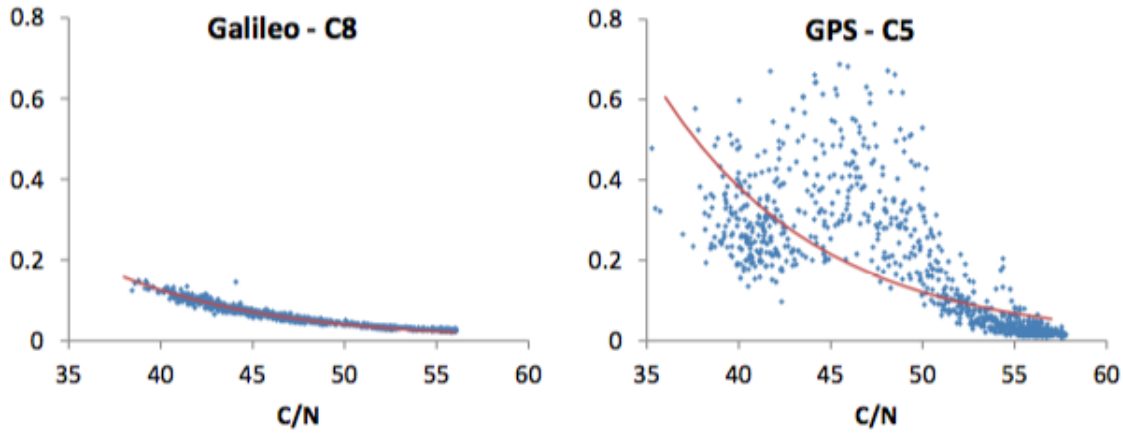

Figure 2.11: Multipath variance comparison for Galileo E5 (C8) and GPS L5 (C5) in function of C/N_0 values. Source: [Caelen, 2014]

From Fig. 2.10 and Fig. 2.11 one can conclude that Galileo E5 AltBOC shows exceptional multipath resistance.

A last point is worth mentioning: the maximum values obtained in [Caelen, 2014] experiments. Maximum multipath values of ± 1.5 m or ±2.5 m were regularly observed on GPS L1 and L5 respectively, whereas these maximum values only reach ±1.5 m on Galileo E1 and Galileo E5a and ±0.5 m on Galileo E5 AltBOC. Maximum observation noise values reached 1 m for all GPS and Galileo code pseudoranges, except Galileo E5 AltBOC whose maximum noise generally fluctuates around 0.3 m.

A recent study conducted by [Gioia et al., 2015] showed real data results for simple single point positioning on both Galieo E1 and E5a signals. Using the four IOV satellites, a first comparison of code pseudorange errors on each of these satellites revealed that satellite precisions are similar. Then, a comparison with GPS positioning reduced to a smaller constellation (in such a way that the geometry influence on Galileo and GPS is equivalent) assessed Galileo E1 superiority over GPS L1. But, it also assessed Galileo E1 superiority over Galileo E5a which was theoretically unexpected (those unexpected results had already been observed by [Simsky et al., 2008a]) . In addition, a combination of Galileo and GPS is tested which proves that a slight improvement can be obtained when Galileo measurements are considered with the from GPS.

Very recently, [Steigneberger & Hauschild, 2015] used the first new FOC constellation satellite that had started to emit in November 2014: E18 (see section 1.1.3). He first analyzed the power of each signal broadcast by these satellites and concluded that E5 was the best transmitted signal, with a very high C/N_0 ratio. As E20, from the IOV constellation has stopped broadcasting E5 signals since May 2014, and today only transmits E1 signal, this E18 satellite completes the constellation of three remaining IOV satellites and allows again new position estimations. The results of a Galileo-only positioning with the four aforementioned satellites using an ionospheric-free combination on E1 and E5 code pseudoranges led to worse results than before, with 3.41 meters of precision on a position (to be compared with [Steigneberger et al., 2013] values). This could be due to the effect of bad geometry and a reduced number of available satellites. Yet, Galileo+GPS combination revealed improved positioning performances in comparison with GPS-only measurements.

2.4 Conclusion

Theoretical considerations expect Galileo E5 AltBOC to outperform present standards in terms of code pseudorange observation precision. Its signal has been designed to be able to mitigate multipath and being more resistant to observation noise.

As concerns the simulated data, a few centimeters level **observation precision** should be expected with Galileo E5 AltBOC when the full Galileo constellation will be available ([Colomina et al., 2012], [Silva et al., 2012], [Lopes et al., 2012]). As regards the **position precision**, the code-plus-carrier combination of [Diessongo et al., 2012], [Diessongo et al., 2014] and [Junker et al., 2011] should allow centimeter precision with new Galileo signals.

When real data are considered, **position precision** on code pseudoranges with Galileo E5 AltBOC seems to be closer to the meter level ([ESA, 2014], [Langley et al., 2012] and [Steigneberger & Hauschild, 2015]). It must be taken into account that as only four satellites were used to compute those results, there was no redundant information. Furthermore, such a configuration leads to high values of geometric dilution of precision (PDOP, see section 4.2.2), which has an important impact on position precision. Therefore, one can conclude that real data

positioning leads to low precision positioning due to bad constellation geometry and the very few number of available satellites (maximum four). However, Galileo E5 AltBOC seems to outperform other Galileo signals in terms of precision, multipath mitigation and noise reduction.

The **observation precision** estimated by [Springer et al., 2013] on real data reached decimeter level on code pseudoranges and millimeter level on phase pseudoranges.

As far as multipath mitigation and observation noise reduction are considered, real data seems to be in accordance with the theoretical expectation. The mitigation of multipath, much more important on Galileo E5 than on other Galileo signals, is demonstrated by [Caelen, 2014]. Similarly, he showed that Galileo E5 was less sensitive to observation noise than other GPS and Galileo signals.

Furthermore, GPS+Galileo positioning seems to improve positioning when compared to GPS-only positioning ([Gioia et al., 2015]).

Chapter 3

Hypothesis and methods

This chapter presents the hypothesis and the research question that set the basis of this dissertation. Then, the methods employed will be briefly discussed and remaining chapters outlined.

3.1 Hypothesis

In chapter 2, the added value of the new Galileo E5 AltBOC signal has been outlined. A first analysis of the signal in itself followed by a discussion about the first results obtained by Galileo's new signals lead to the conclusion that Galileo E5 AltBOC should open very interesting possibilities in term of positioning accuracy. Its very wide bandwidth seems to confer a powerful multipath mitigation capacity associated with a lower observation noise. These characteristics do not seem to appear on all the other Galileo signals, and even not on the new GPS L5 signal.

Therefore, in this dissertation, the assumption is made that positioning with Galileo E5 signal could result in better precision levels than with other GPS and Galileo signals.

3.2 Constraints

The first chapter of this dissertation has demonstrated the difficulty of obtaining precise results with code-only pseudorange measurements due to their high observation noise (position precision of meter level). The conclusion of chapter 1 was that precise positioning (centimeter level on position precision) could only be reached with the phase pseudorange measurements. However, phase positioning requires initial ambiguity resolution, which is a tricky problem that may be even more complicated by the occurrence of cycle slip. Many GNSS users do not possess initial ambiguity resolution algorithms or even receivers able to deal with these observables.

Therefore, in order to make the solution proposed by this dissertation available for general public, only a code-based solution is considered. This constraint will reduce the position precision compared with one that could be reached with the carrier phase. However, as code pseudoranges are non ambiguous, no ambiguity resolution will be required.

Furthermore, the issue of the material used has been barely mentioned in chapter 1 and 2 but its interest is non negligible. As far as code-only positioning is concerned, many solutions propose the use of dual-frequency or even triple-frequency combinations to reach a decimeter-precision level on position. To handle dual or triple-frequency combinations, expensive receivers that are able to handle more than one frequency at the same time, are required.

The solution proposed in this dissertation is meant to be accessible for everyone, even with the more basic GNSS receiver. For this purpose, a new constraint is defined. The code-only solution will be based on single-frequency combinations only. Even if no single-frequency receiver able

to track the Galileo E5 currently only is available on the market, the performance of Galileo E5 could lead to one as positioning results are supposed to be improved by the signal.

3.3 Research question

For many GNSS applications, phase precision of centimeter level on position determination is not needed but meter level of code pseudoranges is not enough. On the basis of the hypothesis made, the code-only solution based on single-frequency combination proposed in this dissertation could lead to decimeter precision instead of meter precision on the estimated position. Indeed, interesting properties of Galileo E5 on code pseudoranges could improve the code-based positioning to a decimeter level. This performance could be achieved with basic GNSS receivers that receive the Galileo E5 signal.

Therefore, the research question arising from the hypothesis and constraints is the following:

"*Could Galileo E5 AltBOC single-frequency code-only measurements be used to bring a decimeter-level accuracy on satellite-based position estimations?*"

3.4 Methods

For the purpose of this dissertation's research question, no particular methods from any previously mentioned authors was followed. The approach considered could therefore be qualified as exploratory. In order to reach the intended goal of decimeter positioning with code-only Galileo E5 single-frequency solution, the existing solutions have been examined considering those criteria. Among them, one stood out, the double difference combination in relative positioning.

In order to achieve decimeter satellite-based positioning using a single-frequency receiver, the single point positioning method was eliminated. Discussed in the chapter 4, this positioning method is considerably affected by errors mentioned in chapter 1 and will therefore not be exploited in the chapter of results (chapter 6). It could never reach the expected precision.

Therefore, the use of single and double difference combinations were envisaged. The single difference, which is used to calculate the double difference, was considered as too imprecise for intended precision achievements.

The double difference combination was considered to be perfectly adapted for the purpose of this dissertation. This combination, detailed in the next chapter, is the basic observable used in on relative positioning. It consists in measurement differences between two receivers. Those differences, first between two receivers and then between two satellites allow removing both satellite-based and receiver-based errors (see section 1.4).

Furthermore, in a particular configuration called *zero baseline*, the atmospheric and multipath biases can be completely eliminated or at least, partially reduced from the double difference combination. With this configuration, the decimeter precisions should be reached. But this configuration is not used in practice. Its main interest is to test the observation precisions that can be reached with the present Galileo constellation. On this basis, longer baseline could be envisaged and studied.

Nevertheless, two other configurations were tested: the *short and medium baselines*. These configurations do not eliminate the atmospheric and multipath errors as zero baseline does. However, the Galileo E5 signal with code-only single-frequency decimeter precision on this configuration could also be reached. This would only depend on distances between receivers and the importance of atmospheric errors, as explained in the next chapter.

3.5 Plan

In order to answer the research question, the following chapters of this dissertation are:

First (Chapter 4), the theoretical principles of the aforementioned combinations will be described and the mathematical reasoning used to answer the research question will be detailed. The parameters used to describe the precision of the measurements will be explained.

Second (Chapter 5), the experimental conditions of the measurements will be handled. The equipment used, the stations characteristics and the data format will be fully described.

Then (Chapter 6), the results of this research, accordingly to the methods proposed in chapter 4, will be exposed.

Finally (Chapter 7), a conclusion integrating all the above-mentioned chapters will allow the reader to summarize the results and compare them to the results obtained by the authors mentioned in chapter 2.

Chapter 4

Theoretical principles

4.1 Introduction

This chapter highlights the theoretical approach used as the basis of the methods employed in this dissertation. The resolution principles from the MATLAB program that served for single point positioning and double difference computations will also be described. Finally, the precision estimations will be discussed. They will be used as references for future analysis (see chapter 6).

4.2 Absolute positioning

As previously mentioned in chapter 2, many satellite-based positioning techniques are available. The following criteria differentiate them:

- the chosen observable (code or phase pseudorange),
- the instantaneity or not of the positioning (real time or post-processing),
- the number of receivers used to determine a position (absolute positioning versus relative positioning)
- the static or kinematic character of the measurements.

This section explains the principle of the absolute positioning resolution using the least squares method. This **absolute** positioning is based on **code** pseudorange measurements, on a **static** receiver in **real-time** processing. Its formula was given in the first chapter (see section 1.3.3).

4.2.1 Least squares adjustment

A position on earth can be satellite-based located if at least four satellites are available to resolve the four unknowns (X_r, Y_r, Z_r, and δt_r), as previously seen in 1.3.1. When more than four satellites are available, the additional observations are also to be taken into account in the position estimation. This would ensure a more accurate estimation of the unknown values. In order to do so, a calculation technique, namely the *Least Squares Adjustment* (LSA) is suggested.

Given an undetermined system, the least squares adjustment principle relies on the following assessment: "*The most probable value of an unknown is the value that minimizes the weighted sum of the residual squares*":

$$\nu^T P \nu = minimum \tag{4.1}$$

where ν is the vector of residuals and P the weight matrix. The weight matrix allows a consideration of the observation of different qualities within the same least square adjustment. In the single point positioning calculation, the weight matrix will be a unit matrix as one usually considers that every observation has the same precision level. By contrast, a weight matrix will be computed in

the double difference position estimation due to the correlations existing in the double difference. This specification will be discussed in section 4.5.5.

The least squares adjustment fundamentally depends on two models: a mathematical one and a stochastic one. The mathematical one is described in the following section. It is based on the equation (1.10) and serves as a link between the observations and the unknowns. The stochastic one will be detailed in section 4.2.1.

Mathematical model

The code pseudorange equation model is given in equation 4.2. The mathematical model is a simplified view of reality. In this model, one only keeps the parameters which have an influence on the future discussion.

$$P^s_{r,k}(t) = D^s_r + T^s_r + I^s_{r,k} + M^s_{r,k,m} + c.(\delta t^s(t^s_{ref}) - \delta t_r(t_{r,ref})) + d_{r,k,m} + d^s_{k,m} + \epsilon^s_{r,k,m} \tag{4.2}$$

In this equation, the four unknowns of absolute positioning are the clock error of the receiver (δt_r), which can not be corrected, and the three receiver position parameters (X_r, Y_r, Z_r). Some assumptions are made in order to solve the system.

- the ionospheric and tropospheric delays ($I^s_{r,k}$ and T^s_r) are estimated using corrective models (Klobuchar and Staastamonien, respectively, see sections 1.4.2 and 1.4.1).
- the multipath effect ($M^s_{r,k,m}$), satellite and receiver hardware delays ($d_{r,k,m}$ and $d^s_{k,m}$) and also the observation noise ($\epsilon^s_{r,k,m}$) are supposed to be negligible and are neglected in the mathematical model
- the ephemerides sent by the satellite are used to estimate satellite clock error ($\delta t^s(t^s_{ref})$).

In this way, the code pseudorange equation becomes:

$$P^s_{r,k}(t) = D^s_r + T^s_{r,mod} + I^s_{r,k,mod} + c.(\delta t^s(t^s_{ref,mod}) - \delta t_r(t_{r,ref})) \tag{4.3}$$

where $T^s_{r,mod}$, $I^s_{r,k,mod}$ and $\delta t^s(t^s_{ref,mod})$ are the modeled tropospheric, ionospheric and satellite clock errors.

One of the unknowns clearly appears in the equation, the receiver clock error $\delta t_r(t_{r,ref})$, but the remaining three are contained in the geometric range term (D^s_r):

$$D^s_r = \sqrt{(X^s - X_r)^2 + (Y^s - Y_r)^2 + (Z^s - Z_r)^2} \tag{4.4}$$

Therefore, one can write:

$$D^s_r = f(X_r, Y_r, Z_r) \tag{4.5}$$

As the equation 4.4 is a non-linear formula, one needs to linearize it in order to be able to estimate the positioning unknowns using the least squares adjustment. To do so, the Taylor linearization theorem is applied on the basis of *a priori* values of the unknowns ($X_{r,0}$, $Y_{r,0}$ and $Z_{r,0}$):

$$\begin{aligned} X_r &= X_{r,0} + \Delta X_r \\ Y_r &= Y_{r,0} + \Delta Y_r \\ Z_r &= Z_{r,0} + \Delta Z_r \end{aligned} \tag{4.6}$$

This leads to rewrite an *a priori* 4.4:

$$\begin{aligned} D^s_{r,0} &= \sqrt{(X^s - X_{r,0})^2 + (Y^s - Y_{r,0})^2 + (Z^s - Z_{r,0})^2} \\ &= f(X_{r,0}, Y_{r,0}, Z_{r,0}) \end{aligned} \tag{4.7}$$

And the Taylor theorem (approximated to its first order) gives:

$$\begin{aligned} f(X_r, Y_r, Z_r) = f(X_{r,0}, Y_{r,0}, Z_{r,0}) - \frac{\partial f(X_{r,0}, Y_{r,0}, Z_{r,0})}{\partial X_{r,0}}.\Delta X_r - \frac{\partial f(X_{r,0}, Y_{r,0}, Z_{r,0})}{\partial Y_{r,0}}.\Delta Y_r - \\ \frac{\partial f(X_{r,0}, Y_{r,0}, Z_{r,0})}{\partial Z_{r,0}}.\Delta Z_r \end{aligned} \tag{4.8}$$

And then:

$$D^s_r = D^s_{r,0} - \frac{(X^s - X_{r,0})}{D^s_{r,0}}.\Delta X_r - \frac{(Y^s - Y_{r,0})}{D^s_{r,0}}.\Delta Y_r - \frac{(Z^s - Z_{r,0})}{D^s_{r,0}}.\Delta Z_r \tag{4.9}$$

To simplify, the following variables will be used in the next equations:

$$\begin{aligned} d^s &= -\frac{(X^s - X_{r,0})}{D^s_{r,0}} \\ e^s &= -\frac{(Y^s - Y_{r,0})}{D^s_{r,0}} \\ f^s &= -\frac{(Z^s - Z_{r,0})}{D^s_{r,0}} \end{aligned} \tag{4.10}$$

Therefore, the code pseudorange equation becomes:

$$P^s_{r,k}(t) = D^s_{r,0} + d^s.\Delta X_r + e^s.\Delta Y_r + f^s.\Delta Z_r + T^s_{r,mod} + I^s_{r,k,mod} + c.(\delta t^s(t^s_{ref,mod}) - \delta t_r(t_{r,ref})) \tag{4.11}$$

If one groups together all the *a priori* and modeled terms in one parameter $P^s_{r,k,0}(t)$:

$$P^s_{r,k,0}(t) = D^s_{r,0} + T^s_{r,mod} + I^s_{r,k,mod} + c.\delta t^s(t^s_{ref,mod}) \tag{4.12}$$

Then the equation (4.11) becomes:

$$P^s_{r,k}(t) - P^s_{r,k,0}(t) = d^s.\Delta X_r + e^s.\Delta Y_r + f^s.\Delta Z_r - c.(\delta t_r(t_{r,ref})) \tag{4.13}$$

As stated in chapter 1, four unknowns need to be solved in order to determine a position. This implies having at least four observation equations to resolve these four unknowns and thus, having four satellites visible from the receiver.

The minimum number of four observation equations required for positioning are therefore given by:

$$\begin{aligned} P^1_{r,k}(t) - P^1_{r,k,0}(t) &= d^1.\Delta X_r + e^1.\Delta Y_r + f^1.\Delta Z_r - c.(\delta t_r(t_{r,ref})) \\ P^2_{r,k}(t) - P^2_{r,k,0}(t) &= d^2.\Delta X_r + e^2.\Delta Y_r + f^2.\Delta Z_r - c.(\delta t_r(t_{r,ref})) \\ P^3_{r,k}(t) - P^3_{r,k,0}(t) &= d^3.\Delta X_r + e^3.\Delta Y_r + f^3.\Delta Z_r - c.(\delta t_r(t_{r,ref})) \\ P^4_{r,k}(t) - P^4_{r,k,0}(t) &= d^4.\Delta X_r + e^4.\Delta Y_r + f^4.\Delta Z_r - c.(\delta t_r(t_{r,ref})) \end{aligned} \tag{4.14}$$

According to the previous equations:

$$P^s_{r,k}(t) - P^s_{r,k,0}(t) - (d^s.\Delta X_r + e^s.\Delta Y_r + f^s.\Delta Z_r - c.(\delta t_r(t_{r,ref}))) = 0 \tag{4.15}$$

Yet, since assumptions were made at the beginning of this chapter, (4.15) is never true in practice. A residual is always found due to the model's imperfections, the observation noise neglected, etc. Therefore, a residual vector $\underline{\nu}$ must be considered as well. This vector only regroups the stochastic errors, not the systematic ones. This is the reason why a first modeling of the systematic errors has been done at the beginning of this section. The least squares process tends to minimize such residual terms. The mathematical model corresponding to such a relation between the unknowns and the observations is given by:

$$\underline{W} - \underline{\nu} + A.\underline{x} = 0 \tag{4.16}$$

where $\underline{W}$ is the vector containing the observations, $\underline{\nu}$ is the vector of residuals, A is the matrix containing the partial derivatives resulting from the Taylor linearization and $\underline{x}$ is the vector of unknowns.

$$A = \begin{pmatrix} d^1 & e^1 & f^1 & -c \\ d^2 & e^2 & f^2 & -c \\ d^3 & e^3 & f^3 & -c \\ d^4 & e^4 & f^4 & -c \end{pmatrix} \quad \underline{x} = \begin{pmatrix} \Delta X_r \\ \Delta Y_r \\ \Delta Z_r \\ \delta t_r(t_{r,ref}) \end{pmatrix} \quad \underline{\nu} = \begin{pmatrix} \nu_1 \\ \nu_2 \\ \nu_3 \\ \nu_4 \end{pmatrix} \quad \underline{W} = \begin{pmatrix} P^1_{r,k}(t) - P^1_{r,k,0}(t) \\ P^2_{r,k}(t) - P^2_{r,k,0}(t) \\ P^3_{r,k}(t) - P^3_{r,k,0}(t) \\ P^4_{r,k}(t) - P^4_{r,k,0}(t) \end{pmatrix}$$

This model is known as the *observation equation model*. In such a model, the number of unknowns is u, the number of observations is n and is equal to the number of equations of observations. Therefore, the matrix has the following dimensions: A $(n \times u)$, $\underline{x}$ $(u \times 1)$, $\underline{\nu}$ $(n \times 1)$ and $\underline{W}$ $(n \times 1)$.

Stochastic model

As the satellite-based positioning techniques use indirect observations to determine a position, propagation of error is required in order to estimate the effect of observation errors on the parameters to be determined. In case of independent and non-linear[1] variables, the variance-covariance matrix of the unknowns Σ_y is obtained thanks to the following formula:

$$\Sigma_y = J.\Sigma x.J^T \tag{4.17}$$

where Σ_x is the variance matrix of the observations and J, the *Jacobian*, is the matrix of the first order partial derivative terms.

For a number n of observations and a number u of unknowns, the dimensions of those matrices are: $(n \times n)$ for Σx, $(u \times n)$ for J and $(u \times u)$ for Σy. And thus, this equation can be written as:

$$\Sigma_y = \begin{pmatrix} \sigma_1^2 & \cdots & \sigma_1.\sigma_u \\ \vdots & \ddots & \vdots \\ \sigma_u.\sigma_1 & \cdots & \sigma_u^2 \end{pmatrix} = \begin{pmatrix} \frac{\delta f_1}{\delta y_1} & \cdots & \frac{\delta f_1}{\delta x_n} \\ \vdots & \ddots & \vdots \\ \frac{\delta f_u}{\delta x_1} & \cdots & \frac{\delta f_u}{\delta x_n} \end{pmatrix} . \begin{pmatrix} \sigma^2_{x_1} & \cdots & 0 \\ \vdots & \ddots & \vdots \\ 0 & \cdots & \sigma^2_{x_n} \end{pmatrix} . \begin{pmatrix} \frac{\delta f_1}{\delta x_1} & \cdots & \frac{\delta f_u}{\delta x_1} \\ \vdots & \ddots & \vdots \\ \frac{\delta f_1}{\delta x_n} & \cdots & \frac{\delta f_u}{\delta x_n} \end{pmatrix} \tag{4.18}$$

with σ^2 the variance terms, $\sigma.\sigma$ the covariance terms and $\dfrac{\delta f_u}{\delta x_n}$ the partial derivatives terms.

[1] (the distance, which comprises three of the four unknowns, is a non-linear term)

4.2.2 Dilution of precision

The precision of the positioning is not only linked to the observation precision, it also depends on the constellation geometry. The *Dilution Of Precision* (DOP) is a parameter that characterizes the impact of the constellation geometry on the positioning. The relation between those three parameters is given by:

$$\sigma_{pos} = DOP.\sigma_{obs} \tag{4.19}$$

where σ_{pos} is the precision of the positioning and σ_{obs} the precision of the observations.

This parameter does not directly affect the signal, and therefore it can not be found in the code and carrier phase equations aforementioned (1.3.3 and 1.3.4). Still, its influence is crucial, particularly when only a reduced number of satellites are simultaneously observed in the constellation, as it is the case for Galileo.

This parameter can be estimated by the cofactor matrix $Q_{\underline{\hat{x}}}$ diagonal terms in the absolute positioning case:

$$\begin{pmatrix} q_{XX} & q_{XY} & q_{XZ} & q_{Xt} \\ q_{YX} & q_{YY} & q_{YZ} & q_{Yt} \\ q_{ZX} & q_{ZY} & q_{ZZ} & q_{Zt} \\ q_{tX} & q_{tY} & q_{tZ} & q_{tt} \end{pmatrix} \tag{4.20}$$

Three parameters can be determined on the basis of this matrix : the GDOP (*Geometric Dilution of Precision*), the PDOP (*Position Dilution of Precision*) and the TDOP (*Time Dilution of Precision*).

$$\begin{aligned} GDOP &= \sqrt{q_{XX} + q_{YY} + q_{ZZ} + q_{tt}} \\ PDOP &= \sqrt{q_{XX} + q_{YY} + q_{ZZ}} \\ TDOP &= \sqrt{q_{tt}} \end{aligned} \tag{4.21}$$

In addition to those parameters, vertical and horizontal values of the DOP can also be estimated (VDOP and HDOP, respectively).

4.3 Relative positioning

In the previous section, absolute positioning was mentioned and particularly, single point positioning. This section discusses the relative positioning case. This kind of positioning consists in making use of more than one receiver to determine a position. For instance, two receivers could be used and their measures combined in order to mitigate common error sources. The difference with absolute positioning is that measurements are directly combined in the treatment. This technique is based on the double difference, itself the basis of the main analysis of this dissertation.

The double difference studied in this dissertation is, according to the criteria for differentiating elements of positioning techniques given in section 4.2, a **relative** positioning technique including **code** measurements on **static** receivers in **real-time** processing.

In relative positioning, amongst the two receiver positions considered, one must be known. The second one is to be determined by the positioning. Therefore, relative positioning can be seen as a baseline vector $\underline{b_{AB}}$ estimation between a known position $\underline{X_A}$ and an unknown position $\underline{X_B}$ [Hofmann-Wellenhof et al., 2008] (see equation (4.22)).

$$\underline{X_B} = \underline{X_A} + \underline{b_{AB}} \tag{4.22}$$

4.4 Combinations

The main goal of this thesis is to assess Galileo E5 AltBOC signal added-value over other GPS and Galileo signals. To assess this superiority, combinations of observations will be formed. In fact, combinations may reduce the influence of factors such as atmospheric biases, satellite-based errors or receiver-based errors. As seen in chapter 1, these biases degrade what can be called the *observation precision*. The observation precision is the precision that can be expected independently from the DOP values or number and elevation of satellites included in the calculations. By contrast, this parameter suffers from receiver-based and satellite-based biases, as well as atmospheric interferences which are varying parameters, mainly linked to the receiver position.

Many combinations exist but some require two frequencies. The outcomes of such dual-frequency combinations depend on two signals. In this dissertation, where only Galileo E5 signal accuracy is investigated, employing such dual-frequency combinations would have complicated comparisons between signals. Besides, receivers able to realize such combinations are more expensive than single-frequency ones. The solution that this dissertation aims to provide is an actionable solution, both in terms of implementation and price.

Furthermore, amongst possible combinations using single-frequency, some use both phase and code pseudoranges. This implies being able to solve the initial ambiguity integer. The equations leading to such a resolution were not considered within the context of this dissertation as requiring powerful algorithms, and therefore not available for every GNSS user.

Finally, combinations between Galileo and GPS signals could also have been considered since both systems are compatible but this would have led to dual-frequency combinations. Moreover, the ability of Galileo to compete with GPS will be discussed in this dissertation. Therefore, combining both systems would not be appropriate for the purpose of this dissertation.

On the basis of previous assessments, two combinations were considered and are outlined in the paragraphs below. The first one, the *single difference*, must necessarily be explained in order to define the second combination called *double difference*. Apart from that purpose, this former combination will not be mentioned further as results it would provide will not be able to compete with those expected with the double difference.

4.4.1 Single difference

The single difference combination consists in subtracting two simultaneous observations from two different receivers $(1, 2)$ looking at the same satellite (i). Code pseudoranges single differences are first considered.

The equation of the code pseudorange measured from the first receiver (1) looking at the satellite (i) (see section 1.3.3) at an epoch of time t is:

$$P^i_{1,k}(t) = D^i_1 + T^i_1 + I^i_{1,k} + M^i_{1,k,m} + c.(\delta t^i(t^i_{ref}) - \delta t_1(t_{1,ref})) + d_{1,k,m} + d^i_{k,m} + \epsilon^i_{1,k,m} \quad (4.23)$$

The equation of the code pseudorange measured from the second receiver (2) looking at the same satellite (i) (see section 1.3.3) at an epoch of time t is:

$$P^i_{2,k}(t) = D^i_2 + T^i_2 + I^i_{2,k} + M^i_{2,k,m} + c.(\delta t^i(t^i_{ref}) - \delta t_2(t_{2,ref})) + d_{2,k,m} + d^i_{k,m} + \epsilon^i_{2,k,m} \quad (4.24)$$

The single difference of those code observations $P^i_{12,k}(t)$ is given by:

$$P^i_{12,k}(t) = P^i_{1,k}(t) - P^i_{2,k}(t)$$

$$= (D^i_1 - D^i_2) + (T^i_1 - T^i_2) + (I^i_{1,k} - I^i_{2,k}) + (M^i_{1,k,m} - M^i_{2,k,m}) + [c.(\delta t^i(t^i_{ref}) - \delta t_1(t_{1,ref}))- c.(\delta t^i(t^i_{ref}) - \delta t_2(t_{2,ref}))] + (d_{1,k,m} + d^i_{k,m} - d_{2,k,m} - d^i_{k,m}) + (\epsilon^i_{1,k,m} - \epsilon^i_{2,k,m})$$

$$= D^i_{12} + T^i_{12} + I^i_{12,k} + M^i_{12,k,m} + c(\delta t_2(t_{2,ref}) - \delta t_1(t_{1,ref})) + d_{12,k,m} + \epsilon^i_{12,k,m} \tag{4.25}$$

with the indexes $*^i_{12}$ representing the single difference terms.

One may notice that, in this last equation, the clock error from the satellite is eliminated. It only happens when observations are perfectly simultaneous between the two receivers. Moreover, the tropospheric delay (T^i_*) and the ionospheric delay ($I^i_{*,k}$), both correlated with distance, see their common part erased thanks to this difference. By contrast, the multipath $M^i_{*,k,m}$ effect is not reduced as it is purely dependent on the location of the receiver antenna of the receiver. Therefore, both multipath effects are combined. One also observes that the hardware delays relative to the satellite are eliminated.

As previously mentioned (see section 1.4), satellite-based biases are eliminated by using a combination of observations from two different receivers on the same satellite. This is the principle of the single difference combination.

Similarly, in order to remove receiver-based biases, a combination of observations from the same receiver on two satellites should be used. The double difference discussed in the next section is based on this last principle.

4.4.2 Double difference

In a double difference, two receivers $(1, 2)$ simultaneously observe two satellites (i, j) (see Fig. 4.1). Single differences are first computed on each observed satellite and then the two single differences obtained are subtracted.

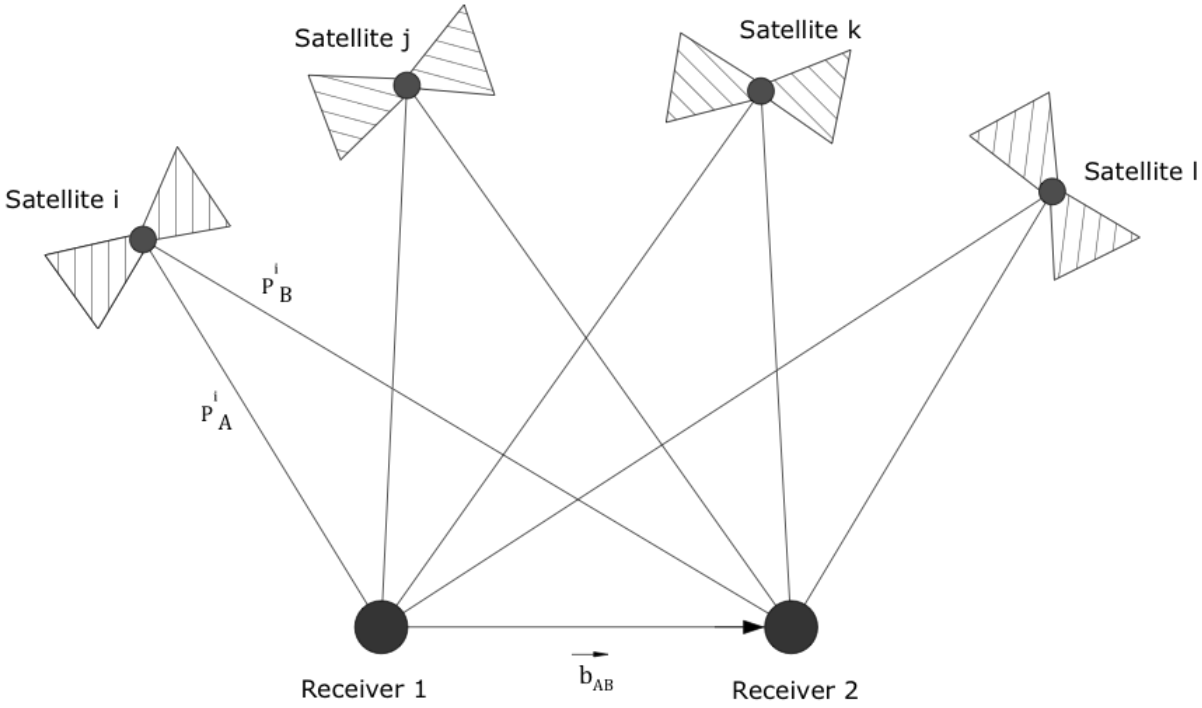

Figure 4.1: Double difference positioning principle

The code pseudorange single difference for two receivers and a satellite i at a time t is given by (see equation (4.25)):

$$P^i_{12,k}(t) = D^i_{12} + T^i_{12} + I^i_{12,k} + M^i_{12,k,m} + c(\delta t_2(t_{2,ref}) - \delta t_1(t_{1,ref})) + d_{12,k,m} + \epsilon^i_{12,k,m} \tag{4.26}$$

The code pseudorange single difference for the same receivers and a satellite j at a time t is given by (see equation (4.25)):

$$P^j_{12,k}(t) = D^j_{12} + T^j_{12} + I^j_{12,k} + M^j_{12,k,m} + c(\delta t_2(t_{2,ref}) - \delta t_1(t_{1,ref})) + d_{12,k,m} + \epsilon^j_{12,k,m} \tag{4.27}$$

The double difference equation is:

$$\begin{aligned} P^{ij}_{12,k}(t) &= P^i_{12,k}(t) - P^j_{12,k}(t) \\ &= (D^i_{12} - D^j_{12}) + (T^i_{12} - T^j_{12}) + (I^i_{12,k} - I^j_{12,k}) + (M^i_{12,k,m} - M^j_{12,k,m}) + \\ &[c(\delta t_2(t_{2,ref}) - \delta t_1(t_{1,ref})) - c(\delta t_2(t_{2,ref}) - \delta t_1(t_{1,ref}))] + [d_{12,k,m} - d_{12,k,m}] + (\epsilon^i_{12,k,m} - \epsilon^j_{12,k,m}) \\ &= D^{ij}_{12} + T^{ij}_{12} + I^{ij}_{12,k} + M^{ij}_{12,k,m} + \epsilon^{ij}_{12,k,m} \end{aligned} \tag{4.28}$$

As announced in the previous section, subtracting two observations of satellite on the same receivers eliminates the receiver-based biases. Thus, only the tropospheric delays, ionospheric delays, multipath and observation noise remain in the equation. The receiver clock error is suppressed by

the double difference, eliminating one of the positioning unknowns.

The following discussion will focus on different possible configurations. Their advantages and drawbacks will also be discussed as well as the expected contributions of the Galileo E5 AltBOC signal.

4.5 Configurations

In order to validate the hypothesis, several configurations have been considered on the double difference combination: the zero baseline, the short baseline and the medium baseline. These will be described and the theoretical possibilities in terms of precision that might be expected when using Galileo E5 AltBOC signal will be examined.

4.5.1 Short and medium baselines

The short baseline configuration happens when the two receivers used in the double difference computation are separated by a distance of a few meters to 10 kilometers [Tiberius et al., 2002]. One speaks of medium baseline configuration when the receivers are 10 kilometers to 100 kilometers apart, and of long baseline when distances are larger. In any case, these three configurations lead to the same conclusions.

With the short baselines, in the remaining terms of the code double difference equation (see equation (4.28)), the common part of the troposphere and ionosphere terms will cancel out. The multipath, depending on the receiver location, will not be mitigated. On the contrary, its effect on both receivers will be combined. The observation noise will also altered the signal.

In medium baseline configuration, the distances between receivers will play an important role as only the common part of double difference errors will be eliminated. Therefore, the effects of ionospheric and tropospheric residuals will be more important as the distance increases. Concerning multipath, its value will only depend on the receiver locations. Similarly to the short baseline case,the observation noise will also altered the signal. The noise inherent to the receiver is receiver dependent. Thus, the receivers used in such configurations are worth being mentioned as differences could exist among them.

The Galileo E5 signal, claimed by [Caelen, 2014] to present low observation noise as well as a remarkable ability to mitigate multipath should be noticeable even on such configurations. However, if ionospheric and tropospheric delays are larger than the E5 band noise, the advantage of using E5 will disappear.

4.5.2 Zero baseline

The zero baseline configuration implies that the satellite signal is observed by two receivers connected to the same antenna through a *splitter*. This device, designed to split the signal between the two receivers, was first assumed to introduce noise by [Caelen, 2014]. As it has to amplify the signal power before splitting it in two parts, this assumption had to be considered. But it turned out that this device was harmless as similar noise has been observed by [Caelen, 2014] on short and zero baseline configurations.

In this particular configuration, most errors are suppressed from the double difference. The ionospheric and tropospheric errors as well as multipath are eliminated from the equation (4.28). Indeed, multipath depends on the antenna location, which is the same for both receivers in this configuration. Furthermore, the part of the observation noise due to signal travel from the satellite to the splitter cancels out. Only the noise due to the 2 involved receivers will remain. As two

receivers are considered, the inherent noises are different and remain as the unique error source.

The observation precision expected in such a configuration will therefore be better than with the short baseline configuration. As regards the Galileo E5 influence, its reduced observation noise should lead to very precise values. But, as explained in chapter 2, four different demodulations of the signals are possible. Out of these four techniques, three of them will generate a loss of Galileo's abilities. The receivers used in the zero baseline configuration, and particularly their demodulation technique, will therefore have an influence on the observation precision result.

4.5.3 Least squares adjustment

The least squares method applied on relative positioning relies on the same principle as in absolute positioning: minimizing the weighted square of the residuals. In relative positioning, the position of one receiver is supposed to be known. If one calls this known receiver position 1, position 2, corresponding to the second receiver position, needs to be determined by the least squares method computation.

As in absolute positioning, four assumptions are considered:

- the receivers are sufficiently close to one another to allow errors elimination by the differencing. This hypothesis is not verified on long baselines.
- the tropospheric and ionospheric delays (T_{12}^{ij} and $I_{12,k}^{ij}$) are supposed to be eliminated by the double difference
- multipath values are very low for each receiver and the result of their differencing ($M_{12,k,m}^{ij}$) is negligible
- the observation noise ($\epsilon_{12,k,m}^{ij}$) is also negligible

The code double difference equation (4.28) is therefore given by:

$$P_{12,k}^{ij}(t) = D_{12}^{ij} \tag{4.29}$$

The unknowns of the code equation are gathered in the D_{12}^{ij} term (see equation (4.30)). There are only three of them as the receiver clock error has been removed by the double difference combination principle.

$$\begin{gathered} D_{12}^{ij} = D_1^i - D_1^j + D_2^j - D_2^i \\ \text{with } D_2^* = \sqrt{(X^* - X_2)^2 + (Y^* - Y_2)^2 + (Z^* - Z_2)^2} \end{gathered} \tag{4.30}$$

Those three unknowns are the components of the receiver B position (X_2, Y_2, Z_2). If *a priori* values can be estimated for these three components ($X_{2,0}$, $Y_{2,0}$, $Z_{2,0}$), a similar Taylor first order approximation as in absolute positioning can be calculated.

On this basis, the code double difference would become:

$$\begin{aligned} P_{12,k}^{ij}(t) = D_1^i - D_1^j + D_{2,0}^j - D_{2,0}^i + (\frac{(X^i - X_{2,0})}{D_{2,0}^i} - \frac{(X^j - X_{2,0})}{D_{2,0}^j})\Delta X_2 + \\ (\frac{(Y^i - Y_{2,0})}{D_{2,0}^i} - \frac{(Y^j - Y_{2,0})}{D_{2,0}^j})\Delta Y_2 + (\frac{(Z^i - Z_{2,0})}{D_{2,0}^i} - \frac{(Z^j - Z_{2,0})}{D_{2,0}^j})\Delta Z_2 \end{aligned} \tag{4.31}$$

To simplify the writing, the following variables are introduced:

$$\begin{aligned} d^{ij} &= \frac{(X^i - X_{2,0})}{D^i_{2,0}} - \frac{(X^j - X_{2,0})}{D^j_{2,0}} \\ e^{ij} &= \frac{(Y^i - Y_{2,0})}{D^i_{2,0}} - \frac{(Y^j - Y_{2,0})}{D^j_{2,0}} \\ f^{ij} &= \frac{(Z^i - Z_{2,0})}{D^i_{2,0}} - \frac{(Z^j - Z_{2,0})}{D^j_{2,0}} \end{aligned} \tag{4.32}$$

As three unknowns need to be solved, three double differences need to be computed in order to estimate a position.

If the known and modeled terms are gathered in $D^{**}_{12,0}$, one obtains for the i,j satellites :

$$D^{ij}_{12,0} = D^i_1 - D^j_1 + D^j_{2,0} - D^i_{2,0} \tag{4.33}$$

The following equation gathers the minimal three double differences observations required to obtain a position estimation.

$$\begin{aligned} P^{ij}_{12}(t) - D^{ij}_{12,0} &= d^{ij}.\Delta X_2 + e^{ij}.\Delta Y_2 + f^{ij}.\Delta Z_2 \\ P^{ik}_{12}(t) - D^{ik}_{12,0} &= d^{ik}.\Delta X_2 + e^{ik}.\Delta Y_2 + f^{ik}.\Delta Z_2 \\ P^{il}_{12}(t) - D^{il}_{12,0} &= d^{il}.\Delta X_2 + e^{il}.\Delta Y_2 + f^{il}.\Delta Z_2 \end{aligned} \tag{4.34}$$

The *observation equation model* at the basis of the least squares solution of the double difference can finally be written:

$$\underline{W} - \underline{\nu} + A.\underline{x} = 0 \tag{4.35}$$

where $\underline{W}$ is the independent term, $\underline{\nu}$ is the vector of residuals, A is the matrix containing the partial derivatives resulting from the Taylor linearization and $\underline{x}$ is the vector of unknowns.

$$A = \begin{pmatrix} d^{ij} & e^{ij} & f^{ij} \\ d^{ik} & e^{ik} & f^{ik} \\ d^{il} & e^{il} & f^{il} \end{pmatrix} \qquad \underline{x} = \begin{pmatrix} \Delta X_2 \\ \Delta Y_2 \\ \Delta Z_2 \end{pmatrix} \qquad \underline{\nu} = \begin{pmatrix} \nu_{ij} \\ \nu_{ik} \\ \nu_{il} \end{pmatrix} \qquad \underline{W} = \begin{pmatrix} P^{ij}_{12}(t) - D^{ij}_{12,0} \\ P^{ik}_{12}(t) - D^{ik}_{12,0} \\ P^{il}_{12}(t) - D^{il}_{12,0} \end{pmatrix}$$

For the purpose of satellite-based positioning on the basis of double differences, at least four satellites should be simultaneously observed to be able to form three double differences. Therefore, four **independent** individual observations from each receiver will lead to four **independent** single differences. From these four single differences, three **dependent** double differences will be computed. Table 4.1 illustrates this principle.

Individual observations	Single differences	Double differences
P_1^i P_2^i	P_{12}^i	
P_1^j P_2^j	P_{12}^j	P_{12}^{ij}
P_1^k P_2^k	P_{12}^k	P_{12}^{ik}
P_1^l P_2^l	P_{12}^l	P_{12}^{il}

Table 4.1: Double differences dependence. The i, j, k, l indices correspond to observed satellites while the $1, 2$ indices represent the two receivers

From Table 4.1, one can observe that double differences are dependent observations. Due to such dependency, the double difference stochastic model will be different from the one presented in the absolute positioning case. Its formula is given by:

$$\begin{pmatrix} \sigma_1^2 & \cdots & \sigma_1\sigma_u \\ \vdots & \ddots & \vdots \\ \sigma_u\sigma_1 & \cdots & \sigma_u^2 \end{pmatrix} = \begin{pmatrix} \frac{\delta f_1}{\delta y_1} & \cdots & \frac{\delta f_1}{\delta x_n} \\ \vdots & \ddots & \vdots \\ \frac{\delta f_u}{\delta x_1} & \cdots & \frac{\delta f_n}{\delta x_n} \end{pmatrix} . \begin{pmatrix} \sigma_{x_1}^2 & \cdots & \sigma_{x_1}\sigma_{x_n} \\ \vdots & \ddots & \vdots \\ \sigma_{x_n}\sigma_{x_1} & \cdots & \sigma_{x_n}^2 \end{pmatrix} . \begin{pmatrix} \frac{\delta f_1}{\delta x_1} & \cdots & \frac{\delta f_u}{\delta x_1} \\ \vdots & \ddots & \vdots \\ \frac{\delta f_1}{\delta x_n} & \cdots & \frac{\delta f_u}{\delta x_n} \end{pmatrix} \tag{4.36}$$

where $\sigma_*\sigma_*$ is the covariance term added by the dependency characteristic of the double differences and x_n are the double difference observations.

4.5.4 Precision

In relative positioning, the single and double difference precisions (σ_{SD} and σ_{DD}) can be obtained from individual observation precisions (σ_1 for observations made at receiver 1, and σ_2 for the observations of receiver 2) by applying the error propagation law. As the single and double differences only rely on independent observations, the following precisions are obtained:

$$\begin{aligned} \sigma_{SD}^2 &= \sigma_1^2 + \sigma_2^2 \\ \sigma_{DD}^2 &= 2.\sigma_1^2 + 2.\sigma_2^2 \end{aligned} \tag{4.37}$$

If the A and B receivers are similar, same manufacturer, same model , the σ_1^2 and σ_2^2 will be equal and therefore:

$$\begin{aligned} \sigma_{SD}^2 &= 2.\sigma_1^2 \\ \sigma_{DD}^2 &= 4.\sigma_1^2 \end{aligned} \tag{4.38}$$

In practice, the σ_{DD}^2 could be associated with the variance of the independent term of the double difference in the zero and short baseline cases. However, some restrictions need to be placed on the previous assumption. In the zero baseline case, only the observation noise inherent to the receiver remains, not the entire observation noise. Therefore, the estimated value of precision will be under-estimated. On the contrary, in the short baseline case, if the entire observation noise is present, the multipath also enters into account in the precision computation. One must therefore neglect the multipath to consider the equivalence between the variance of the independent term and the double difference precision.

4.5.5 Correlation of the combinations

The relative positioning includes a notion of correlation of the observables. This correlation can be divided in two parts: the physical correlation and the mathematical correlation. The physical correlation refers to the fact that observations collected by two receivers are made on the same satellite. This correlation does not show an important impact on the computation and is not taken into account. By contrast, the mathematical correlation of signals, introduced by differentiating must be considered [Hofmann-Wellenhof et al., 2008].

The mathematical correlation observed on the double differences must therefore be discussed and considered in the computation. In this way, its influence on the double difference variance-covariance matrix will be derived.

If three satellites i,j and k are simultaneously observed by two receivers 1 and 2 location at time t, the single differences used to form the double differences could be written:

$$\begin{aligned} P_{12}^{ij} &= P_{12}^{i} - P_{12}^{j} \\ P_{12}^{ik} &= P_{12}^{i} - P_{12}^{k} \end{aligned} \tag{4.39}$$

Under matrix format, these equations become:

$$DD = C.SD \tag{4.40}$$

with

$$DD = \begin{pmatrix} P_{12}^{ij} \\ P_{12}^{ik} \end{pmatrix}$$

$$C = \begin{pmatrix} -1 & 1 & 0 \\ -1 & 0 & 1 \end{pmatrix}$$

$$SD = \begin{pmatrix} P_{12}^{i} \\ P_{12}^{j} \\ P_{12}^{k} \end{pmatrix}$$

The variance-covariance matrix of the double differences is given by:

$$\Sigma_{DD} = C.\Sigma_{SD}.C^T \tag{4.41}$$

As seen in the section 4.5.4, $\sigma_{SD}^2 = 2.\sigma^2$.

The result of matrix C multiplication leads to:

$$\Sigma_{DD} = 2.\sigma^2.\begin{pmatrix} 2 & 1 \\ 1 & 2 \end{pmatrix} \tag{4.42}$$

This last equation assesses the double difference mathematical correlation. Therefore, a weight matrix needs to be created and applied the computation. This weight or correlation matrix is given by the inverse of the Σ_{DD} matrix.

$$P(t) = \Sigma_{DD}^{-1} = \frac{1}{2.\sigma^2}.\frac{1}{3}.\begin{pmatrix} 2 & -1 \\ -1 & 2 \end{pmatrix} \tag{4.43}$$

In order to generalize the previous formula, the equation (4.44) expresses the weight matrix of a double difference combination composed of n_{DD} double differences at time t:

$$P(t) = \frac{1}{2.\sigma^2} \cdot \frac{1}{n_{DD}+1} \cdot \begin{pmatrix} n_{DD} & -1 & -1 & \cdots \\ -1 & n_{DD} & -1 & \cdots \\ -1 & \cdots & \ddots & \cdots \\ \vdots & \cdots & \cdots & n_{DD} \end{pmatrix} \tag{4.44}$$

In this dissertation, the σ taken as references for the correlation matrix computation are the values given by [Springer et al., 2013]. The Table 4.2 gathers them:

	GPS			
	L1	L2	L5	
σ (m)	0.380	0.485	0.360	
	Galileo			
	E1	E5a	E5b	E5
σ (m)	0.360	0.340	0.350	0.130

Figure 4.2: σ reference values

4.6 Conclusion

While chapter 3 described the methods, chapter 4 addressed the theoretical principles applied in this dissertation. These methods are supposed to be applicable for all the GNSS users, whatever the equipment.

First, the single point positioning was discussed. The least squares method used to resolve positioning equation was described. This type of positioning has been characterized as absolute, static, executed in real-time processing but only on code measurements. This restriction comes from the fact that the initial ambiguity of phase pseudoranges requires the resolution of complex algorithms that are not available to every user. The stochastic model of the least squares adjustment provides a way to obtain estimated parameter precisions from observation precisions.

Secondly, the relative positioning, in static mode and real-time processing under format of double difference combination was addressed. This kind of positioning has been explained on code position resolution. Moreover, the remarkable features of the zero baseline configuration have been discussed. This configuration allows removing many errors affecting the signal.

Finally, a last point that is worth mentioning is the correlation of the combinations. A weight matrix must be considered in the resolution algorithm of the double difference due to the mathematical correlation introduced by the differences done between the observations. Thanks to this matrix application, the precision on individual observations can be easily computed on the basis of the independent term of the double difference.

Chapter 5

Application

Zero, short and medium baselines configurations are defined by specific GNSS receiver positions. The precise coordinates associated with each of these positions as well as the characteristics of each receiver and antenna will be described in this chapter. The spatial segment, comprising the satellite availability for each studied GNSS, will also be mentioned. Finally, the data format and the computation program will be briefly explained.

5.1 User segment

In order to calculate positions, four ground stations were used for data collection. Two of them, located in the Sart-Tilman, provided data for the zero-baseline experimentation. The ground stations of Brussels and Waremme were used for the short and medium baselines experiments. In this dissertation, "WARE" stands for Waremme station, "BRUX" for Brussels, "ULG1" and "ULG0" for the two stations of Sart-Tilman.

5.1.1 Precise coordinates

Precise coordinates were computed for those stations thanks to the *Center Point RTX - Post-processing* application from Trimble, a receivers manufacturer. This function determines precise coordinates of a fixed station based on GNSS measurements for a whole specific day, providing better than two centimeters horizontal accuracy. For this purpose, the Trimble Center-Point RTX, described as a correction service for GNSS, computing and broadcasting corrections to the receivers via satellites, combines GPS, Beidou, GLONASS and QZSS satellite systems to compute the user position in post-processing mode. Tables 5.1, 5.2, 5.3and 5.4 show the precise coordinates of the four reference stations.

ITRF2008 at Epoch 2014.16		
Coordinate	**Value**	σ
X	4 039 066.467 m	0.004 m
Y	393 662.043 m	0.004 m
Z	4 904 422.369 m	0.004 m
Latitude	50° 34' 57" 20446 N	0.002 m
Longitude	05° 34' 0" 02039 E	0.004 m
Elevation	302.175 m	0.006 m

Figure 5.1: ULG0 precise coordinates

ITRF2008 at Epoch 2014.16		
Coordinate	**Value**	σ
X	4 039 066.467 m	0.004 m
Y	393 662.043 m	0.004 m
Z	4 904 422.369 m	0.004 m
Latitude	50° 34' 57" 20446 N	0.002 m
Longitude	05° 34' 0" 02039 E	0.004 m
Elevation	302.156 m	0.006 m

Figure 5.2: ULG1 precise coordinates

ITRF2008 at Epoch 2014.23		
Coordinate	**Value**	σ
X	4 031 947.048 m	0.004 m
Y	370 151.207 m	0.004 m
Z	4 911 906.091 m	0.004 m
Latitude	50° 41' 23" 55436 N	0.002 m
Longitude	05° 14' 43" 12321 E	0.004 m
Elevation	187.872 m	0.006 m

Figure 5.3: WARE precise coordinates

ITRF2008 at Epoch 2015.23		
Coordinate	**Value**	σ
X	4 027 881.440 m	0.004 m
Y	306 998.660 m	0.004 m
Z	4 919 498.980 m	0.004 m
Latitude	50° 47' 53" 03055 N	0.002 m
Longitude	04° 21' 30" 83553 E	0.004 m
Elevation	158.144 m	0.005 m

Figure 5.4: BRUX precise coordinates

These fixed coordinates are the *a priori* values used in the single point positioning and double difference computations (see sections 4.2.1 and 4.5.3).

5.1.2 Material

Receivers

Nowadays several GNSS receiver types exist. They can be distinguished according to three criteria.

First, some receivers are able to process multiple GNSS signals: the *multi-GNSS* receiver.

Secondly, a few receivers allow the tracking of more than one frequency while others do not. The former are called *multi-frequency* receivers, the latter *single-frequency* receivers. *Single-frequency* receivers operate only with the standard upper L-band (1560-1610 MHz) that includes namely GPS L1 and Galileo E1 whereas *multi-frequency* receivers handle GPS L2, L5, Galileo E5a, E5b and E5a+b. In this dissertation, only these frequencies will be considered.

Eventually, a third criterion differentiates receivers: the type of observables. This may be either code pseudoranges exclusively or code and phase pseudoranges measurements.

Every receiver in each of the stations mentioned earlier is multi-GNSS, multi-frequency code and phase receivers.

The University of Liège owns four receivers of two separate manufacturers. Two of them are products of Trimble company (Trimble NetR9 receivers) whereas the two others are designed by Septentrio (Sept PolarX4 and Sept PolarXS). Brussels and Waremme stations both equipped with Septentrio receivers: a Sept PolarX4 and a Sept PolarX4TR. Disparities exist between these receivers: some of them directly derive from product engineering [Caelen, 2014].

Antennae

The University of Liège owns two antennae made by Trimble (TRIMBLE TRM 59800 SCIS). They are positioned on the roof the B5a building. This type of antenna is called choke ring antenna. Its particular shape mitigates the influence of the multipath on the received signals.

The Brussels' antenna is produced by Javad (Javad ring antenna DM). It is also a choke ring antenna.

In Waremme, the antenna is a choke ring antenna from Ashtech, a Trimble integrated technology (ASH 701945E M). This antenna is by far the oldest of the four used in this dissertation. It might have a negative influence on the results presented.

Splitter

The *splitter*, mentioned in section 4.5.2, is a device that amplifies the received signal with the aim of splitting it into two receivers connected to the same antenna. This device is required in zero baseline configuration . Nonetheless, it was also used in the short baseline realized in the Sart-Tilman site as both Trimble and Septentrio short baselines have been observed simultaneously thanks to the two same antennas. The splitter is an amplifier splitter of type ALDCBS1X2 GPS.

5.1.3 Configurations

Zero, short and medium baseline configurations have been tested at the different sites available.

The zero baseline experiments only took place on the Sart-Tilman site. As four receivers were available, the two Trimble receivers were used to create one zero baseline and the two Septentrio composed the other. Same label receivers have been put together, as receiver specificities change from one manufacturer to another manufacturer. As two antennae are present in this site, each one was used to create a zero baseline. The first one, called "ULG0" used to create the Trimble zero baseline while the"ULG1" antenna served to realize the Septentrio baseline, as illustrated in Fig. 5.5.

The short baseline was also created in the Sart-Tilman site, with the same four receivers. The Septentrio and Trimble receivers were spread between the two "ULG0" and "ULG1" antenna.

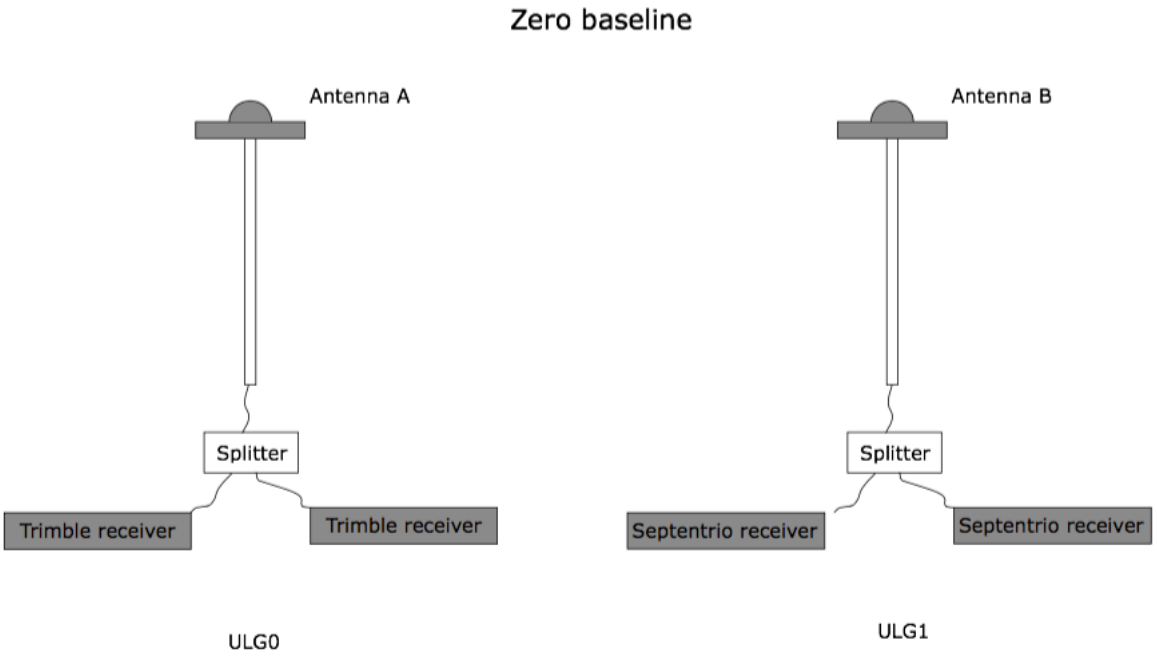

(a) Zero baselines in Sart-Tilman site

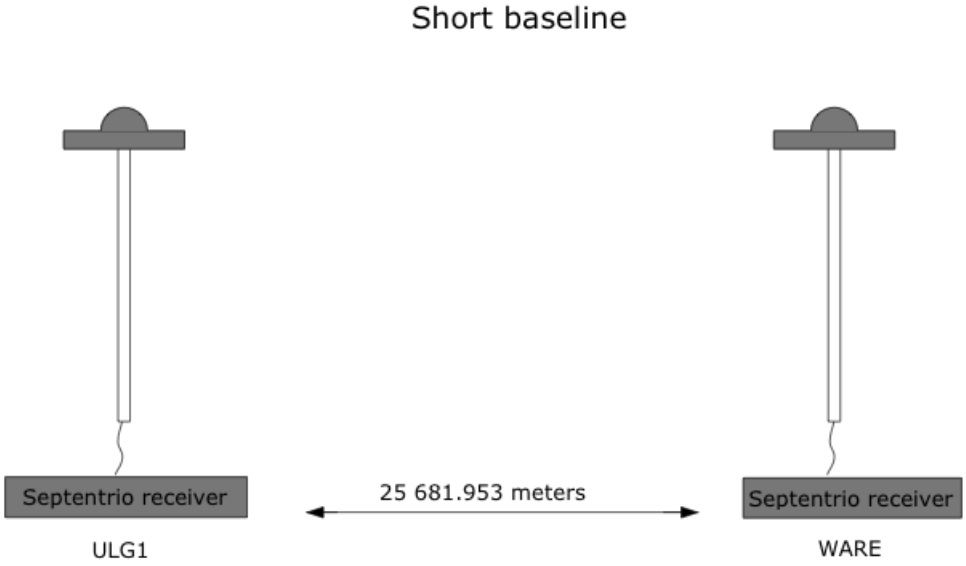

(b) Medium baseline between Sart-Tilman and Waremme

Figure 5.5: Zero and medium baseline representation

The medium baselines were created between the antennae placed in the "ULG1" position in the Sart-Tilman and the Waremme and Brussels stations. Each of these stations are equipped with a Septentrio receiver, avoiding to combine two different receiver types (Trimble and Septentrio receivers). The Waremme medium baseline is illustrated by Fig. 5.5.

Table 5.1 summarizes these configurations, the distance between the stations (baseline length) and the period of observation of each baseline. The abbreviation DOY in this Table stands for *Day Of Year*. In this calendar system, for a normal year, the 1^{st} of January is the DOY 1 and the 31^{st} of December is the DOY 365.

Zero baselines				
Station	**Receivers**	**Distance**	**DOYs**	**Year**
ULG0	Trimble NetR9	0 m	343-353	2014
ULG1	Septentrio X4 and XS	0 m	343-353	2014
ULG1	Septentrio X4 and XS	0 m	60-180	2015
Short baselines				
Stations	**Receivers**	**Distance**	**DOYs**	**Year**
ULG0-ULG1	Trimble NetR9	5.177 m	180-93	2015
ULG0-ULG1	Septentrio X4 and XS	5.177 m	180-93	2015
Medium baselines				
Stations	**Receivers**	**Distance**	**DOYs**	**Year**
ULG1-WARE	Septentrio X4 and XS	25 681.953 m	80-100	2015
ULG1-BRUX	Septentrio X4 and XS	88 676.492 m	80-100	2015

Table 5.1: Receiver configurations

5.1.4 Receiver observation noise

Among the aforementioned stations, [Caelen, 2014] estimated the observation noise that might be expected on Brussels and Sart-Tilman receivers. Since his analysis in 2014, the Brussels antenna position remained fixed. But, the two antennae of Sart-Tilman were positioned in different locations than the one presented in section 5.1.1, for the purpose of his own analysis. Nonetheless, the values of noise given in Table 5.2 results from a combination eliminating atmospheric and multipath errors. Therefore, the difference between the values were estimated by [Caelen, 2014] to be mainly due to the differences between receiver models than by the site.

Table 5.2 provides values of this observation noise on Brussels and Sart-Tilman receivers. They depend on signal frequency. They were normalized on the basis of a 45 dB Hz reference ratio. However, this normalization have to be handle carefully as observation at low elevation will show worse values and satellites at higher elevation will engender better values.

	GPS-codes		**Galileo-codes**		
Receivers	L1	L5	E1	E5a	E5
Brussels - Septentrio X4	0.120	0.175	0.075	0.089	0.030
Sart-tilman - Trimble NetR9	0.242		0.144	0.115	0.132
Sart-tilman - Septentrio X4	0.175	0.140	0.115	0.076	

Table 5.2: Receiver noise in meters in function of the frequency observed. Source : [Caelen, 2014]

From this table, the Septentrio receivers both share similar noise values. By contrast, the Trimble receiver shows higher values of noise. We therefore could except more precise observations with the Septentrio receivers than with the Trimble receivers. This should be taken into account in further analysis.

If a comparison between signals' noise is done, it clearly appears that Galileo's new signals are less noisy than the GPS ones.

5.2 Space Segment

The space segment comprises the analysis of the satellites and their signals.

In this dissertation, data were collected every 30 seconds. Therefore, successive observation epochs correspond to successive 30 seconds.

5.2.1 Constellations

The GPS and Galileo constellations are presented in the Tables 5.3 and 5.4. These constellation tables are called almanacs, they gathered status data from every satellites.

PRN	Launched	Usable	PRN	Launched	Usable
	Block IIA			**Block IIR-M**	
32	11-26-90	2-26-08	17	9-26-5	12-16-05
26	7-7-92	7-23-92	31	9-25-06	10-12-06
9	6-26-93	Decomissionned	12	11-17-06	12-13-06
4	10-26-93	11-22-93	15	10-17-06	10-31-07
3	3-28-96	Decomissionned	29	10-17-07	1-2-08
10	7-16-96	8-15-96	7	3-15-08	3-24-08
8	11-6-97	Decomissionned	5	8-17-09	8-27-09
	Block IIR			**Block IIF**	
13	7-23-97	1-31-98	25	5-28-10	8-27-10
11	10-7-99	1-3-00	1	7-16-11	10-14-11
20	5-11-00	6-1-00	24	10-4-12	11-14-12
28	7-16-00	8-17-00	27	5-15-13	6-21-13
14	11-10-00	12-10-00	30	2-21-14	5-30-14
18	1-30-01	2-15-01	6	5-17-14	6-10-14
16	1-29-03	2-18-03	9	8-2-14	9-17-14
21	3-31-03	4-12-03	3	10-29-14	12-12-14
22	12-21-03	1-12-04	26	3-25-15	4-20-15
19	3-20-04	4-5-04	8	7-15-15	
23	6-23-04	7-9-04			
2	11-6-04	11-22-04			

Table 5.3: Almanac of GPS constellation. Source: [GPS-World-Staff, 2015]

As explained in chapter 1, GPS L5 is only broadcast by the last satellite generation in orbit, the Block IIF satellites. From Table 5.3, one of the last GPS satellite launched (PRN 26) became operational in April 2015, during the observation period of the Septentrio zero baseline. Similarly, during the Trimble and Septentrio 2014 observation period, the satellite PRN 3 became operational. These additional satellites improve the position estimated with GPS L5. The reasons being that more satellites will be available and therefore, the probability to reach a better PDOP is higher. Furthermore, the redundancy of information sent by the satellites will be taken into account in the mean square adjustment and improve the position estimation.

One can conclude from Table 5.4 that positioning with Galileo is limited as only three satellites available in the constellation are considered as fully operational. The other four satellites from the FOC constellation are under commissioning, signifying that even if their signals reach the receivers, the observations they transfer have not been validated yet.

From Table 5.4, it is worth mentioning that even if the E20 satellite is declared "Not available" because of malfunctioning, its signals are still captured by the receivers. But, as E20 has stopped emitting Galileo E5a, E5b and E5 signals (see section 1.1.3), only Galileo E1 will benefit from a temporary 5-satellite constellation. Secondly, one may notice that the 2 most recently launched satellites (E22 and E26) joined the Galileo constellation during Septentrio zero baseline

period. If not already commissioned, these satellites broadcast the Galileo signals and these signals are tracked by the receivers used in this dissertation.

PRN	Launched	Operational
	Test prototypes	
GIOVE-A	12-28-05	Decomissionned
GIOVE-B	4-27-08	Decomissionned
	In Orbit Validation	
E11	10-21-11	12-10-11
E12	10-21-11	1-16-12
E19	10-12-12	12-1-12
E20	10-12-12	Not available
	Full Operational Capability	
E18	08-22-14	Under commisionnig
E14	08-22-14	Under commisionnig
E26	3-27-15	Under commisionnig
E22	3-27-15	Under commisionnig

Table 5.4: Almanac of Galileo constellation. Source: [GPS-World-Staff, 2015]

5.2.2 RINEX format

The *Receiver Independent Exchange Format* (RINEX) format is the standard exchange format between receivers for pos-processing applications. It has been developed by the *International GNSS Service* (IGS). The main purpose of this format is to facilitate the exchange of GNSS data. The version used in this dissertation is the version 3.00 that consists of three ASCII file types :

- observation data file
- navigation message file
- meteorological data file

In the observation data file, the observation codes are defined by three characteristics : the observation type (t), the frequency number (n) and any attribute that is worth being mentioned (a). This third characteristic has been created since new GPS and Galileo signals combined frequencies (-I and -Q for instance). These signal properties are mentioned in this attribute.

Table 5.5 illustrates those characteristics called *tna* characteristics. The signal strength is the ratio C/N_0 mentioned in chapter 2.

t: observation type	C: code	L: carrier phase	D: Doppler	S: signal strength
n: frequency	1,2,...,8			
a: attribute	tracking mode (-I, -Q) or channel, etc.			

Table 5.5: RINEX observation code tna. Source: [IGS et al., 2013]

The RINEX format codifies each of the GPS and Galileo signal. In order to agree on the terminology used in this dissertation, Table 5.6 shows the relation between the signal naming convention used in this dissertation and the naming proposed by the RINEX format for all the Septentrio X4, XS and Trimble observed signals.

GNSS system	Frequency name	Channel	Code	Phase
GPS	L1	C/A	C1C	L1C
		z-tracking	C1W	L1W
	L2	C/A	C2C	L2C
		L2C (L)	C2L	L2L
		L2C (M+L)	C2X	L2X
		z-tracking	C2W	L2W
	L5	Q	C5Q	L5Q
Galileo	E1	C	C1C	L1C
		B+C	C1X	L1X
	E5a	Q	C5Q	L5Q
		I+Q	C5X	L5X
	E5b	Q	C7Q	L7Q
		I+Q	C7X	L7X
	E5 (E5a+b)	Q	C8Q	L8Q
		I+Q	C8X	L8X

Table 5.6: RINEX GPS and Galileo observation codes. Source: [IGS ET AL., 2013]

From this table, it is the frequency name that will be used to define signals. However, as a frequency name often corresponds to different channels, one must specify which channel is used. And, as many receivers are used and as the channel observed depends on the receiver model, receivers and associated channels are described in Table 5.7.

Receiver	GNSS	Frequency name	Channel	Code	Phase
Septentrio X4 and XS	GPS	L1	C/A	C1C	L1C
		L2	z-tracking	C2W	L2W
		L5	Q	C5Q	L5Q
	Galileo	E1	C	C1C	L1C
		E5a	Q	C5Q	L5Q
		E5b	Q	C7Q	L7Q
		E5 (E5a+b)	Q	C8Q	L8Q
Trimble NetR9	GPS	L1	C/A	C1C	L1C
		L2	z-tracking	C2W	L2W
		L5	Q	C5Q	L5Q
	Galileo	E1	B+C	C1X	L1X
		E5a	I+Q	C5X	L5X
		E5b	I+Q	C7X	L7X
		E5 (E5a+b)	I+Q	C8X	L8X

Table 5.7: Observed channels in function of the receiver

5.2.3 RTP format

The RTP format is the ASCII format of data used in this dissertation. It has been developed by R. Warnant of the University of Liège for the Geomatics unit's needs. Based on RINEX code and phase pseudoranges, this format also adds pre-calculated ionospheric and tropospheric corrections, satellite clock error estimation, broadcast and precise orbits. These parameters are therefore directly available for positioning.

5.3 MATLAB program

The single point positioning, single and double differences have all been computed thanks to MATLAB scripts. Each of the positioning method has been implemented as a script function, all bound to the main program. Fig. 5.6 illustrates the program structure.

From Fig. 5.6, one can observe that after the call of the setup function, the different configuration functions are used, according to the options recorded by this setup function.
Then, the procedure is similar for all configurations. The data from the header of the RTP file are collected as well as the observations it contains. Among the extracted observation data, the extraction function selects the data corresponding to the options entered.
After computation, statistics are computed and all the results are saved. Similarly, graphics and figures of PDOP, position deltas in the X,Y,Z and North, East, Up dimensions are computed and saved.

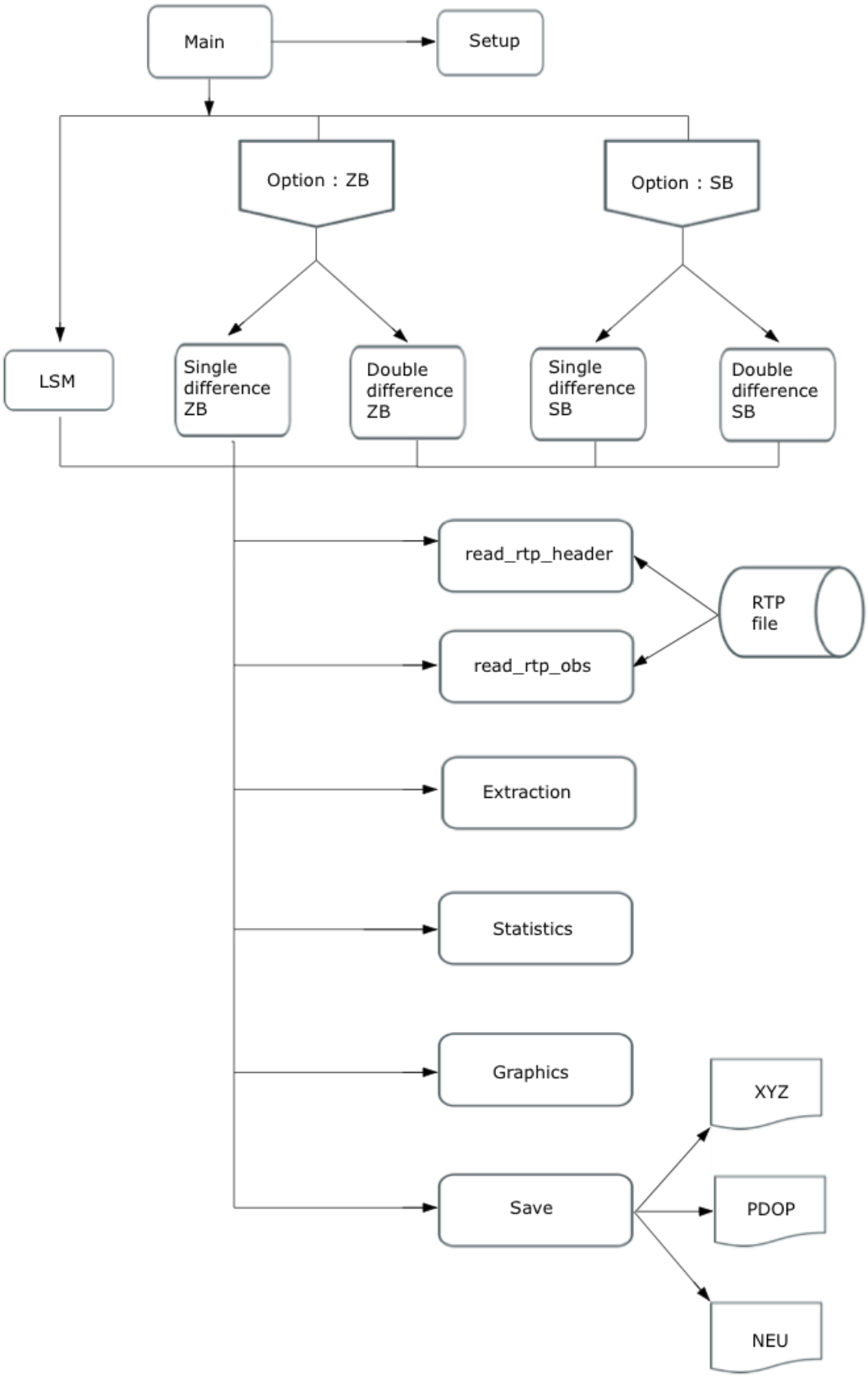

Figure 5.6: Structure of the MATLAB program

5.4 Conclusion

This chapter describes the practical application of this dissertation.

First, the user segment was explored. The fixed coordinates used in the computation, evaluated with a few millimeters precision thanks to the Trimble application, were presented. The precision on their determination has an important impact on the position estimation precision. The materials such as receivers, antennae and splitter devices were described and defined. The localization of the stations used and their respective configurations were given and illustrated. Finally, values of observation noise observed by [Caelen, 2014] were displayed in order to introduce a first comparison between receivers. It appears that the Septentrio receivers should lead to more precise positioning as less noise is observed on these receivers, all other things being equal.

The second section of this chapter detailed the space segment. The constellations presently available for both GPS and Galileo signals are shown and discussed. It can be concluded from those observations that positioning with Galileo is limited as only three satellites available in the constellation are considered as operational. The other four satellites from the FOC constellation are still under commissioning, meaning that even though their signals reach the receivers, the signals they emit have not been fully validated yet. The formats of observation data were also described: RINEX and RTP. The RINEX format is the standard format of GNSS data exchange while the RTP format extracts raw pseudoranges from RINEX and adds information in the observation file such as the precise orbits, ionospheric and tropospheric corrections.

Finally, the MATLAB program used to compute the different configurations was illustrated.

Chapter 6

Results

In this chapter, the double difference theoretically explained in chapter 4, will be implemented and its results detailed. In order to determine if Galileo E5 code pseudoranges could be used to achieve decimeter level of precision on estimated positions, the three GPS frequencies (L1, L2 and L5) as well as the three supplementary Galileo signals (E1, E5a and E5b) will serve as a comparison point. The discussion that follows will therefore incorporate a GPS and Galileo complete analysis.

As already mentioned, the Galileo constellation only comprises eight satellites (commissioned or under commissioning process) at present time. Nonetheless, almost all the results presented in this section rely on only four visible satellites to determine positions. Actually, the new satellites launched were adjusted in their orbital planes, changing the constellation. Therefore, the number of visible satellites remains four in most of the days of observation but more observation epochs are available.

The estimation of a position will be altered by the reduced constellation. This alteration is mainly due to two main factors.

Firstly, higher PDOP values will be observed in the case of a reduced constellation than in the case of full constellation. The reason being that the chances of meeting an inaccurate satellite geometry are higher.

Secondly, between the few satellites observed, a great number show low elevation values. At low elevation, the signal broadcasted by the satellite is greatly altered than in high elevation. This is because the signal has to travel a longer distance in the atmosphere when visible only at low elevation.

A third parameter, which is not directly linked to the constellation but depends on it, is worth being discussed. As four satellites are needed to compute a position, no redundancy of observations will be available with the Galileo constellation. Redundant observations are used by the least squares process to reach more precise solutions. A limited constellation will therefore automatically lead to less precise position estimation.

Consequently, in the aim of having the highest number of valid observation periods, two constraints will be applied on the visible satellites to be part of the computation of the double difference:

- Firstly, the minimum elevation will be fixed to 0. This way, all the visible satellites will be included, thereby increasing the chances of meeting long observation periods. This constraint, even if allowing higher number of visible satellites, increases the number of observations made at low elevation. These observations being altered, the positioning result will suffer from this choice. Moreover, the Trimble receivers estimate satellites orbits. Therefore, when a satellite rises over the horizon, this receiver is directly able to observe it, as it has computed its orbit and knows where to search in order to find the satellite. The Septentrio receivers are not able to estimate the satellites' direction of observation and therefore, only received low elevation observations when the satellite elevations decrease to reach the horizon.

- Secondly, the maximum acceptable PDOP value will be fixed to 10. The double difference PDOP values considered here are not equivalent to PDOP values obtained in single point positioning. Those single point positioning PDOP values are most of the time 2 or 3 times higher than the double difference PDOP values. This second constraint avoids having huge PDOP peaks. These peaks show important repercussion on the estimated position, leading to meters errors where the centimeter precision could have been reached otherwise. An example of single point positioning PDOP and double difference PDOP is given in section 6.1.2.

Precision needs to be made concerning the first point aforementioned. The minimum elevation fixed to 0 is not systematically applied on all Galileo satellites. Indeed, the E20 satellites, which experienced technical problems in 2014, stopped emitting Galileo E5a, E5b and E5a+b but still broadcast the E1 signal. However, it does not broadcast ephemerides. For this reason, its coordinates can not be computed, making its use impossible for single point positioning. Nevertheless, as double differences contain a difference of satellite-to-receiver distances (see terms D_{12}^{**} in equation (4.30)) which are similar in the case of the zero baseline, the satellite E20 will be used for the zero baseline tests. Let us recall that this assertion remains valid as long as the two receivers make simultaneous measurements on the signals emitted by two satellites involved in the double difference. Therefore, the analysis of the zero baselines will be done by including the E20 satellite, while the short baseline will add a new constraint to the first point: the minimum elevation will be fixed to 0 but the computation will not comprise satellite E20 in the estimation of the position.

In order to better understand the general results obtained on each signal, brief analyses of those signals have been done individually for each receiver considered in the zero baseline configuration. These analyses should help for the interpretation of the result tables given for each configuration. General results shape, as well as PDOP or low elevation influence, will be treated and will serve as reference for further explanations.

6.1 Double difference

In this section, each observation epoch that meets the aforementioned constraints and which contains Galileo E5 signal will be taken into consideration to compute statistics. However, with the Galileo reduced constellation, the Galileo signals more often suffers from high PDOP peaks or low elevation satellites presence. In order to provide a more realistic analysis of the Galileo satellite system, the GPS constellation is reduced to a 4-satellites system. The highest satellite observed at each epoch as well as the three lowest satellites of these epochs are maintained. This choice have been done on the basis of the observation of the Galileo satellites behaviour. It often appears that one satellite is at high elevation while the others are located at low elevations (between 0 degrees and 25 degrees). This choice will lead to PDOP values similar to those of Galileo as GPS geometry will be closer to that of Galileo. The comparison between the full constellation GPS, the reduced 4-satellite constellation of GPS and the Galileo present constellation is proposed in every configuration cases.

The Appendix gathers the PDOP statistics concerning the observation periods studied. The PDOP mean has a significative impact on the position precision. It was also envisaged to study satellite elevation in this Appendix but the elevation statistics are less representative of the actual constellation. Also, in the case of Galileo, when four satellites are observed, one is often situated at high elevation (between 70 and 50) while the others are situated at lower elevations (between 0 to 25). The mean elevation value is therefore influenced by the high elevation satellite. On the contrary, GPS L1 and L2, which show a mean of 11 simultaneously observed satellites, often meet only 3 satellites at high elevation while the other elevation values are lower. For this reason, the elevations of the GPS satellites are most of the time lower than elevation of Galileo satellites. Therefore, elevations will be mentioned in the text for particular cases but will appear in the Appendix.

6.1.1 Zero baseline

In chapter 5, different configurations applicable on double differences have been discussed. The zero baseline, which allows the removal of satellite-based biases, receiver-based biases, atmospheric errors, multipath and a part of the observation noise, will be the first configuration handled in this chapter. In this particular configuration, assessing the superiority of Galileo E5 should be easier than with other configurations. Only the part of observation noise inherent to receiver affects the signal. As explained in chapter 2, observation noise have been demonstrated to be very low on Galileo E5 in comparison with other signals ([Caelen, 2014]).

Below are the parameters that will be taken into account in order to assess the precision of the signals.

- The precision of the pseudorange measurements (observations) σ_{obs}, obtained by the use of the formula (4.38).
- The standard deviation on North, East an Up position components: σ_N, σ_E, σ_U
- The standard deviation of the P_{12}^{ij} term: $\sigma_{P_{12}^{ij}}$ (see equation (4.29)).
- The standard deviation of the independent term: σ_{ind}
- The mean of the on North, East an Up position components: μ_N, μ_E, μ_U
- The precision on the estimated position σ_{pos} which will be given by the MRSE (*Mean Radial Spherical Error*) given by:

$$\sigma_{pos} = \sqrt{\sigma_N^2 + \sigma_E^2 + \sigma_U^2} \tag{6.1}$$

As the Table 5.1 shows, two zero baselines are studied in this dissertation. The first one is composed of two Septentrio receivers, the Septentrio XS and the Septentrio X4. They are both connected to the antenna B, on the ULG1 position, thanks to a *splitter*. The second zero baseline is made of two Trimble NetR9 receivers linked to the antenna A located on the ULG0 position.

Results from *Days of Year* (DOYs) 343 to 353 of year 2014 were collected on both baselines but only the Trimble baseline will be discussed in detail on the basis of this data. Indeed, Septentrio baseline in 2014 knows a critical lack of Galileo E5 data, due to Septentrio XS particularity. This receiver owns a limited number of channels, making it able to track only a limited number of signals at the same time. During the observation period, Septentrio XS only received Galileo E5 on a single day out of the 10 days of observations. Therefore, as in double difference common observations are required, the zero baseline made by the Septentrio receivers suffered from this lack of received satellite signals resulting in shorter Galileo observation periods. As a consequence, only the 2015 data, with more satellites available for Galileo, will be presented in the next sections.

Since 2014, Galileo constellation has changed. The Tables 5.3 and 5.4 summarize GPS and Galileo satellites in orbit at the time of the observation and their capacity to emit a valid signal.

From Table 5.3, which represents the GPS almanac at the time of the analysis, the main concern is about GPS L5 new frequency. As explained in the introduction (chapter 1), GPS L5 is only broadcasted by the last satellite generation in orbit, the Block IIF satellites. As can be seen from Table 5.3, the last GPS satellite launched (PRN 3) in 2014 became operational during the observation period (DOY 343 to 353 of 2014, id est. : from December 9^{th} to December 19^{th} of 2014). Such Block IIF constellation allows at least 4 satellites to be observed from our stations for a few epochs of the day.

The L1 and L2 GPS signals are broadcasted by every satellite. They are therefore expected to

give stable results as a high number of satellites reduce the PDOP and allow redundancy in the least squares adjustment.

The second Table 5.4 illustrates the difficulty of estimating a position using Galileo only. Indeed, only three satellites have been declared fully operational at time of writing. The two new satellites from the FOC constellation launched at the observation period (E18 and E14) are still in validation process. Still, they broadcasted Galileo signals at observation time and then, could be used to calculate positions even if they are still not declared fully operational. Nevertheless, this limited constellation provides four visible satellites at a given station for a reduced number of epochs of the day, which is sufficient to perform satellite-based positioning.

It is worth mentioning that even if the E20 satellites is declared "Not available" because of malfunctioning, its signals are still tracked by the receivers. But, as E20 has stopped emitting Galileo E5a, E5b and E5 signals (see section 1.1.3), only Galileo E1 will benefit from a temporary 5-satellites constellation.

6.1.2 Trimble receivers

As explained in the introduction of this chapter, the constraint concerning the minimum elevation affects more Trimble receivers than Septentrio receivers. Trimble receivers will track more observation epochs with Galileo satellites as they also track satellites at their rise above the horizon. But, as these observations are more altered by atmospheric biases, the positioning results will also be affected. On the other hand, when satellite elevation is higher, PDOP values increase in such a way that the quality of the positioning is also affected. Therefore, the precision values obtained with Trimble positioning are expected to be quite high.

The Fig. 6.1 illustrates the differences between Septentrio and Trimble receivers number of epochs of observation.

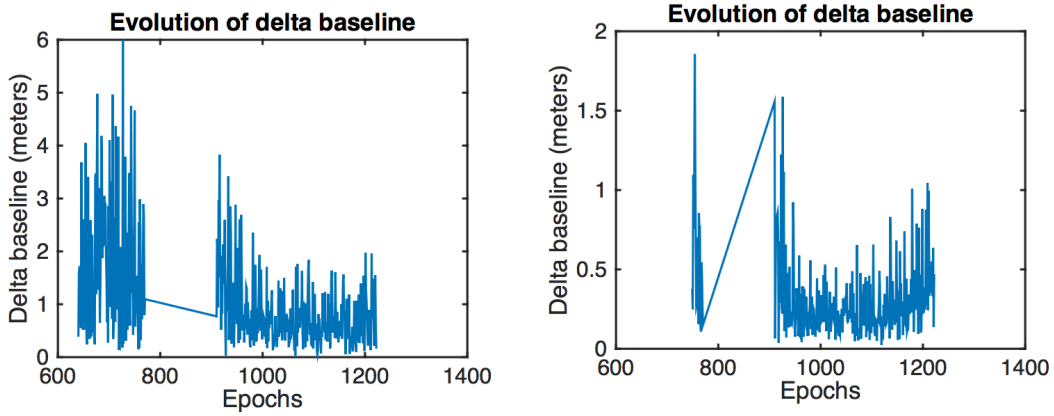

(a) Galileo E5a delta baseline on double difference in zero baseline with Trimble receivers (DOY 346 of 2014)

(b) Galileo E5a delta baseline on double difference in zero baseline with Septentrio receivers (DOY 346 of 2014)

Figure 6.1: Example of differences in the number of observed epochs between Septentrio and Trimble receivers on DOY 346.

From Fig. 6.1, one can observe that 109 epochs are missing on the Septentrio delta baseline, the epochs needed for satellite 19 to grow from 2 degrees of elevation to 20 degrees. They correspond to the observations at the rise of the satellites. One may also notice the important hole in the results between epoch 777 to epoch 909. It is due to a PDOP peak excessing the 10 maximum limit fixed.

Epochs with PDOP values superior to 10 were automatically suppressed. These epochs presenting high values correspond to the epochs where the four satellites observed showed an elevation higher than 20 degrees. The position precision obtained is automatically degraded by these PDOP values.

In order not to be biased by the initial part of the distribution, the Septentrio results on these ten days have been used to limit the extension of the Trimble results. Therefore, the days on which Septentrio results were available on at least one of the Galileo signals (7 days out of 10), the initial part of the distribution was removed in order to start with the same epoch as in the Septentrio results. Therefore, only 7 days will be used to compute statistics.

From the 10 days observation period with the two Trimble receivers in a zero baseline configuration, some days stand out from the rest (for instance, DOYs 344 and 350). Four days are affected by very high PDOP values on Galileo observations while the others suffer from the low elevation of Galileo satellites. Furthermore, one other day shows interesting results but only very few epochs of observations are available on the Galileo signals. The DOY 344 and 350 do not suffer from these biases or lack of observations. They will therefore be used to the present general shape of Galileo and GPS results.

Figures 6.2 and 6.4 illustrate the GPS L1, L2 and L5 results obtained during the whole observation period (DOY 343 to DOY 353) as GPS satellite visibility at a given station repeats itself in an identical way after a sidereal day. Therefore, in zero baseline configuration, each observation day should give the same results on GPS signals.

GPS L1 and L2 results

The Trimble receivers show very consistent results for GPS L1 and L2 signals. Fig. 6.2 gives an illustration of the GPS L1 and L2 results general shape during the observation period. For the sake of readability of the presented figures, the values of the standard deviations represented by a black line on the North, East and Up figures are given in a the Table 6.1. Likewise, the value of the means of North, East and Up deviations, drawn in red, are also presented in the Table 6.1.

Fig. 6.2 represents the deviations of the estimated position on North, East and Up local directions. As precise initial coordinates have been fixed (see section 5.1.1), the results of the average errors should be close to zero. The variance of those parameters is an indicator of the precision of the computed position. If the delta shows a high variance value, the precision of the estimated position will decrease. Therefore, a reliable signal received in appropriate conditions (low PDOP, full constellation satellite and very few low elevation satellites) should present low variance and a mean value close to 0.

The independent term represented on Fig. 6.2 is the key parameter which allows the assessment of the observation precision. Indeed, in zero baseline mode, this term should only be influenced by the observation noise. Therefore, its variance is an indicator of the precision of the observations.

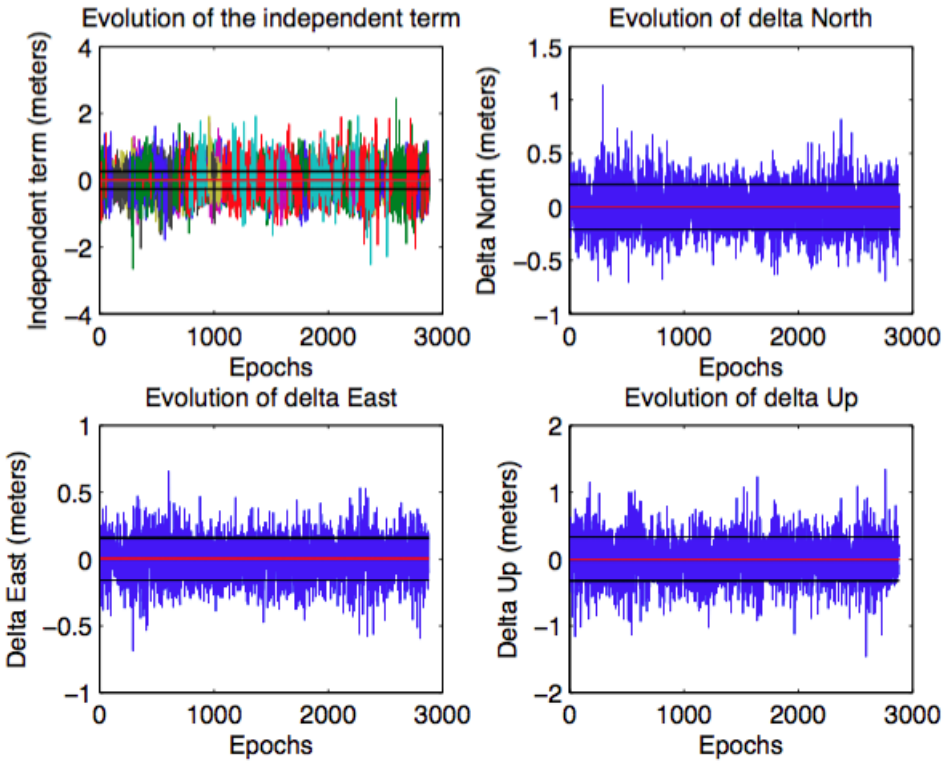

(a) GPS L1(C1C) with Trimble NetR9 baseline (DOY 344)

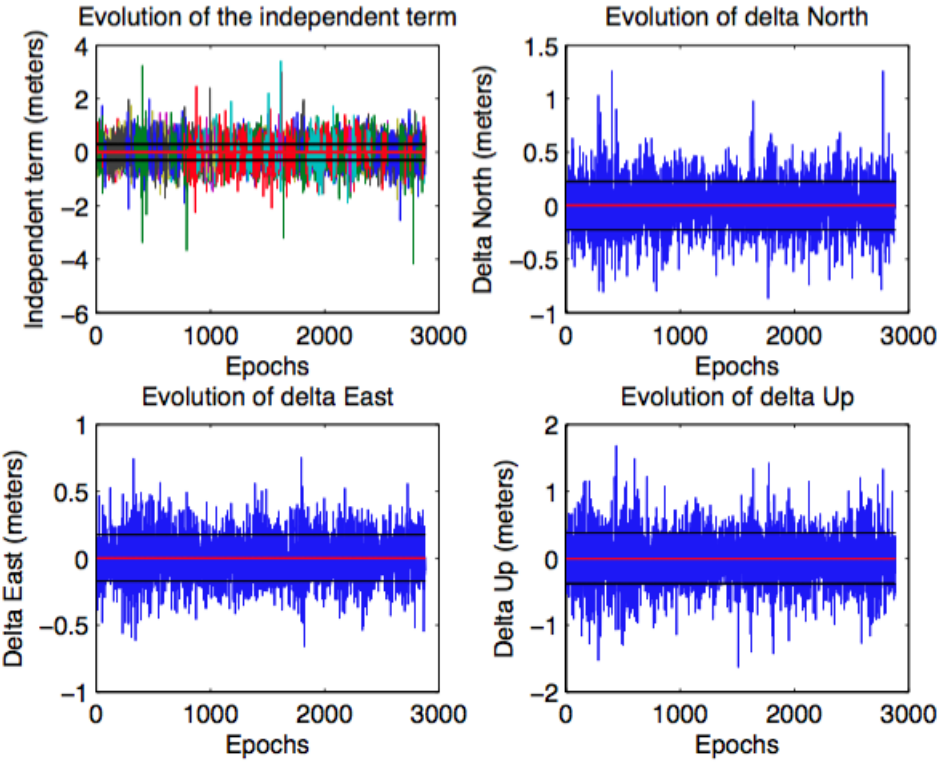

(b) GPS L2 (C2W) with Trimble zero baseline (DOY 344)

Figure 6.2: GPS L1 and L2 independent terms and code double difference positioning on the DOY 344 of year 2014 observed on the Trimble zero baseline. The red lines represent the average values, the black lines the standard deviations. On the independent term figures, the different colors correspond to the different double differences used in the computation

The observation precision should not be confused with the position precision aforementioned. On one hand, the observation precision characterizes the quality of the signal. It depends on the errors affecting the signal, such as atmospheric errors, satellite-based biases or receiver-based biases, multipath and observation noise. In zero baseline configurations, only the observation noise inherent to the receiver affects the signal. On the other hand, the positioning precision is an indicator of the precision obtained on the estimated position and depends on the geometry of the constellation, the number of available satellites and the redundancy of observations.

In the zero baseline case, the independent term and the P_{12}^{ij} (see Table 6.1) are supposed to be equivalent as the D_{12}^{ij} must be equal to zero (see section 4.5.3). Furthermore, as observation precision calculation is based on the standard deviation of the independent term, the smallest the independent term variance is, the best the observation precision.

The stable results of GPS L1 and L2 can be attributed to the the high number of visible satellites broadcasting these signals at any observation epoch (from 6 to 15 satellites).

GPS L1	North	East	Up	Independent term	P_{12}^{ij}
Standard deviation (m)	0.211	0.159	0.323	0.260	0.260
Mean (m)	-0.001	0.001	-0.005	0.003	0.003
Observation precision (m)	0.130				
Position precision (m)	0.418				
GPS L2	North	East	Up	Independent term	P_{12}^{ij}
Standard deviation (m)	0.228	0.173	0.382	0.299	0.299
Mean (m)	0.003	0.000	-0.012	0.001	0.001
Observation precision (m)	0.149				
Position precision (m)	0.478				

Table 6.1: Standard deviations and means in meters of Fig. 6.2

Table 6.1 gathers the statistics concerning GPS L1 and L2 figures on DOY 344. One can observe that GPS L1 seems to show better observation and position precisions than GPS L2. Nevertheless, the results obtained are very close. As predicted, the mean values of North, East and Up deviations are roughly equal to 0.

GPS L5 results

The GPS L5 signal is more difficult to handle (Fig. 6.4). Only 4 or 5 satellites simultaneously broadcast the signal to the ULG0 station at a given epoch. Therefore, the number of observation epochs is reduced when compared to GPS L1 and L2 signals. And, among those satellites, some show very low elevation values, which decreased the precision of the position estimation. Moreover, the geometry of the constellation is the reason behind the high PDOP values at certain epochs of the day. Finally, few epochs of observations are available, which affects the statistics calculated on this signal.

Among the 10 days of observation, a change in the general GPS L5 double difference shape can be observed. From Fig. 6.4, it can be seen that its general shape is constituted of two parts.

One presents high values of North, East and Up deviations. They are caused by the decrease of elevation of satellite 25 which induces a raise of the PDOP values. This shape corresponds to days juste before satellite 3 became operational.

From DOY 348 to DOY 353, the shape is modified by the addition of this new satellite in the observations. GPS L5 shape becomes more complicated, separated into four periods (Fig. 6.4). The

first one is representative of the real positioning quality that could be expected with the present GPS L5 satellite constellation (no peak of PDOP and only satellite 3 at low elevation values). The second one also includes satellite 3 observations but at higher elevation even though PDOP values are higher. Then, the PDOP decreases for a short number of epochs as the number of satellites increases to 5. The third part presents very high PDOP values, due to the apparition of the satellite 30 in the fourth-satellites constellation. This high PDOP deteriorates results on that part. Finally, a very small amount of results with low PDOP completes this shape.

The Fig. 6.3 illustrates the behaviour of the PDOP and the number of satellites over the DOY 350 observation period.

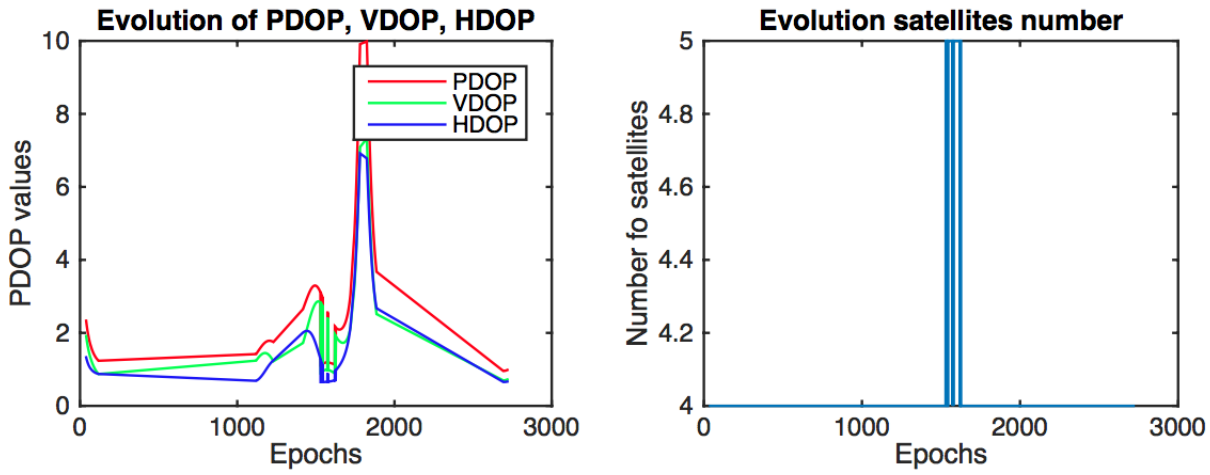

Figure 6.3: PDOP values and number of satellites on DOY 350 of year 2014 illustrating the addition of the satellite 3 to the GPS L5 satellites constellation

It is worth noticing that if the results affected by the PDOP peak, in the second GPS L5 shape, are removed from the analysis (from epoch 1745 to epoch 1886), the position precision is improved from $\sigma_{pos} = 1.518$ to $\sigma_{pos} = 1.012$ on DOY 350.

The two shapes of the GPS L5 code double difference are shown in Figure 6.4 and their characteristics are described in the Table 6.2.

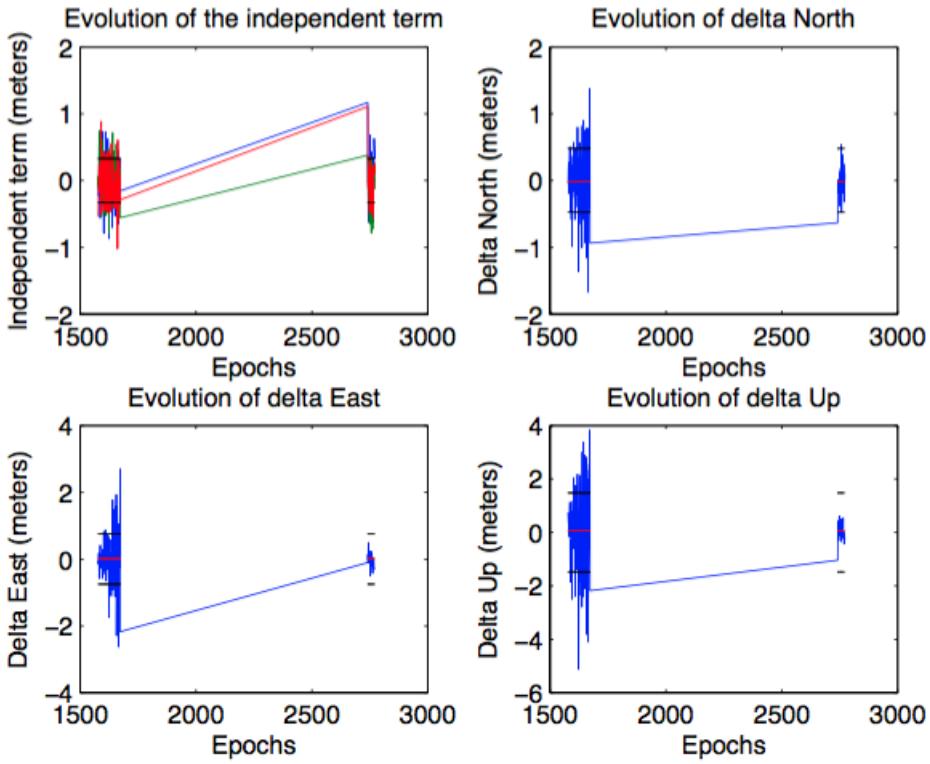

(a) GPS L5 (C5Q) with Trimble zero baseline (DOY 344)

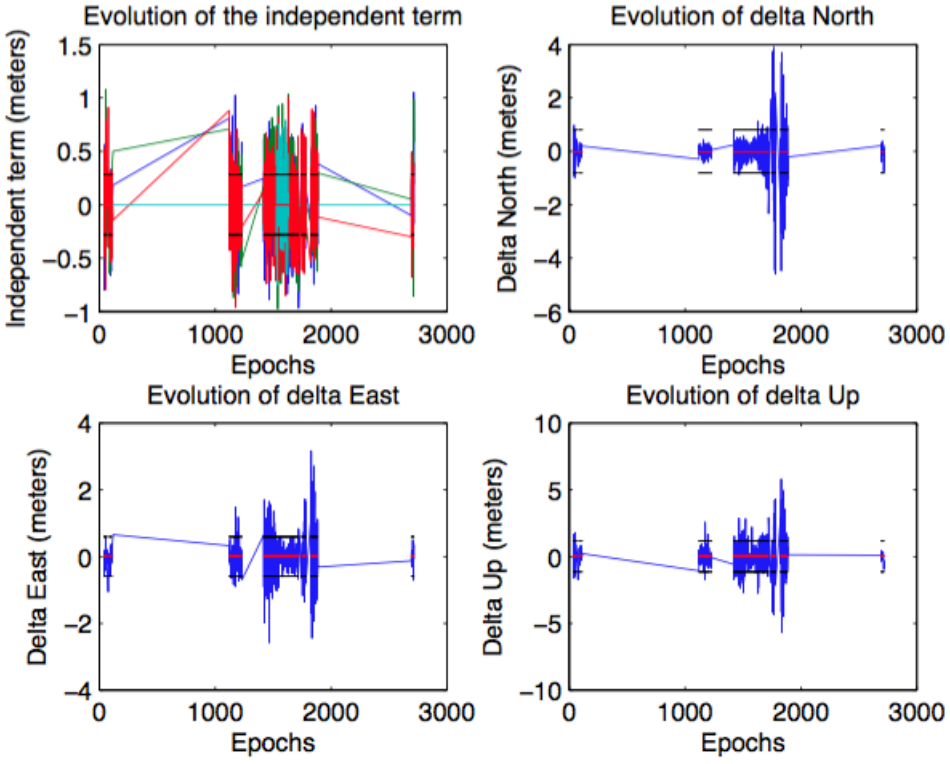

(b) GPS L5 (C5Q) with Trimble NetR9 zero baseline (DOY 350) with satellite 3

Figure 6.4: GPS L5 independent terms and code double difference positioning on the DOY 344 of year 2014 observed on the Trimble zero baseline. The red lines represent the average values, the black lines the standard deviations. On the independent term figures, the different colors correspond to the different double differences used in the computation

Table 6.2, which gathers GPS L5 statistics, shows a disparity between results using satellite 3 or not. The observation precision and the position precision seem to be improved by the arrival of this new satellite. Still, the position precision observed is more higher than with GPS L1 and L2, for reasons aforementioned (high PDOP values, low elevation satellite influence and lower number of visible satellites). Nonetheless, observation precision value reached with the addition of the satellite 3 outperform the GPS L2 one. Although GPS L5 suffers a lot from high PDOP and a limited number of visible satellites, the GPS L5 signal, if placed under similar observation conditions to GPS L2, it could reach better position precision as it observation precision is similar to GPS L2 one.

GPS L5 (without satellite 3)	North	East	Up	Independent term	P_{12}^{ij}
Standard deviation (m)	0.478	0.753	1.474	0.328	0.328
Mean (m)	-0.015	0.010	-0.064	-0.026	-0.026
Observation precision (m)	0.167				
Position precision (m)	1.723				
GPS L5 (with satellite 3)	North	East	Up	Independent term	P_{12}^{ij}
Standard deviation (m)	0.803	0.594	1.143	0.280	0.280
Mean (m)	-0.021	0.008	0.029	-0.003	-0.003
Observation precision (m)	0.140				
Position precision (m)	1.518				

Table 6.2: Standard deviations and means in meters of Fig. 6.4

The standard deviation values of the North, East and Up errors given in Table 6.2 are higher for GPS L5 than in GPS L1 and L2 cases. Moreover, average PDOP value on the GPS L5 signal is about 3 while only 1 or even less is reached on GPS L1 and L2 values (see Appendix). These elements deteriorate the position precision when using GPS L5.

Galileo signals results

Fig. 6.5 and 6.6 present the positioning results obtained with Galileo signals. They are available on a smaller number of epochs (over the whole observation period, approximatively from 50 to 500 epochs, depending on the DOY) than the GPS L1 and L2 ones due to their reduced constellation. This observation has also been made for GPS L5, whose number of simultaneous observed satellites does not exceed 5. The computed results only consider common epochs of signal observation. By this assessment, one must understand that when Galileo E5 is not seen, the results are not computed for Galileo E1, E5a and E5, and reversely.

Galileo E5 PDOP values are better than other Galileo signals for each day observed. This is due to the introduction of the correlation matrix of the double difference (see section 4.5.5). Observation precision values are required to construct this matrix. [Springer et al., 2013]'s observation precisions have been chosen as reference values (see Table 4.2). This matrix is included in the PDOP combination. Therefore, the PDOP values of Galileo E5 signal, which show better precision value, are lower than the others. The mean value of PDOP for Galileo E5 on this ten days period is 2.476. These value reach 5.858, 5.616, 5.719 in Galileo E1, E5a and E5b cases (see Appendix).

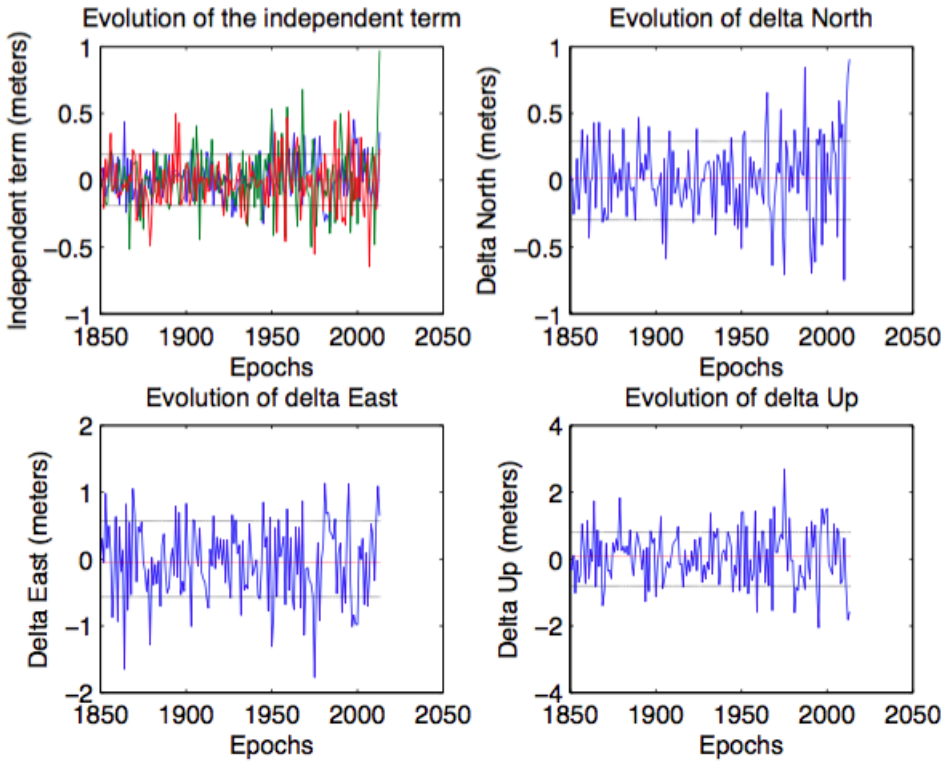

(a) Galileo E1 (C1C) with Trimble zero baseline (DOY 344)

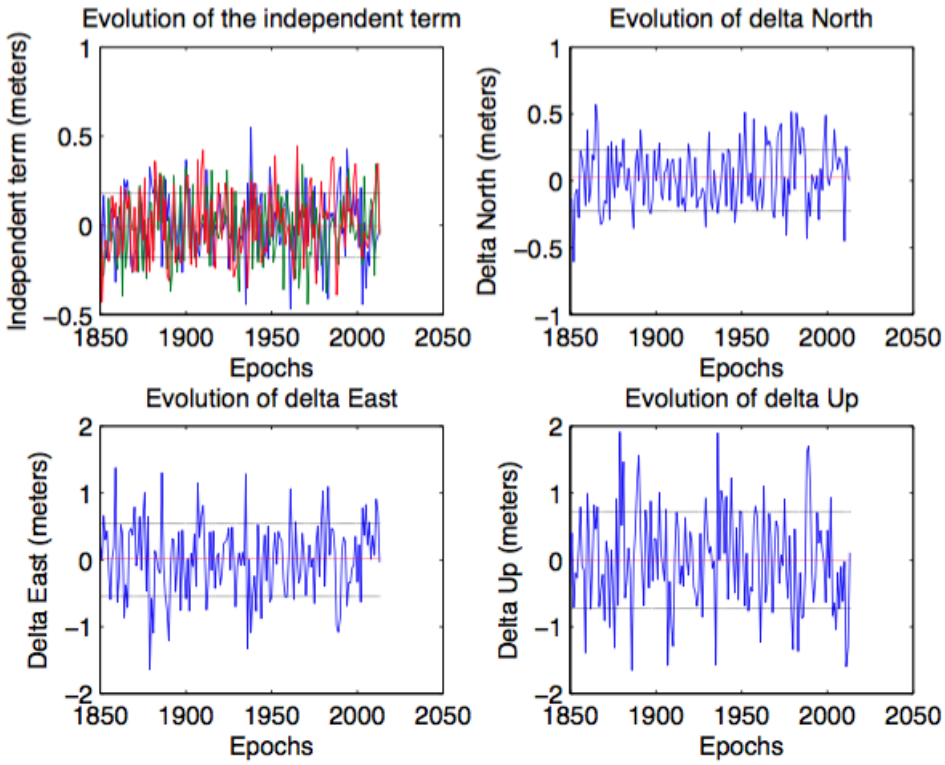

(b) Galileo E5a (C5X) with Trimble zero baseline (DOY 344)

Figure 6.5: Galileo E1 and E5a independent terms and code double difference positioning on the DOY 344 of year 2014 observed on the Trimble zero baseline. The red lines represent the average values, the black lines the standard deviations. On the independent term figures, the different colors correspond to the different double differences used in the computation

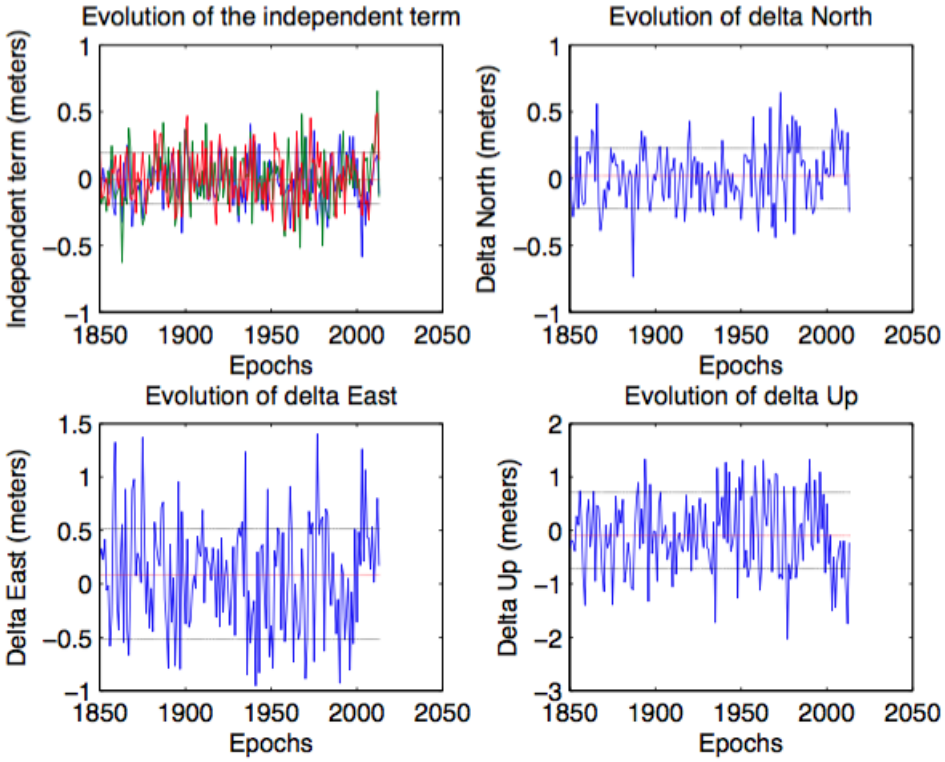

(a) Galileo E5b (C7X) with Trimble zero baseline (DOY 344)

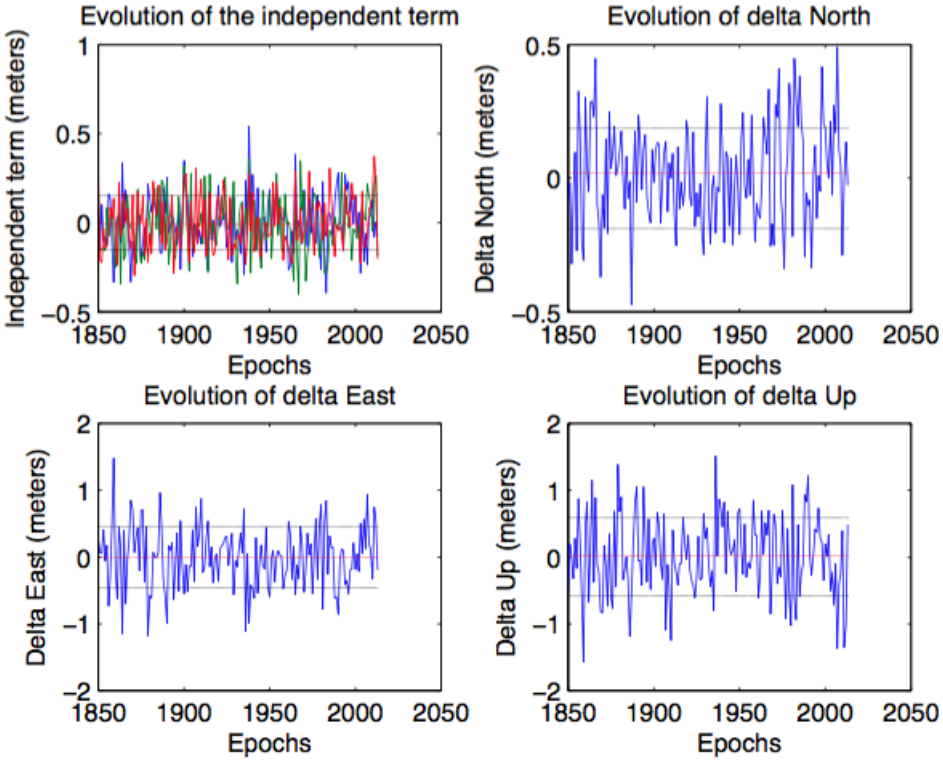

(b) Galileo E5 (C8X) with Trimble zero baseline (DOY 344)

Figure 6.6: Galileo E5b and E5 independent terms and code double difference positioning on the DOY 344 of year 2014 observed on the Trimble zero baseline. The red lines represent the average values, the black lines the standard deviations. On the independent term figures, the different colors correspond to the different double differences used in the computation

From Fig. 6.5 and 6.6, the PDOP of the double difference, which is a notion different from the PDOP of the single point positioning, is always under 3.5 on Galileo measurements and raises values to about 8 for GPS L5 signal. As a point of comparison, in a single point positioning computation realized the same DOY, the PDOP of Galileo signal reaches 7.5 and does not go beyond 4 whereas the GPS L5 PDOP values reach 10 at their maximums.

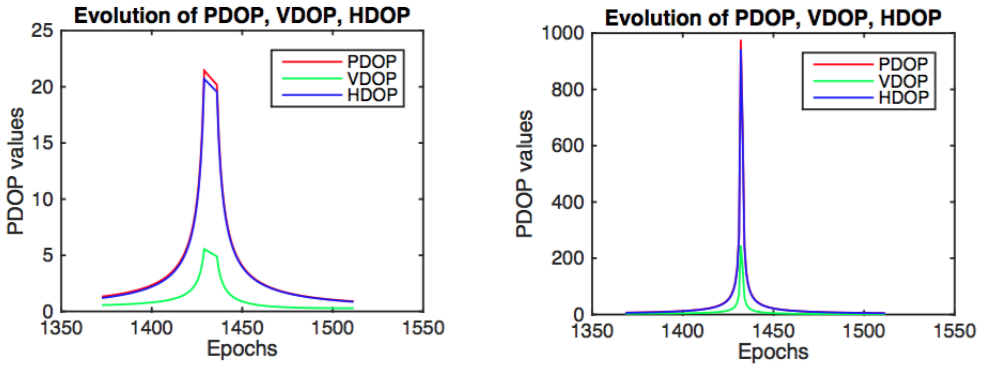

(a) Galileo E5 (C8X) in code double difference on ULG0 (Trimble receivers zero baseline) (DOY 347)

(b) Galileo E5 (C8X) in code single point positioning on ULG0 (DOY 347)

Figure 6.7: PDOP values between code single point positioning with Galileo E5a+b and code double difference with Galileo E5a+b on the ULG0 station on DOY 347 of 2014

Fig. 6.7 shows the mitigation of the PDOP in the double difference computation in comparison with PDOP values in single point positioning. The figures were obtained from DOY 347 analysis, where a high PDOP peak was observed.

When PDOP values from single positioning are compared to PDOP values from double difference, the PDOP peaks are positioned in the same manner but reduced in the double difference analysis (see Fig. 6.7). The high PDOP values in the double difference reflect very high PDOP values in single point positioning. Therefore, in this analysis, the double difference PDOP values are limited to 10 in order to avoid extremes values in the results.

Even if the number of observed satellites at a given epoch is reduced, thanks to the quality of the signals, Galileo observation precisions are better than GPS ones (see Table 6.3). Compared with GPS, Galileo clearly shows the best precision values with an observation precision better than 10 centimeters for every of its signals. Particularly, Galileo E5 presents the best value of observation precision with about 8 centimeters precision.

Yet, Galileo position precision does not allow the same precision as obtained with GPS L1 and L2 code pseudoranges measurements. The values presented for this DOY 344 are close to the average value of position precision for this 10 days period. While GPS L1 and L2 position precision ranges around 40 centimeters, the Galileo values are closer to the 1 meter (see Table 6.3).

This difference between observation precision and position precision is interesting. It reveals the importance of having a higher number of satellites, which leads to smaller PDOP values and redundant observations. Due to their 4 visible satellites constellation, Galileo signals, that show by far the best observation quality, present a precision on the positioning of the order of the meter.

From Table 6.3, the standard deviations of the North, East and Up errors are higher than in GPS L1 and L2 cases. These values are closer to the GPS L5 results. As in GPS L5 case, they

also result from more varying observation conditions.

Galileo E1	North	East	Up	Independent term	P_{12}^{ij}
Standard deviation (m)	0.294	0.569	-0.809	0.192	0.192
Mean (m)	0.015	-0.047	0.072	-0.002	-0.002
Observation precision (m)	0.096				
Position precision (m)	1.032				
Galileo E5a	North	East	Up	Independent term	P_{12}^{ij}
Standard deviation (m)	0.227	0.546	0.724	0.181	0.181
Mean (m)	0.027	0.014	-0.012	-0.004	-0.004
Observation precision (m)	0.091				
Position precision (m)	0.934				
Galileo E5b	North	East	Up	Independent term	P_{12}^{ij}
Standard deviation (m)	0.225	0.514	0.707	0.190	0.190
Mean (m)	0.021	0.085	-0.099	-0.008	-0.008
Observation precision (m)	0.095				
Position precision (m)	0.903				
Galileo E5	North	East	Up	Independent term	P_{12}^{ij}
Standard deviation (m)	0.188	0.456	0.587	0.154	0.154
Mean (m)	0.018	-0.003	0.018	-0.006	-0.006
Observation precision (m)	0.077				
Position precision (m)	0.767				

Table 6.3: Standard deviations and means in meters of Fig. 6.5 and 6.6

It should be noted that Galileo E1, which is the only Galileo satellite to benefit from the satellite E20 emissions, is represented in the figure 6.5 without this E20 satellite. The addition of satellite E20 in the constellation does not always lead to 5 visible satellites for Galileo E1. On the contrary, it is often the fourth satellite of the constellation. However, it allows positioning results on a higher number of epochs when considered. Indeed, it completes a three visible satellite constellation that would not allow positioning with the other frequencies. In DOY 344 case, considering the E20 satellite adds 318 epochs of observations to the initial 164 number obtained with Galileo E1 without E20, E5a, E5b and E5.

In Table 6.4 of results, the comparison has been made between observation and position precisions considering or not the E20 satellite. When not considered, the same epochs of observation than in Galileo E5a, E5b and E5 cases are used to compute statistics.

General results

The average, minimum, maximal and standard deviation values of observation precision (σ_{obs}) and position precision (σ_{pos}) of the whole observation period (DOY 343-353) are gathered in the next Table 6.4. As mentioned in the introduction paragraph, the observations with double difference PDOP values higher than 10 have been removed from the statistical analysis. Similarly, no elevation mask was used as many Galileo satellites appear only at low elevation.

	GPS				
$\sigma_{obs}(m)$	L1	L2	L5	L5 (incl. satellite 3)	
Mean	0.135	0.151	0.166	0.139	
Min	0.130	0.144	0.158	0.138	
Max	0.141	0.158	0.170	0.140	
Standard deviation	0.004	0.005	0.004	0.001	
$\sigma_{pos}(m)$					
Mean	0.425	0.475	1.675	1.462	
Min	0.417	0.457	1.648	1.365	
Max	0.431	0.507	1.723	1.518	
Standard deviation	0.006	0.017	0.042	0.084	
$\sigma_{pos}(m)$ limited to 4 satellites					
Mean	2.652	2.254			
Min	2.616	2.082			
Max	2.687	2.389			
Standard deviation	0.028	0.123			
	Galileo				
σ_{obs} (m)	E1	E5a	E5b	E5	E1(incl. E20)
Mean	0.076	0.0967	0.100	0.079	0.073
Min	0.059	0.090	0.095	0.077	0.066
Max	0.096	0.117	0.110	0.08	0.079
Standard deviation	0.014	0.010	0.005	0.001	0.005
$\sigma_{pos}(m)$					
Mean	1.609	1.615	1.612	1.531	0.720
Min	0.802	0.934	0.903	0.767	0.446
Max	2.811	2.041	2.185	2.228	1.799
Standard deviation	0.734	0.464	0.473	0.502	0.532

Table 6.4: Precision of observations and positions in meters obtained with code double differences on the DOY 343-353 period observed by the Trimble receivers on ULG0 station in zero baseline mode.

From Table 6.4, the following conclusions can be drawn:

- Firstly, as already observed in the previous figures, the **observation precisions** of the Galileo signals are better than 10 centimeters. On this basis, a classification of the signals can be done. The best results are shown by Galileo E1, followed by Galileo E5 and then E5a and E5b.
  In the zero baseline double difference, the only remaining error affecting the signal is the receiver inherent part of the observation noise. However, from Table 5.2, the highest observation noise values were expected on Galileo E1 when Trimble receivers are used. Galileo E1 without satellite 20 showed the highest PDOP values in this study. Therefore, it defines the minimal number of epochs observed. Galileo E5, with its low PDOP values showed often more observation epochs but had to be restrained to the Galileo E1 observation epochs. Still, after analysis of Galileo results when all its observation epochs are considered, this classification remains unchanged. This unexpected result could be due to this demodulation technique used by the Trimble receivers. As seen in chapter 2, four demodulation techniques of the AltBOC signal exist but only one conserves the great properties of the signal. The receiver conception being a well kept secret, this assumption remains unproved.

- Concerning Galileo E1, the addition of the fifth satellite improves the **observation precision**. In fact, values systematically lower when E20 is considered can be observed. The minimal values given in this table are similar to GPS L1 or L2. Yet, E20 shows lower signal to noise

ratio on the signals transmitted than the other satellites. It should therefore be more affected by the noise than other satellites thus leading to worse observation results.

- Furthermore, as it often constitutes the fourth satellite of the constellation and sometimes the fifth satellite, PDOP values are lowest than when this satellite is considered (2.775 when E20 is considered versus 5.858 when E20 is not considered). This gives an idea of the effect of high PDOP values on **position estimation**. The addition of this satellite also allows considering more observation epochs in the computation.

- As far as the **position precision** is concerned, Galileo E5 signal shows the best results among the Galileo signals (except for Galileo E1 signal considered with E20). At equal elevation values, this is explained by the lower PDOP values presented by the Galileo E5 signal (for reasons aforementioned) due to signal expected quality.

- The study of GPS signals according to both their observation precision and position precision leads to the following classification: GPS L1 provides the best results, followed by GPS L2 and finally GPS L5. Yet, when the satellite 3 is added to the GPS L5 constellation, an improvement in the **observation precision** can be seen. GPS L5 is then in second place of the classification, which is a position more appropriate in view of the expected results for this signal ([Springer et al., 2013]).

- Similarly, this addition modifies the mean of **position precision**. The reason is that the addition of satellite 3 changes the visible geometry, leading to a PDOP decrease (from 3.413 to 2.774 when considering the satellite 3). This satellite also increases the number of observations and may help in obtaining position estimations by joining an incomplete constellation (see Fig. 6.4).

- A last point that is worth being mentioned concerning GPS L1 and L2 signals is the **standard deviation of the position precision**. Its value is extremely small compared to the one observed on Galileo signals. This makes GPS L1 and L2 very reliable signals over time, thanks to the high number of satellites (12 to 15) which bring redundant information and low PDOP values (see Appendix).

- When GPS and Galileo results are compared, it is obvious that **position precision** is better on the GPS signals (around 40 centimeters for both GPS L1 and L2 signals). GPS L5 has a meter and a half of precision, hence is closer to the Galileo results (between 1.531 meters on Galileo E5 to 1.615 meters on Galileo E5a).

- When the results of the reduced constellation of GPS are compared to the Galileo results, a clear superiority of Galileo signals appears. In such a GPS reduced constellation, the PDOP values of GPS L1 and L2 are respectively, 2.838 and 3.466, and these values are even lower than the Galileo ones (except for Galileo E5). However, Galileo signals reach better positioning values than GPS when its constellation is reduced thanks to their low observation precision value. Values of elevations of this reduced constellation are very similar to those observed with Galileo (approximatively 40 degrees for Galileo versus 37.5 degrees for GPS L1 and 39 for GPS L2).

To conclude with Trimble results from Table 6.4, Galileo signals reach meter precision whereas GPS ones reach decimeter precision on the estimated position. Even if only a reduced part of the observation noise alters the signal quality, the position is altered by PDOP values, low satellite number and low elevation satellites on Galileo and GPS L5. Hence, Galileo shows less accurate results on positioning than those obtained with GPS. Still, when the comparison is done with the GPS reduced constellation, the results of GPS L1 and L2 are worse than those obtained with Galileo.

6.1.3 Septentrio receivers

The Septentrio data in 2014 provided only one day of observation which included Galileo E5 signal. For this reason, data from 2015 has also been collected in order to compute statistics. This lack of Galileo E5 observation is due to a particularity of the Septentrio XS receiver, already mentioned in the Trimble case introduction. As less channels are available, the number of epochs of observation of the Galileo signal was limited. Therefore, a sort has been realized in the 2015 data collection in order to only consider *days of year* presenting more than 30 epochs of observation on Galileo E5 signal. But among these days, many results were degraded by high PDOP values. Out of the collection of data 2015, some days revealed lower PDOP values and a large number of observations. Such conditions were met every 10 days of observations.

The data collected in the year 2015 consisted in 120 successive days (from DOY 60 to DOY 180). Two days in each 10-days period have been selected for their low PDOP values and high number of observations on Galileo E5 (approximately 200 epochs). Therefore, among the 120 initial days of observation, only 24 days of observations were computed. And among those 24 days, 12 days did not include Galileo observations and one only measured 5 epochs of observation. The 11 others days were used to compute statistics.

This selection of days among others should give a better estimation of the position precision that might be expected when the full Galileo constellation will be available. It is worth noticing that the last 3 days of observations (DOY 153, 154 and 173) included observations from new satellites E22 and E26 observations.

Figures 6.8, 6.9, 6.10 and 6.11 and represent the GPS and Galileo results of the code double differences on each of the studied signal on DOY 84 of 2015. During the period of observation (from the 1^{st} March to the 29^{th} of June), one more GPS satellite of the Block IIF became fully operational (the satellite 26, in the 20^{th} of April). The Galileo constellation also changed as the satellites E22 and E26, launched in March 2015, will appear in the constellation.

General observations

A very first general observation can be made on the Septentrio receiver results regarding precision. Both **position and observation precision** appear to be better with Septentrio than with the Trimble receiver. This can be easily observed on the Fig. 6.9, 6.10, 6.11 and 6.8 where the variances of the Galileo and GPS distributions are reduced on North, East and Up positions as well as on the independent term.

Such a reduction of the variance on the independent term was expected by [Caelen, 2014] observation noise given in Table 5.2. The Septentrio receivers showed lower values of observation noise than the Trimble receiver. Therefore, a higher **signal quality** was expected on those receivers.

As concerned the **position precision**, average PDOP values of both Galileo and GPS double difference results were similar to those of the Trimble receivers. The mean elevation values observed also appeared to be equivalent. Therefore, as most of the time the additional satellites of the GPS and Galileo constellation did not offer the possibility of a fifth visible satellite, the position precision improvement observed with Septentrio receivers is mainly due to the improvement of the observation precision.

Secondly, the Septentrio receiver observations appear not to be simultaneous. This particularity implies two effects.

- As observations are not simultaneous, the clock errors of each receiver are different. If one supposes that the clock error of the receivers could reach 0.5 milliseconds, the offset of time

between the two observations made by the two receivers could lead to observe a clock error of 0.5 on one receiver, and -0.5 on the other. Therefore, in the double difference, the difference between those two clock errors would lead to an error of one millisecond instead of suppressing them.

- Similarly, as the satellites are not observed at the same moment by the two receivers, the orbital coordinates of the satellites are different. Therefore, the D_{12}^{ij} term is not equal to zero as the distance from the receivers to the satellites varies with the considered receiver for the same observed satellite. And then, the P_{12}^{ij} and independent term are not equivalent. The independent term is reduced and therefore the positioning results are better than it should be.

The combination of these effects is observed in the results (see Tables 6.5 and 6.6). It allows explaining the offset on the East error which can be observed from the results.

GPS results

From Fig. 6.9, a few peaks arise from the GPS L2 double difference results. These peaks are also present in the distribution of GPS L2 obtained with Trimble. But, in Trimble case, they are not visible due to the larger variance observed for this receiver. These peaks are due to a diminution of visible satellites (6 or 7) or very small PDOP peaks when too many satellites are located in high elevation.

The second important point when observing GPS L1 and L2 figures is the jump that occurs during the observation period. This jump is due to a particular characteristic of the Septentrio receivers. When the clock error becomes larger than a given threshold, it is automatically readjusted by the receiver, giving rise to a jump in the receiver clock time scale. It can be seen from Fig. 6.9 that such a clock jump affects the position estimation (mainly the East component).

Double difference results on GPS L5 also appear to be better than in Trimble case. The standard deviations on North, East and Up errors only reach 0.120, 0.099 and 0.177 whereas values of 0.478, 0.753 and 1.474 were observed on Trimble. These differences are engendered both by a diminution of the PDOP (average value of 3.093 in Trimble case for and average value of 2.26 in Septentrio case) and an improvement of the quality of the tracked signal (from 15 centimeters to 4 centimeters). This diminution of the PDOP might be due to the rearrangement of the orbits of the GPS satellites caused by the arrival of an additional satellite. As regards the improvement of signal quality, it is mainly due to the Septentrio receiver accuracy but also to the fact that Trimble receivers tracked more low elevation satellites. Therefore, the quality of the received signal was altered on Trimble receivers.

Still, the GPS L5 signal (Fig. 6.8) is altered by high PDOP peak, that can be found on each day of the analyzed period.

Table 6.5 presents the parameters associated to the Fig. 6.9 and 6.8.

From this table, one can observe that a clear offset appears on the East deviation, for whatever signal considered. This offset could be explained by the non simultaneity of the observations.

On the DOY 84, GPS L5 is the best signal observed, both in terms of **observation and position precision** (5 centimeters of observation precision and 23 centimeters on position). This quality in observation and position was expected on this signal but the Trimble results of 2014 did not assess it. Otherwise, the three signals show similar values of **position precision** but different values of **observation precision** due to different PDOP values (values under 1 for GPS L1 and L2 and above 2.5 for GPS L5).

GPS L1	North	East	Up	Independent term	$P_{12}^{i,j}$
Standard deviation (m)	0.124	0.128	0.201	0.191	0.294
Mean (m)	-0.006	0.121	-0.004	-0.002	-0.011
Observation precision (m)	0.096				
Position precision (m)	0.269				
GPS L2	North	East	Up	Independent term	$P_{12}^{i,j}$
Standard deviation (m)	0.100	0.111	0.182	0.158	0.276
Mean (m)	-0.000	0.119	0.002	0.002	-0.011
Observation precision (m)	0.079				
Position precision (m)	0.236				
GPS L5	North	East	Up	Independent term	$P_{12}^{i,j}$
Standard deviation (m)	0.120	0.099	0.177	0.101	-0.010
Mean (m)	-0.004	0.138	-0.006	0.004	0.270
Observation precision (m)	0.051				
Position precision (m)	0.235				

Table 6.5: Standard deviations and means in meters of Fig. 6.9 and 6.8

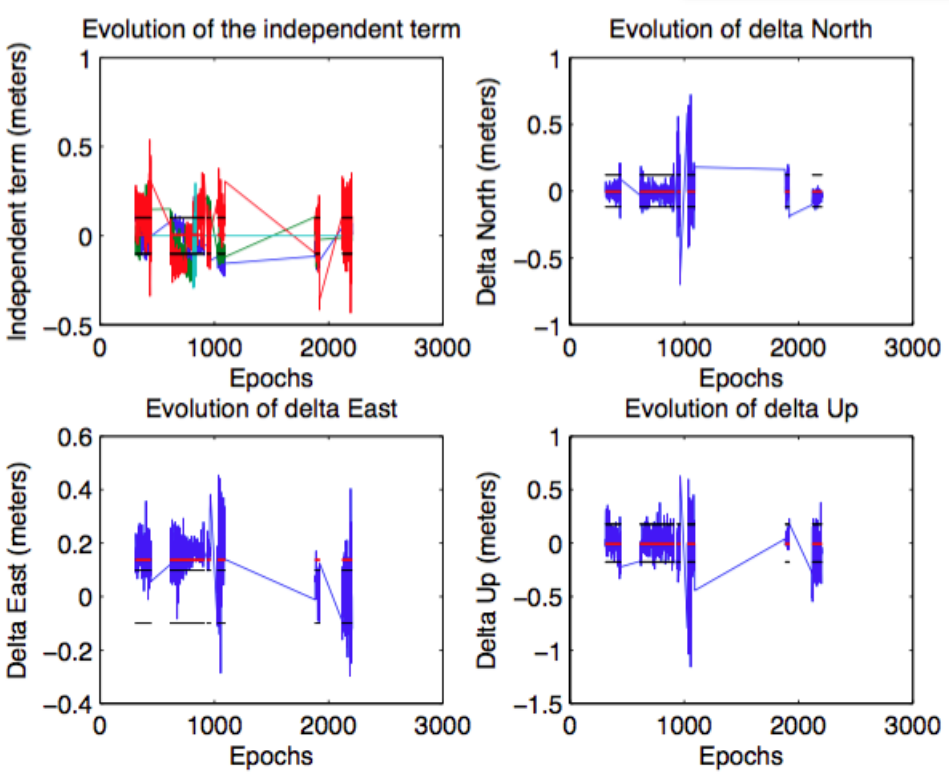

Figure 6.8: GPS L5 (C5Q) independent term and code double difference positioning on the DOY 84 of year 2015 observed on the Septentrio zero baseline. The red lines represent the average values, the black lines the standard deviations. On the independent term figures, the different colors correspond to the different double differences used in the computation

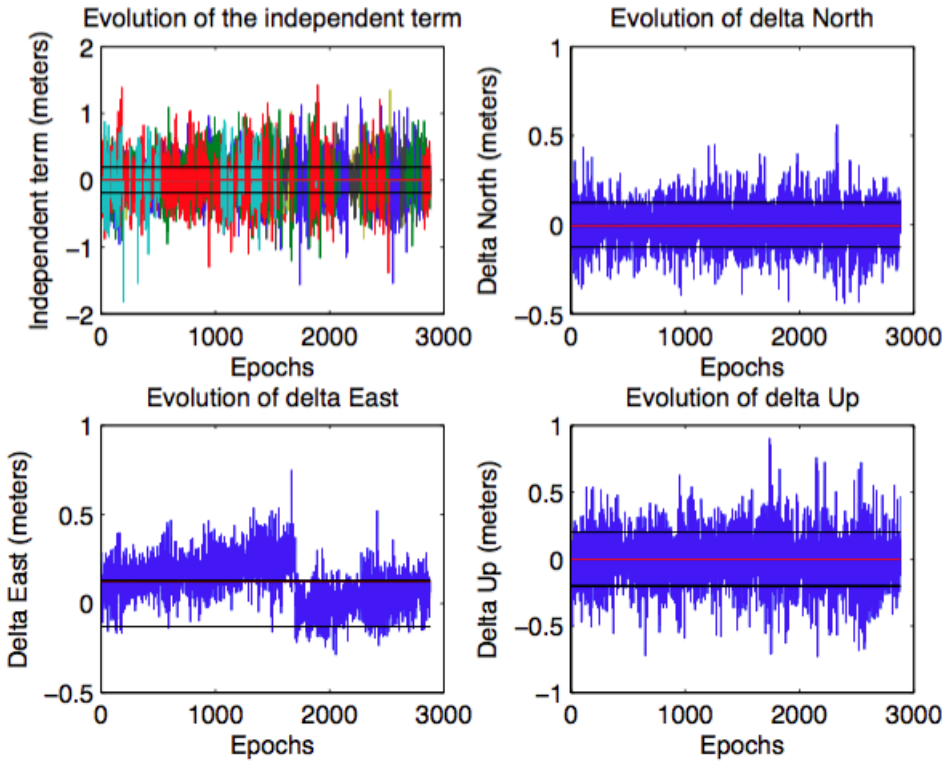

(a) GPS L1 (C1C) with Septentrio zero baseline (DOY 084)

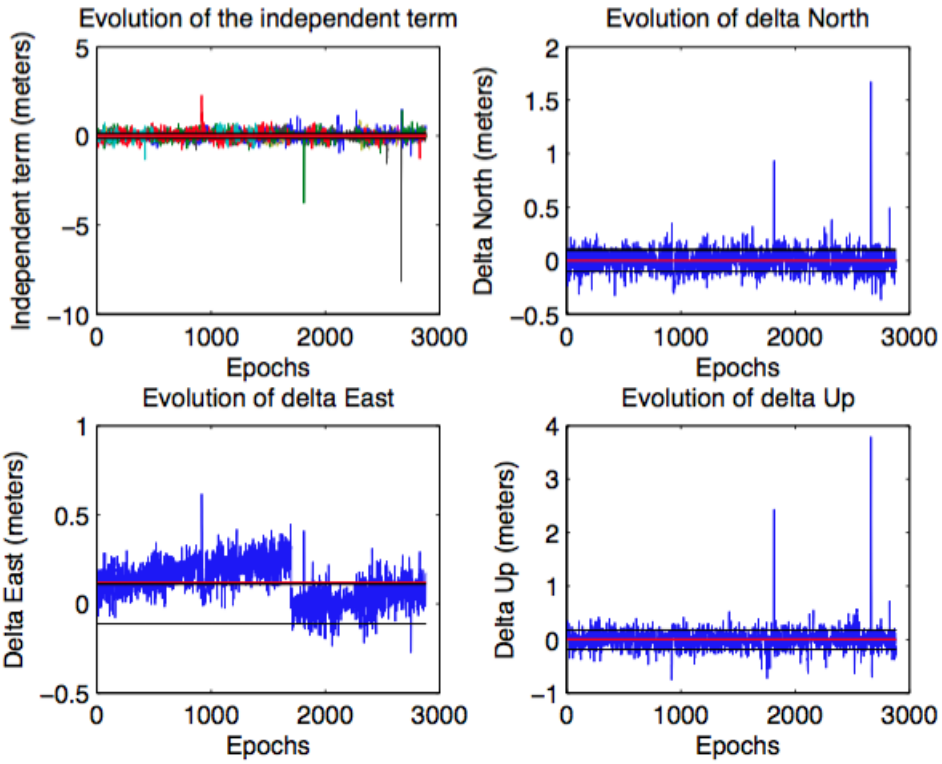

(b) GPS L2 (C2W) with Septentrio zero baseline (DOY 084)

Figure 6.9: GPS L1 and L2 independent terms and code double difference positioning on the DOY 84 of year 2015 observed on the Septentrio zero baseline. The red lines represent the average values, the black lines the standard deviations. On the independent term figures, the different colors correspond to the different double differences used in the computation

Galileo results

Figures 6.10 and 6.11 illustrate the Galileo double difference results. The variance of the North, East and Up errors are very low as compared to the Trimble ones. And thus, the obtained position precisions are also better with the Septentrio receivers.

In each figure, a hole in the results is observed. It is due to a PDOP peak that appears at the very beginning of the observations. The size of this peak increases from Galileo E5a to E5b to E1 and the smallest peak observed is for Galileo E5. The reason is linked to the observation precision used in the correlation matrix creation. As already mentioned, [Springer et al., 2013]'s results have been taken as a reference (see Table 4.2). Therefore, PDOP values are smaller on Galileo E5 and this is the reason why more epochs of observation are available. In the statistics analysis, all the results have been reduced to the minimal number of observations obtained on Galileo signals.

This DOY maintains PDOP values of 6 on each side of the PDOP peak. However, an exception is made for Galileo E5 whom values are closer to 2 for reason aforementioned.

Table 6.6 presents the statistics associated to the Fig. 6.10 and 6.11.

Galileo E1	North	East	Up	Independent term	$P_{12}^{i,j}$
Standard deviation (m)	0.202	1.011	0.231	0.114	0.113
Mean (m)	0.009	0.092	-0.057	0.055	-0.140
Observation precision (m)	0.057				
Position precision (m)	1.057				
Galileo E5a	North	East	Up	Independent term	$P_{12}^{i,j}$
Standard deviation (m)	0.166	0.768	0.179	0.086	-0.127
Mean (m)	0.005	0.002	-0.094	0.068	0.091
Observation precision (m)	0.043				
Position precision (m)	0.806				
Galileo E5b	North	East	Up	Independent term	$P_{12}^{i,j}$
Standard deviation (m)	0.191	0.900	0.213	0.097	0.099
Mean (m)	0.007	0.145	-0.045	0.052	-0.147
Observation precision (m)	0.049				
Position precision (m)	0.945				
Galileo E5	North	East	Up	Independent term	$P_{12}^{i,j}$
Standard deviation (m)	0.059	0.413	0.084	0.023	0.043
Mean (m)	0.025	0.131	-0.061	0.058	-0.143
Observation precision (m)	0.012				
Position precision (m)	0.426				

Table 6.6: Standard deviations and means in meters of Fig. 6.10 and 6.11

With Septentrio, Galileo signals show better results than with the Trimble receivers. The **position precision**, reaching 1.5 meters in Trimble case only reaches values under 1 meter. Similarly, values of **observation precision** decreased from 7-8 centimeters with Trimble to reach 4-5 centimeters with Septentrio.

As in GPS case, an offset can be observed on the East error. It might be associated to the combined effect of the orbit and clock effects resulting from the non simultaneity of observation. In the same way, the P_{12}^{ij} are not equivalent to the independent term.

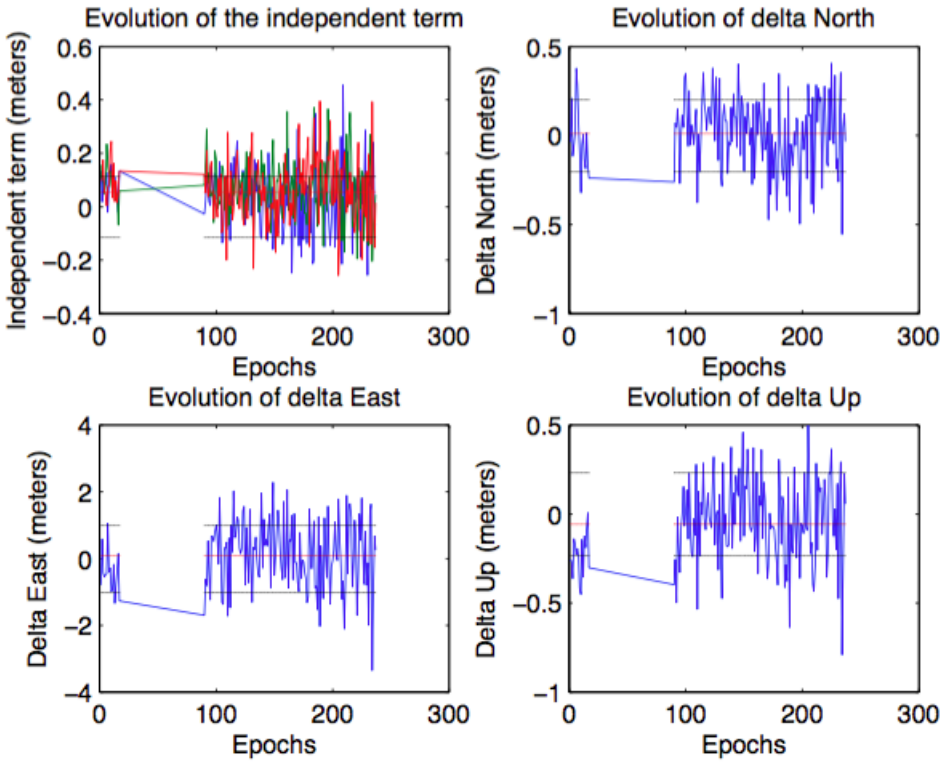

(a) Galileo E1 (C1C) with Septentrio zero baseline (DOY 084) limited to 4 satellites

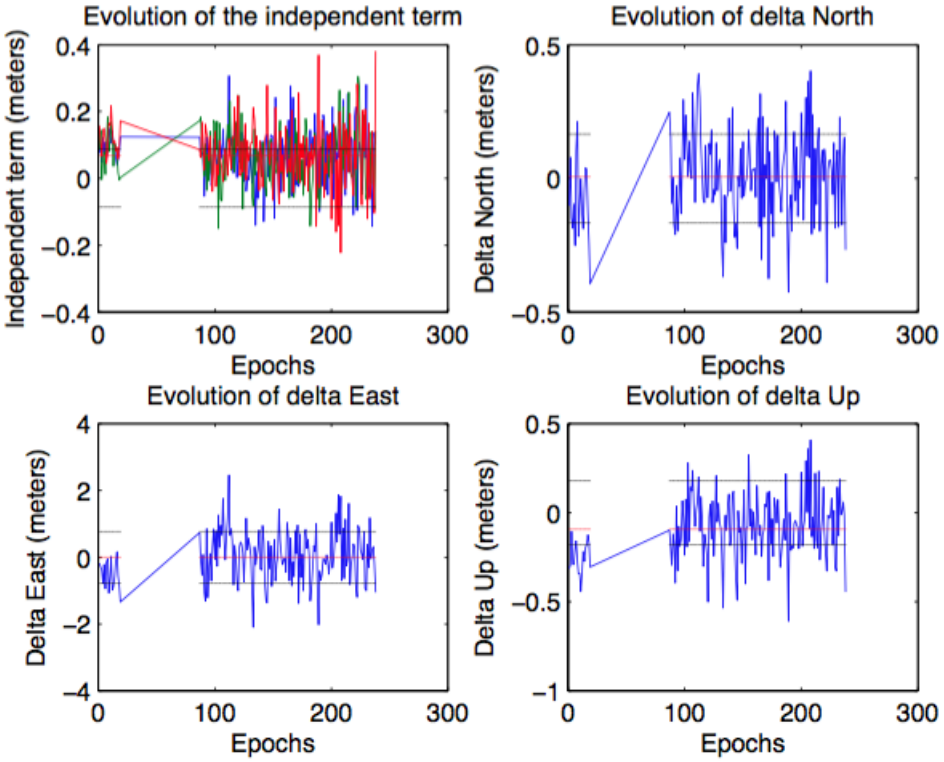

(b) Galileo E5a (C5Q) with Septentrio zero baseline (DOY 084)

Figure 6.10: Galileo E1 and E5a independent terms and code double difference positioning on the DOY 84 of year 2015 observed on the Septentrio zero baseline.The red lines represent the average values, the black lines the standard deviations. On the independent term figures, the different colors correspond to the different double differences used in the computation

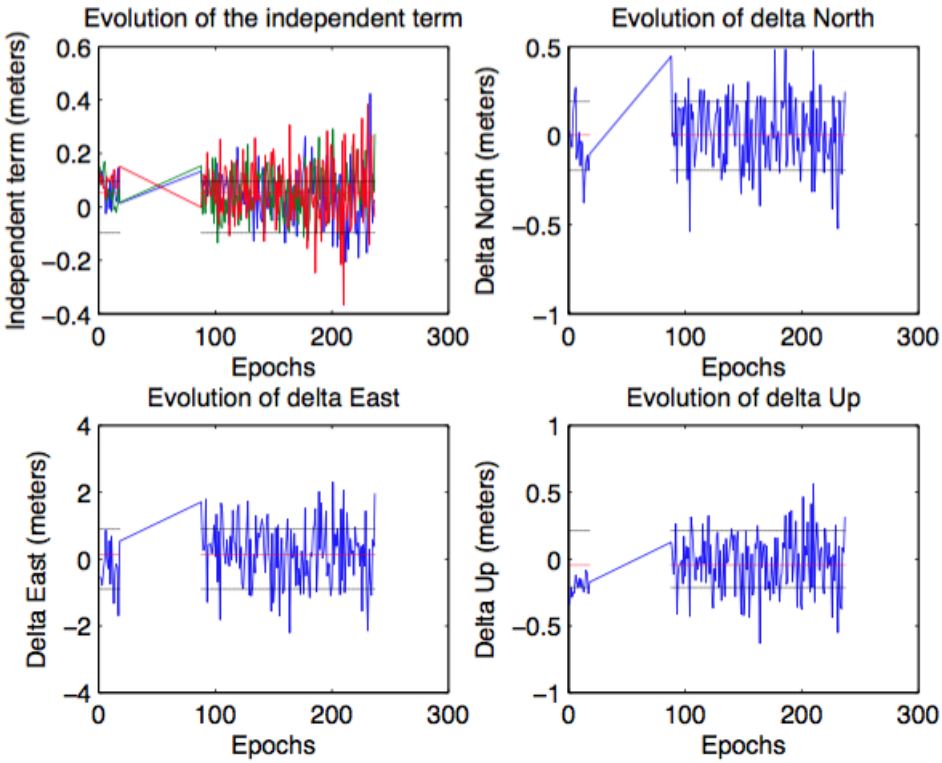

(a) Galileo E5b (C7Q) with Septentrio zero baseline (DOY 084)

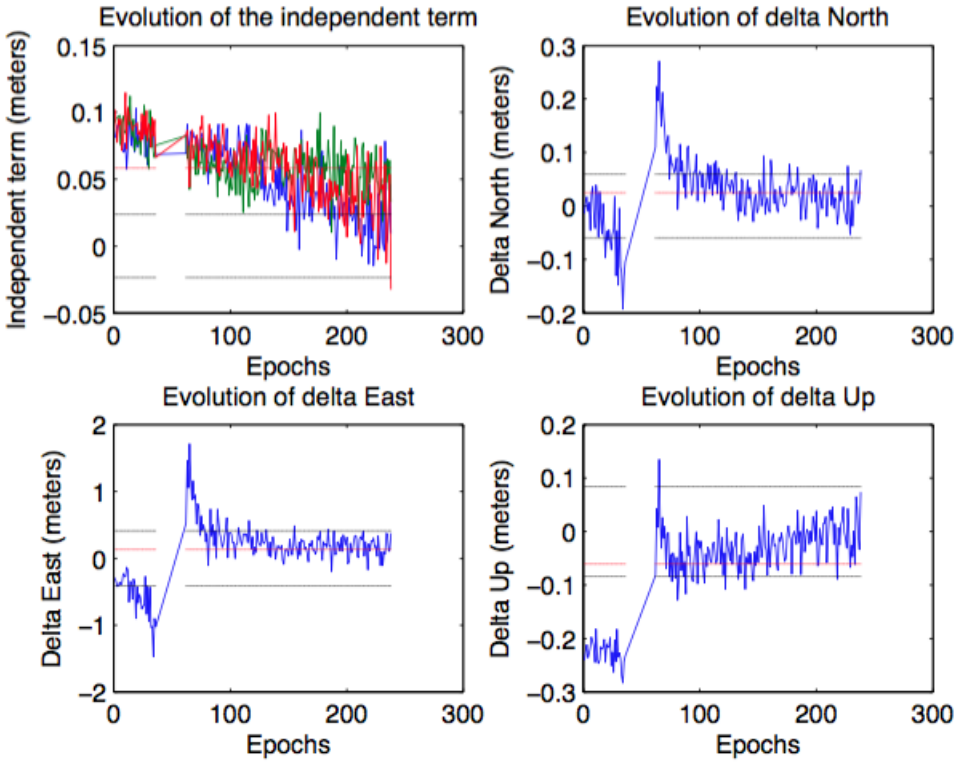

(b) Galileo E5 (C9Q) with Septentrio zero baseline (DOY 084)

Figure 6.11: Galileo E5b and E5 independent terms and code double difference positioning on the DOY 84 of year 2015 observed on the Septentrio zero baseline.The red lines represent the average values, the black lines the standard deviations. On the independent term figures, the different colors correspond to the different double differences used in the computation

General results

Table 6.7 collects the statistics on the 11 days of observation chosen.

	GPS				
$\sigma_{obs}(m)$	GPS L1	GPS L2	GPS L5		
Mean	0.089	0.067	0.041		
Min	0.083	0.058	0.031		
Max	0.097	0.079	0.055		
Standard deviation	0.006	0.009	0.010		
$\sigma_{pos}(m)$					
Mean	0.261	0.210	0.221		
Min	0.250	0.197	0.179		
Max	0.275	0.236	0.270		
Standard deviation	0.008	0.013	0.029		
$\sigma_{pos}(m)$ limited to 4 satellites					
Mean	1.854	1.177			
Min	1.639	0.996			
Max	2.103	1.356			
Standard deviation	0.180	0.122			
	Galileo				
σ_{obs} (m)	E1	E5a	E5b	E5	E1(sat E20)
Mean	0.051	0.039	0.040	0.010	0.056
Min	0.035	0.027	0.028	0.005	0.046
Max	0.071	0.052	0.056	0.026	0.065
Standard deviation	0.013	0.009	0.010	0.006	0.007
σ_{pos}	E1	E5a	E5b	E5	E1(sat E20)
Mean	0.846	0.623	0.664	0.190	0.691
Min	0.466	0.297	0.316	0.055	0.547
Max	1.251	0.899	0.998	0.504	0.948
Standard deviation	0.276	0.194	0.245	0.133	0.119

Table 6.7: Precision of observations and positions in meters obtained with code double differences on the DOYs 60-120 period of year 2015 observed by the Septentrio receivers on Sart-Tilman ULG1 position in zero baseline mode

From Table 6.7, many conclusions can be drawn:

- Galileo E5 is highly superior to all other considered signals. Its superiority is both assessed on the **observation and position precision** with mean value of observation precision of 1 centimeter and a position precision of 19 centimeters.
- Among the Galileo signals, the E5a frequency is always slightly more precise as far as **observation and position precision** are concerned than E5b. Galileo E1 signal shows the lowest value in terms of both **position and observation precision**.
- Regarding GPS, the L5 signal seems to outperform GPS L1 and L2 as far as **observation precision** is concerned. With values close to the GPS L2, GPS L5 also shows a great improvement in **position precision** than when observed with the Trimble receivers. As already discussed, this position precision can be explained by lower PDOP values, the rearrangement of the satellite planes and the lower observation precision.
- Values of GPS for the reduced constellation are not as essential as in Trimble case as the Galileo E5 superiority is shown even without considering it. Nonetheless, the advantages of

a numerous satellites constellation over low numbered satellites constellation clearly appears from these results. The mean PDOP value is approximately 3, which is still lower than the 5 observed on Galileo E1, E5a and E5b. However, as in Trimble case, Galileo position precision, even with higher PDOP is better than GPS results with the reduced constellation.

- From the minimum values given, one can observe that 5 millimeters have been reached with Galileo E5 on **observation precision** and 5 centimeters on **position precision** on a particular DOY.

- The contribution of the satellite E20 to the Galileo E1 signal is more important in terms of **position precision** than in terms of observation precision, as already observed in the Trimble case.

- As in Trimble case, it is important to highlight the stability of GPS L1 and L2 values along the observation days. This particularity results in their high number of satellites and observations. Nonetheless, the GPS and Galileo signals also show low standard deviation values but only on the **observation precision** (except for Eb).The GPS L5 and Galileo signal tends to be more variable when position precision is concerned.

- The choice of "good" days of observation for the Galileo signals among the 120 initial days might also have contributed to reach better position (low PDOP) and observation (high elevation) precisions.

- When both signals are compared, it is clear that Galileo, with its constellation of visible satellites reduced to four or five, is not able to compete with GPS L1 and L2 concerning the **position precision** apart from Galileo E5 signal which even outperforms GPS results. Nonetheless, values obtained are at a decimeter precision, which is what was initially expected (see chapter 3). The GPS L5 signal shows better results with its new satellites than when observed with Trimble. This improved constellation allows it to show very low position precision for a higher observation precision than Galileo E5. Indeed, its observation precision could be compared with Galileo E5a or E5b ones but it leads to better position results.

- Still, with a reduced constellation, GPS presents worse precisions than Galileo, which is positive for the future results with full Galileo constellation. However, Galileo E5 seems to be able to reach better position precision than the GPS L1 and L2 signals on these days with low PDOP values.

6.1.4 Zero baselines comparison

When comparing Tables 6.7 with Table 6.4, both gathering statistics concerning the double difference results, important differences need to be commented.

Firstly, the precisions obtained with the Septentrio baseline are better than those with the Trimble baseline, in both terms of **observation and position precision**. This observation had also been made by [Caelen, 2014] as concerns the **observation precision**. He compared the two receivers in zero baseline and observed a lower noise generated by the receiver with Septentrio than with Trimble. Furthermore, he also noticed a better tracking precision on the GPS L5 frequency with the Septentrio. This last assessment is also verified in this dissertation.

This improvement of the observation precision is the reason of the improvement of the position precision. Indeed, values of PODP remain similar (see Appendix) on both baselines.

Concerning the improvement of the Galileo observation precision, the code pseudoranges recorded by the Septentrio receiver are different from those recorded by the Trimble receiver. In addition to the lowest observation noise of the Septentrio receiver, the codes recorded by Septentrio may show

a lower signal to noise ratio than the one tracked by the Trimble receiver (see Table. 5.7).

Galileo E1 and GPS L5 are the signals that show the most different values from Trimble results to Septentrio results. Galileo E1 was the most accurate regarding the observation precision and the second more accurate for the position precision with Trimble. It occupies the last place on the Septentrio baseline generally speaking. On the contrary, the GPS L5 signal, which showed the worse results in position precision with Trimble, even with the addition of the satellite 3, shows results similar to the GPS L1 and L2 with Septentrio.

When compared with the classification of signals given by [Springer et al., 2013] in the Table 4.2, the Septentrio classification seems to perfectly match this order, for every signal considered. However, values of observation precisions obtained in this dissertation are better than those reached by [Springer et al., 2013].

To conclude, decimeter precision can be reached on **position** estimation for every of the considered signals with Septentrio. With Trimble, only the minimum values reach such a position precision level on the Galileo signals. As regards the GPS signals, GPS L1 and L2 reach the decimeter precision on each baseline while GPS L5, even when considering its minimum value, is not able to achieve position precision at decimeter level on the Trimble baseline. Furthermore, values obtained with GPS L1 and L2 are the best positioning values on both baseline (except for Galileo E5 and GPS L5 with Septentrio receivers).

On the contrary, the best **observation precision** values are obtained with Galileo signals on both baselines (except for GPS L5 with the Septentrio receivers). This last point concerning the observation precision is by far the most important. It allows considering precise positioning with Galileo signals when the complete constellation will be available, reducing thereby the PDOP values and high number of low elevation satellite observed.

6.1.5 Short and medium baselines

In this section, it is no longer question of Galileo E1 with or without E20 satellites. Indeed, as mentioned before, the satellite E20 does not broadcast ephemerides and it is mandatory to have satellite coordinates in the short baseline configuration.

Four short and medium baselines were analyzed in this dissertation.

- Two short baselines: in the Sart-Tilman site, between ULG0 and ULG1 positions with both Trimble and Septentrio receivers (5.177 meters according to fixed coordinates)
- A first medium baseline : between Sart-Tilman and Waremme (25 681.953 meters according to fixed coordinates)
- A second medium baseline : between Sart-Tilman and Brussels (88 676.492 meters according to fixed coordinates).

The two short baselines benefit from the arrival of new Galileo satellites : E26 and E22. Even if still under commissioning at time of writing, they both started to emit valid signals that were used in this computation.

In this configuration, other errors will affect the signals. Namely, the atmospheric errors, the multipath and the additional observation noise. It will be interesting to compare their effect on short and medium baselines. The zero baseline, which is not affected by these errors, will also be used in the comparison.Indeed, the zero baseline configuration can be seen as a calibration of the relative positioning. The results obtained in this configuration allow realizing the observation noise

part due to the receiver. But in practice, code positioning with the Galileo E5 signal at a decimeter precision level should be achieved with one unique receiver and a reference station sending its own code pseudoranges. This reference station will be located at a certain distance from the receiver. Therefore, study of short and medium baselines will be critical for the validation of the hypothesis of this dissertation.

The variables used to study the short baselines remain the same as in the zero baseline case except for the P_{12}^{ij}. This term will no more be equal to the independent term as the distances between receivers and satellites are not equivalent with the short baseline analysis.

Over the short baseline, the atmospheric errors will be completely cancel, and results are expected to be better than on medium baselines.

In the hereunder results, the GPS L5 signal is also considered reduced to four satellites in order to compare it with the Galileo signals. Indeed, with the arrival of new satellites in its constellation, its PDOP values have decreased from 3 in zero baseline to 1.7. With PDOP values close to 3, this signal was comparable to the Galileo signals but no more with PDOP 1.7. Therefore, when reducing to four its constellation, in a similar way than with the GPS L1 and L2 signals, the PDOP values obtained reach 3, as for the 2 other GPS signals (see Appendix). These PDOP values are closer to the Galileo signals values (closer to 4 in this configuration (except for Galileo E5)).

Similarly to the zero baseline case, the Galileo results were considered only when all the Galileo signals were tracked simultaneously.

In the medium baselines, the observation precision is not computed anymore. Indeed, as atmospheric errors and multipath are added on the equation of the signal in addition to the observation noise, compute an observation precision on this basis has non sense. With the short baselines, as only a few multipath is added to the observation noise, the observation is still computed. One must consider that on these short distances, the multipath can be neglected.

Short baseline with Trimble receivers

Figures of results show the same general shape as the figures presented in the zero baseline configuration. For this reason, they will not be discussed. The Table 6.8 summarizes statistics estimated over the 180 to 193 DOYs of the year 2015. Among them, only ten days presented results with Galileo E5. The satellite E26 started to appear in many DOYs of observation but not always as a fifth satellite.

The ten days on which statistics are based present high and low PDOP, high and low elevation satellites. Like in the zero baseline case, no distinction have been made between them. The only restriction was the PDOP maximum value set to 0.

Contrary to the zero baseline case, no sort have been done on results to eliminate the results obtained at lower elevations by comparing them to the Septentrio results. The reason is that only 5 days of results are available with Septentrio (where the Galileo signals are observed) and on among them only show 12 epochs of observation. Therefore, not to reduce the results too much and also in order to benefit from the new satellites launched, the results were not sorted.

The statistics of these 10 days observation are given in Table 6.8 .

	GPS			
$\sigma_{obs}(m)$	GPS L1	GPS L2	GPS L5	
Mean	0.338	0.244	0.299	
Min	0.332	0.240	0.284	
Max	0.347	0.254	0.335	
Standard deviation	0.004	0.005	0.019	
$\sigma_{pos}(m)$				
Mean	1.062	0.759	1.792	
Min	1.027	0.730	1.553	
Max	1.086	0.791	2.503	
Standard deviation	0.018	0.022	0.284	
$\sigma_{pos}(m)$ limited to 4 satellites				
Mean	6.841	3.665	3.395	
Min	6.330	3.382	2.983	
Max	7.508	4.317	4.370	
Standard deviation	0.392	0.300	0.451	
	Galileo			
σ_{obs} (m)	E1	E5a	E5b	E5
Mean	0.233	0.209	0.226	0.122
Min	0.191	0.178	0.188	0.107
Max	0.272	0.257	0.299	0.139
Standard deviation	0.027	0.025	0.034	0.011
$\sigma_{pos}(m)$				
Mean	3.116	2.522	2.825	1.571
Min	1.149	1.203	1.387	0.945
Max	5.511	4.059	4.637	2.619
Standard deviation	1.416	0.932	1.015	0.520

Table 6.8: Precision of observations and positions in meters obtained with code double differences on the DOYs 180-193 period observed by the Trimble receivers located in the Sart-Tilman in short baseline mode

From the Table 6.8, many observations can be done.

- In a general way, all present results are more higher on this table than on the zero baseline table of the Trimble receivers. The observation precision of 8 centimeters on Galileo E5 reaches now 12 centimeters. Still, Galileo E5 remains the best signal in terms of observation precision. But, the observation precisions being higher for each signal, the position precisions, that rely on it, will also show more higher results.

- In the zero baseline case, the Galileo E5 is also the best signal in terms of **position precision**. This is still the case in this configuration. By contrast, Galileo E1, which showed the best results in zero baseline position precision when satellite E20 was included, is now the worse Galileo signal. Nonetheless, the standard deviation of the Galileo E1 signal reveals that this signal had known greater variability than the other which might have altered its average value. If one looks at the minimum values, Galileo E1 is the second best Galileo signal in terms of position precisions.

- Among the GPS signal, GPS L2 is by far the best signal. Once more, one should notice how steady over the time are the results of GPS L1 and GPS L2 frequencies in comparison with all other signals. The GPS L1, which was the best signal in terms of both **position and observation precision** is now the last in terms of observation precision. However, its low

PDOP (under 1, see Appendix) still allows it to be better than GPS L5 as far as **position precision** is concerned.

- When both GNSS are compared, the best **observation precisions** are obtained by Galileo, like in the zero baseline analysis. They evolved from zero baseline 10 centimeters precision to more that 20 centimeters in this configuration. Similarly, the GPS precisions ranged from 15 centimeters to 25-35 centimeters on average in short baseline. This increase is due to the influence of multipath and the entire observation noise on the signals, which were not present in zero baseline (only the part of observation noise depending on the receiver was present).

- When looking at the **position precisions** of both GPS and Galileo systems, no comparison can be made, the results being better on all the GPS signals thanks to their lower PDOP values (around 1 for GPS L1 and L2, 1.7 for GPS L5 and almost 4 for Galileo signals except for Galileo E5 with 1.5). Therefore, GPS L1 and L2 values are better than Galileo ones, as in the zero baseline case. But Galileo E5 seems to be able to compete with GPS L5. The reason is that both signals share similar PDOP values (approximately 1.5). As the GPS L5 observation is worse than the Galileo E5 one, the Galileo E5 positioning results are better. Nonetheless, when minimum values are considered, the Galileo signals position precision values are more similar to the GPS ones. And then, when conditions of observation are favorable, the Galileo signals could be able to compete with the GPS signals.

- When the constellation of GPS is reduced to 4 satellites, and their PDOP values raise to 3, the position precision becomes quite similar to Galileo signals' ones as concerns GPS L2 and GPS L5. As far as GPS L1 signal is considered, very high values are observed. Those are due to an increase of the observation precision on this signal (from 0.33 meters to 0.55 meters) higher than the one observed on GPS L2 and L5 signals (from 0.24 to 0.38 meters for GPS L2 and from 0.29 to 0.33 meters with GPS L5).

To conclude with this Trimble study, both in zero baseline and short baseline, one can observe that Galileo always shows better observation precision, particularly on Galileo E5. As concerns the position precision, the GPS results are still better than the Galileo results notably due to the high PDOP observed on the Galileo observation. When GPS constellation is reduced to four satellites and the PDOP values are quite similar to Galileo values, the results on position estimation are clearly better with Galileo signals as their observation precision is better.

The decimeter position precision, not reached in zero baseline with the Galileo signals could therefore not have been expected on the short baseline.

Short baseline with Septentrio receivers

The short baseline between the Septentrio receivers only provided 5 days of observations with Galileo E5 observations. Each of these days have been used to compute statistics. Observations with the new E26 satellite of Galileo were included in these results but as in the Trimble case, it did not necessarily allow to reach a 5 satellite visibility.

The results of this short baseline are summarized in the Table 6.9. The observation precisions, better than the Trimble ones in zero baseline, are expected to lead to better results in short baseline than with the Trimble receivers.

Observations from the Table 6.9 are summarized hereunder.

	GPS			
$\sigma_{obs}(m)$	GPS L1	GPS L2	GPS L5	
Mean	0.154	0.124	0.119	
Min	0.149	0.121	0.106	
Max	0.159	0.129	0.138	
Standard deviation	0.004	0.003	0.015	
$\sigma_{pos}(m)$				
Mean	0.462	0.355	0.569	
Min	0.456	0.342	0.510	
Max	0.469	0.364	0.725	
Standard deviation	0.005	0.008	0.089	
$\sigma_{pos}(m)$ limited to 4 satellites				
Mean	3.104	1.912	1.394	
Min	2.823	1.732	1.011	
Max	3.581	2.162	1.990	
Standard deviation	0.300	0.185	0.367	
	Galileo			
σ_{obs} (m)	E1	E5a	E5b	E5
Mean	0.098	0.073	0.080	0.036
Min	0.042	0.043	0.044	0.023
Max	0.123	0.093	0.100	0.045
Standard deviation	0.033	0.020	0.021	0.009
$\sigma_{pos}(m)$				
Mean	1.794	1.085	1.374	0.604
Min	0.860	0.601	0.642	0.258
Max	3.383	1.536	2.278	1.253
Standard deviation	1.033	0.342	0.666	0.396

Table 6.9: Precision of observations and positions in meters obtained with code double differences on the DOYs 180-193 period observed by the Septentrio receivers located in the Sart-Tilman in short baseline mode

- The **observation precisions** are much better than in the Trimble short baseline.
- Galileo E5 is once more the most precise signal as **signal quality** is concerned. Whereas GPS signals observation precisions are all higher than 10 centimeters, the precisions on the Galileo signals are under this value and reach 4 centimeters with E5. Similarly to the zero baseline, the bests results are given by Galileo E5 and then E5a and E5b and finally E1. Moreover, Galileo E5 shows low standard deviation values on both zero and short baseline, which signifies it is not varying a lot over time, just as GPS L1 and L2 signals.
- If one considers the minimum values of position precision, the Galileo signals are able to reach decimeter precision when placed in optimal observation conditions. With Galileo E5, these minimum values are even better than minimum values observed with the GPS signals. The mean values seem to be affected by high values obtained on days of high PDOP (one day of observation reached mean PDOP values of 9 on the three Galileo E1, E5a and E5b signals). This is confirmed by the high values of standard deviation observed on these signals.
- Concerning GPS signals, the classification of best signal in terms of **observation precision** is also conserved from the zero baseline case: GPS L5, then GPS L2 and finally GPS L1. The values have raised since the zero baseline but are lower than in the Trimble short baseline case. As a matter of a fact, the values of observation precision obtained with the Septentrio receivers in short baseline are similar to those obtained with the Trimble receivers in zero

baseline.

- Similarly to zero baseline case, the highest values of PDOP observed on GPS L5 lead to highest values of **position precision**. Still, its results are better than in the Trimble short baseline thanks to its better observation precision on the Septentrio receivers.
- When one considers the reduced constellation of GPS, even if the PDOP average values are close to 3, the average PDOP values of Galileo are not reached (PDOP value of 5 on Galileo E1, E5a and E5) and still the position precision values are very high when compared with the one observed on Galileo signals due to the poorer quality of the GPS signals.

Trimble and Septentrio short baselines comparison

The Trimble short baseline results are very poor in comparison with the Septentrio ones. One reason for such results is that Septentrio treats less data than Trimble and then has less PDOP peaks or satellite elevation issue than the Trimble results. The second reason is the reduced number of days used to estimate statistics with Septentrio. But, on the shortest observation period of Septentrio, PDOP values (see Appendix A) are higher than with the Trimble observation period (average value of 3 on Trimble and 5 on Septentrio). It should also be noted that the arrival of the new Galileo satellites in the results offered new epochs observation in comparison with those observed in zero baseline.

Therefore, both receiver types seem to know alterations, coming from the PDOP or the low elevation satellites. And as differences between the signals were already observed in zero baseline, where PDOP values were equivalent and satellites observed at low elevation by the Trimble receiver had been removed to obtain similar observation periods on both Septentrio and Trimble receiver, it seems that the main factor of the differences observed between Trimble and Septentrio is the receiver itself and its ability to track the signals.

The decimeter precision can not be reached with the Galileo E5 signal on the estimated position in zero and short baseline computed with the Trimble receivers with the present Galileo constellation. By contrast, such a precision on position can be reached with the Septentrio receivers in both zero and short baseline with the signal Galileo E5. It will therefore be interesting to raise the baseline length in order to know until which distance this precision can still be obtained. This will allow knowing the maximum distance between a single receiver position and a reference station sending it the code pseudoranges it needs to compute the double difference solution.

Medium baseline with Waremme

The Waremme-Sart-Tilman baseline offers rare observations on Galileo signals. Even if both receivers are Septentrio X4, and if the period of observation counts 20 days, the antenna placed in Waremme, is an old model and the observation signal to noise ratio usually low. And then, Galileo E5 signal was observed on only 3 days, on a hundreds of epochs. Therefore, results might be biased and must be handled carefully.

The Table 6.10 summarizes the statistics on these 3 days of observation.

	GPS			
$\sigma_{pos}(m)$	GPS L1	GPS L2	GPS L5	
Mean	0.877	0.807	1.645	
Min	0.866	0.787	1.410	
Max	0.884	0.834	1.937	
Standard deviation	0.010	0.024	0.268	
$\sigma_{pos}(m)$ limited to 4 satellites				
Mean	6.747	5.932	2.573	
Min	6.379	5.235	2.371	
Max	7.049	6.594	2.720	
Standard deviation	0.340	0.680	0.181	
	Galileo			
$\sigma_{pos}(m)$	E1	E5a	E5b	E5
Mean	0.817	1.405	0.793	0.349
Min	0.619	0.973	0.685	0.273
Max	1.120	1.662	0.877	0.407
Standard deviation	0.267	0.377	0.098	0.069

Table 6.10: Precision of observations and positions in meters obtained with code double differences on the DOYs 80-100 period observed by the Septentrio receivers of Waremme and Sart-Tilman in short baseline mode

- The position precision obtained on Galileo is better than in the short baseline case because lower PDOP values were observed during this 3 days of observation (PDOP values of 3 instead of 5 in short baseline). This PDOP values are more similar to the zero baseline and therefore, the position precision values are closer to position precision obtained with the zero baseline configuration.
- The Galileo E5 signal still shows the best position precision among every considered signals. The Galileo E5a signal seems to be more altered by the atmospheric and multipath errors than others, showing a higher value on both position precisions for equal values of PDOP.
- As concerns GPS, GPS L5 shows high PDOP values making it reach 1.5 meters on the position precision. Concerning GPS L1 and L2, their position precisions increase to become twice superior than in short baseline with similar PDOP values observed.
- It appears from this Table that the comparison with the GPS reduced satellite constellation is not needed anymore as comparable values of GPS and Galileo signals on the position precisions are obtained with their respective constellations, even if PDOP values are different. This clearly shows the superiority of the Galileo signals over the GPS ones.
- In addition to atmospheric errors and multipath, the obsolescence of the antenna in Waremme also degrades the signal quality.

The 25 kilometers between the two receivers still allow decimeter level precision on position estimation with Galileo. Therefore, a larger baseline is interesting to consider. This will be done in the next subsection with the Brussels baseline.

Medium baseline with Brussels

The medium baseline between Brussels and Sart-Tilman has been done between the Septentrio X4 on the ULG1 station and Brussels' Septentrio receiver. The statistics calculated are presented in the Table 6.11. Among the 20 days of data, 7 days have been selected to estimate statistics because of the presence of Galileo E5 signal.

	GPS			
$\sigma_{pos}(m)$	GPS L1	GPS L2	GPS L5	
Mean	1.089	0.749	3.821	
Min	1.027	0.705	3.535	
Max	1.146	0.805	3.997	
Standard deviation	0.048	0.036	0.169	
	Galileo			
$\sigma_{pos}(m)$	E1	E5a	E5b	E5
Mean	1.934	1.602	1.687	1.151
Min	1.308	0.824	0.922	0.361
Max	2.870	2.226	2.448	2.065
Standard deviation	0.558	0.599	0.569	0.701

Table 6.11: Precision of observations and positions in meters obtained with code double differences on the DOYs 80-100 period observed by the Septentrio receivers of Brussels and Sart-Tilman in short baseline mode

Observations from Table 6.11 are given hereunder.

- The distance between receivers being longer, results are more affected by atmospheric biases.
- The Galileo signals show minimum values in position precision that could compete with the GPS ones and even outperform them. The Galileo E5 signal clearly shows superiority over all other signal when minimum values are considered and over Galileo signals when mean values are considered.
- The precision on the estimated position is better to the one observed on the Waremme baseline for GPS L2 signal but poorer on the two other GPS signals and the Galileo signals. The GPS L5 is altered on this baseline by high PDOP peaks. This is the reason for its high results in positioning precision. As concerns the Galileo signals, PDOP values are higher than with Waremme baseline (PDOP values of 5 instead of 3 in the Waremme baseline for Galileo E1, E5a and E5b and 2 instead of 1 for Galileo E5) and therefore, it is not surprising to obtain poorer positioning results.

To conclude with this baseline, when PDOP values are reduced (this happens on 3 days of observation), the Galileo signals E5a, E5b and E5 reach decimeter level precision. The Galileo E5 signal even reaches 36 centimeters of precision. Among the GPS signals, only the GPS L2 is able to reach the decimeter precision.

6.2 Conclusion

The conclusion of this chapter will allow the confirmation of this dissertation hypothesis .

We have seen that two parameters were mainly used to characterize a signal and a position estimation: the observation and position precisions.

- The observation precision is affected, in the zero baseline case, by the part of the observation noise due to the receiver. In short baseline configuration, the multipath and the other part of the observation noise are added but the multipath is assumed to be very low hence the observation precision can still be evaluated.
- The position precision is computed for each configuration. Its depends notably on the PDOP values, which show very important influence as one could observe it. But this precision is

also affected by low number of satellites observed as the mean squares adjustment is more precise when more observations are available Finally, a third parameter affects this position estimation: the low elevation satellites which send damaged signals.

Among the two receiver types used to compute the double differences, the Trimble receivers clearly showed the worse results. This can mainly be attributed to their higher observation noise.

When considering the results obtained, the Trimble receivers should be avoided if decimeter precision is reached. By contrast, the Septentrio receivers allow reaching decimeter precision with Galileo E5 on zero, short baseline and medium Waremme baseline. Decimeter precision can also be reached on medium Brussels baseline if PDOP values are not to high.

This validates the hypothesis we have made in this dissertation that decimeter precision on position could be reached by Galileo E5a+b signal using only code pseudoranges in single-frequency positioning.

Chapter 7

Conclusion

Satellite-based positioning is becoming more and more precise as new satellites and new signals are designed.

Positioning with carrier phases is by far the most precise method. However, this kind of observable requires more sophisticated material and algorithms to resolve the initial ambiguity.

Therefore, code pseudorange precise positioning appears as a challenge for signal engineers. Indeed, the code pseudorange is the observable used in the commercial devices and applications (the mobile car GPS, the applications of localization on smartphones and tablets, future autonomous cars guided by satellites, to name but a few). The interest of achieving real-time precise positioning with this observable is thus essential for these device manufacturers.

However, the signal broadcast by a satellite is altered during its journey to the receiver. The atmosphere delays the signal and weakens it while many reflecting surfaces deviate it. Furthermore, the propagation inside satellite and receiver cables retards the signal arrival to the receiver. Moreover, the clocks of the satellites and the receiver are not synchronized which induces measurement errors and a noise called observation noise modifies the signal's shape. Other parameters influence and delay this signal in such a way that signal quality is reduced when it is finally tracked by the receiver.

In addition to this, satellite-based positioning implies being able to see at least four satellites. The geometry of the observed satellites has an influence on the precision obtained on the position estimated. It is characterized by a parameter called the PDOP. Nonetheless, the observation of a great number of satellites allows a reduction of the impact of the geometry. The issue of the geometry will therefore impact more the reduced constellation satellite systems such as Galileo.

The European satellite system Galileo is at the forefront of the technology with its new satellites and signals. Among the signals generated by this system, one stands out from the rest. The Galileo E5a+b signal, also called Galileo AltBOC or Galileo E5, offers great positioning possibilities. Indeed, it has been proven that this signal shows a particularly good resistance to multipath and is less sensitive to observation noise than the others. The improvement of positioning precision using this signal is the hypothesis tested in this dissertation has been written.

7.1 Methods

Two constraints have been considered:

First, only the code pseudoranges have been used. This way, the solution proposed could be used by the simplest receiver. But using only codes constrains the precision that could be obtained with this signal. Indeed, the precision on the code positioning is generally close to the decameter

or the meter in best case scenarios. Therefore, improving the precision with the code pseudoranges will lead to an expect precision of decimeters on a position estimation.

Second, the challenge of achieving decimeter positioning is also constrained by a solution using only single-frequency. When decimeter positioning is considered with code pseudoranges, many authors use dual-frequency receivers in order to realize dual-frequency combinations, more precise than single-frequency ones. But dual-frequency receivers are more expensive than simple-frequency ones. Moreover, the single-frequency receivers are also those that are the most used in public devices and applications.

In order to respect these constraints and achieve decimeter precision on position estimation, a method of relative positioning has been implemented: the double difference. The simultaneous observations of two satellites by two receivers allow a reduction or even elimination of many of the aforementioned errors by differencing the measurements.

Different configurations are envisaged with this combination. First, a *zero baseline* configuration, consisting in two receivers connected to the same antenna thanks to a splitter, has been tested. Not used in practice for usual positioning, this configuration has been implemented with the aim of estimating the observation noise due to the receivers. Indeed, atmospheric delays, multipath and a part of the observation noise are eliminated in this configuration.

In practice, when double difference is used in positioning, one user receives code pseudoranges from a reference station located at a certain distance but observing the same satellites simultaneously. Therefore, *short and medium baseline* have been tested. In these cases, the receivers are a few to a hundred kilometers distant from each other. Therefore, atmospheric errors as well as multipath, the clock errors of both receiver and satellites and full observation noise affect the signal. The idea was to define the distance until which the double difference measurements could lead to the decimeter precision. For this purpose, the code pseudoranges from Brussels and Waremme stations have been used in medium baselines and stations of the Sart-Tilman, a few meters apart, have been used to realize the short baselines.

Two different receiver types were tested on those zero and short baselines. Two receivers were manufactured by Trimble and two by Septentrio. [Caelen, 2014] had already proved that low observation noise was present on the Septentrio receivers, leading thus to more precise measurements than the Trimble receivers. It is therefore expected that decimeter precision on position will be reached more easily with the Septentrio receivers as the observed signal is more precise.

7.2 Results

The results obtained in *zero baseline* showed important differences between different receivers.

With the Trimble receivers, the **observation precision** on GPS L1, L2 and L5 signals reach approximatively 15 centimeters. On the Galileo E1, E5a, E5b and E5, the precision obtained never surpasses the 10 centimeters. The Galileo E5 signal shows 8 centimeters of precision.

As concerns the **position precision**, the Trimble receivers lead to 40 centimeters precision on the GPS L1 and L2 signals and 1.5 meters on GPS L5, due to the high values of PDOP presented by this signal. By contrast, values obtained with the Galileo signals are closer to 1.5 meters precision reached by GPS L5 as they also show high PDOP values.

On the Septentrio *zero baseline*, the GPS **observation precision** ranges from 4 centimeters

on GPS L5 to 8 centimeters on GPS L1. This difference between GPS L5 results on the Trimble and Septentrio baselines is due to the fact that the observation periods were not similar. During the Septentrio observation period, new GPS satellites started to broadcast the GPS L5 signal, reducing thereby the PDOP values. Concerning Galileo observation precision, Septentrio allows the attainment of 1 centimeter precision on Galileo E5 to 5 centimeters on Galileo E1.

The **position precision** is by far the best on the Septentrio receivers. Galileo E5 signal allows 20 centimeters precision on positioning while Galileo E1 reaches 80 centimeters. As concerns GPS signals, 20 centimeters precision is reached on each observed signal.

Therefore, it clearly appears that Septentrio results are more precise than Trimble ones and that the decimeter precision expected in this dissertation will be available on these Septentrio receivers. Furthermore, the observation precision reached by Galileo E5, always better than the other signals, proves that this signal shows a better quality that is unequaled by other signals studied.

The *short baselines* in Sart-Tilman (5.177 meters) executed with these two receiver types prove that highest observation and position precisions can be obtained on the Septentrio receivers. Particularly, 60 centimeters precision on positioning was reached by the Galileo E5 signal whereas higher PDOP values than in zero baseline case were observed.

The *medium baselines* were only considered with the more precise Septentrio receivers. Positioning of 40 centimeters was reached on the Waremme baseline (25 681.953 kilometers) with Galileo E5 as lower PDOP values were observed than in the short baseline case. On the Brussels baseline of a length of 88 676.492 kilometers, results were more affected by PDOP and the average value of position precision with Galileo E5 decreased to 1.15 meters. Nonetheless, it appears that when PDOP is lower, decimeter precision can be reached with this signal.

Finally, a comparison of the results obtained with the four simultaneously visible satellites of the Galileo constellation and a reduced GPS constellation showing similar PDOP values than Galileo leads to the conclusion that Galileo E5 signal clearly outperforms all other signals in terms of position precision. This validates the hypothesis that Galileo E5 could provide a better precision than other Galileo and GPS signals.

To conclude, decimeter precision on positioning can be reached in single-frequency positioning with Galileo E5 code pseudoranges. Using relative positioning as we did, the decimeter precision can be reached up to 25 kilometers distance between receivers. This precision could also be reached with longer baselines (even 90 kilometers) on the days presenting PDOP values that are not too high. Therefore, a full constellation of Galileo satellites is expected to outperform precision on positioning even on long baselines.

When these results are compared to those obtained by the authors mentioned in chapter 2, notably the observation precision obtained by [Springer et al., 2013], we have found better precision, both on GPS and Galileo observations. In zero baseline, this is due to the smallest part of the observation noise considered in the computation of the observation precision. But this is also due to the new Galileo satellites addition. The Trimble values are closer to these results in short baseline for GPS signals where the multipath is accounted for in the observation precision computation as well as the observation noise. Nonetheless, the classification of the signals from [Springer et al., 2013] is also observed in this dissertation. This classification is in accordance with the classification of Galileo signals realized by [Simsky et al., 2008a] on the basis of multipath results.

7.3 Prospects

The results of this discussion remain to be tested further as decimeter level on the 90 kilometers' baseline can only be reached by the Galileo E5 signal on days when the observed PDOP values are low. These high PDOP values are induced by the reduced Galileo constellation. Therefore, as more operational Galileo satellites are launched, the better the results in terms of position precision. It will therefore be interesting to repeat the same study when more Galileo satellites are available.

We faced issues with the Septentrio receivers concerning the simultaneity of the observations. We noticed that two Septentrio receivers did not observe the constellations of GNSS at exactly the same time. Two effects were induced by this offset. The orbital coordinates of the satellites were different from one receiver to the other, leading to a D_{12}^{ij} term slightly different from 0. This issue has thus an influence on the results we observed on position precision, reducing the independent term and therefore leading to better precision values. Secondly, the offset on the receiver clock could, instead of being eliminated by the double difference, may lead to a new source of error. The observation precision could therefore be altered. This problem should be resolved in order to validate the results of this dissertation.

Among the observation periods considered, some configurations have faced a lack of observation days presenting results of Galileo E5. This lack was due to a particularity of the Septentrio XS receiver used in the zero and short baseline cases. It was also due to the antenna on the Waremme medium baseline and to the fact that the Septentrio receivers did not track satellites since their raise, contrary to the Trimble receivers. For this reason, the Trimble observation epochs were reduced in order to match those of Septentrio on the same observation days. Therefore, analyzing more observation days on each period would lead to more stable statistics.

Only code pseudoranges have been tested in this dissertation. The precision obtained with Galileo E5 on the carrier phases would also be interesting to analyze. Would a similar superiority of this signal over other signals be observed?

Finally, many authors seems to have encountered better precision values when both GPS and Galileo systems were combined. This could also be the subject of further analysis.

Bibliography

[Avila-Rodriguez et al., 2007] Avila-Rodriguez, J.-A. et al., 2007, The MBOC modulation : A final touch for the Galileo frequency and signal plan. *Inside GNSS*, 2(6), pp. 43–58.

[Caelen, 2014] Caelen, F., 2014, *Contrôle de la qualité des nouveaux codes GPS et Galileo*. Master's thesis, Université de Liège.

[Colomina et al., 2012] Colomina, I. et al., 2012, Galileo's surveying potential: E5 pseudorange precision. *GPS World*, 23(3), pp. 18–33.

[de Bakker et al., 2009] de Bakker, P. F. et al., 2009, Geometry-free undifferenced, single and double differenced analysis of single frequency GPS, EGNOS and GIOVE-A/B measurements. *GPS Solutions*, 13(4), pp. 305–314, doi:10.1007/s10291-009-0123-6.

[de Bakker et al., 2012] de Bakker, P. F. et al., 2012, Short and zero baseline analysis of GPS L1 C/A, L5Q, GIOVE E1B, and E5aQ signals. *GPS Solutions*, 16(1), pp. 53–64, doi:10.1007/s10291-011-0202-3.

[Diessongo et al., 2012] Diessongo, H. T. et al., 2012, Exploiting the Galileo E5 Wideband Signal for Improved Single-Frequency Precise Positioning. *Inside GNSS*, 7(5), pp. 64–73.

[Diessongo et al., 2014] Diessongo, T. H. et al., 2014, Precise position determination using a Galileo E5 single-frequency receiver. *GPS Solutions*, 18(1), pp. 73–83, doi:10.1007/s10291-013-0311-2.

[ESA, 2014] ESA, 2014, Galileo achieves in-orbit validation. *ESA Communication Production*, URL http://www.esa.int/Our_Activities/Navigation, consulted on August 2st, 2015.

[EuropeanUnion, 2010] EuropeanUnion, 2010, European GNSS (Galileo) open service : Signal in space interface control document.

[Gao et al., 2006] Gao, Y. et al., 2006, Precise Point Positioning and its challenges, aided-GNSS and signal tracking. *Inside GNSS*, 1(6), pp. 16–21.

[Gioia et al., 2015] Gioia, C. et al., 2015, A Galileo IOV assessment: measurement and position domain. *GPS Solutions*, 19(2), pp. 187–199, doi:10.1007/s10291-014-0379-3.

[GPS-SSI, 2015] GPS-SSI, 2015, The Global Positioning System. URL http://www.gps.gov/systems/gps/, consulted on May 24st, 2015.

[GPS-World-Staff, 2015] GPS-World-Staff, 2015, The Almanac: orbit data and resources on active GNSS satellites. *GPS World*, 25(8), pp. 46–49, URL http://gpsworld.com/the-almanac/, consulted on August 15st, 2015.

[Hofmann-Wellenhof et al., 2008] Hofmann-Wellenhof, B. et al., *GNSS - Global Navigation Satellite Systems - GPS, GLONASS, Galileo, and more*. SpringerWienNewYork, 2008.

[ICGNSS & UNOOSA, 2010] ICGNSS & UNOOSA, U. N. O. F. O. S. A., 2010, Current and planned global and regional navigation satellite systems and satellite-based augmentation systems.

[IGS et al., 2013] IGS, I. G. S. et al., 2013, RINEX - the receiver independent exchange former - version 3.02.

[Joseph, 2010] Joseph, A., 2010, Measuring GNSS signal strength. *Inside GNSS*, 5(8), pp. 20–25.

[Julien et al., 2015] Julien, O. et al., 2015, Estimating ionospheric delay using GPS/Galileo signals in the E5 Band. *Inside GNSS*, 10(2), pp. 55–64.

[Junker et al., 2011] Junker, S. et al., Precise single-frequency positioning using the full potential of the Galileo E5 signal. In *Proceedings of the 3rd International Colloquium - Scientific and Fundamental Aspects of the Galileo Programme*, Danish Design Center in Copenhagen, Denmark, 2011, p. 6.

[Langley, 1997] Langley, R. B., 1997, GPS Receiver system noise. *GPS World*, pp. 40–45.

[Langley et al., 2012] Langley, R. B. et al., 2012, First results: precise positioning with Galileo prototype satellites. *GPS World*, 23(9), pp. 45–49.

[Lopes et al., 2012] Lopes, H. D. et al., On the evaluation of Galileo E5 AltBOC signals for GNSS-INS integration. In *Proceedings of the 25th International Technical Meeting of The Satellite Division of the Institute of Navigation (ION GNSS 2012)*, Nashville, Tennessee, USA, 2012, vol. 59, pp. 1641–1650.

[Rebeyrol et al., 2007] Rebeyrol, E. et al., 2007, Galileo civil signal modulations. *GPS Solutions*, 11(3), pp. 159–171, doi:10.1007/s10291-006-0047-3.

[Shivaramaiah & Dempster, 2009] Shivaramaiah, N. C. & Dempster, A. G., The Galileo E5 AltBOC: understanding the signal structure. In *Proceedings of the International Global Navigation Satellite Systems Society Symposium on GPS/GNSS*, Holiday Inn Surfers Paradise, Gold Coast, Australia: Menay P/L, 2009, p. 13.

[Silva et al., 2010] Silva, P. F. et al., ENCORE: Enhanced code Galileo receiver for land management applications in Brazil. In *5th ESA Workshop on Satellite Navigation Technologies and European Workshop on GNSS Signals and Signal Processing*, ESTEC, Noordwijk, The Netherlands: IEEE, 2010, pp. 1–8, doi:10.1109/NAVITEC.2010.5708053.

[Silva et al., 2012] Silva, P. F. et al., Results of Galileo AltBOC for precise positioning. In *6th ESA Workshop on Satellite Navigation Technologies and European Workshop on GNSS Signals and Signal Processing*, ESTEC, Noordwijk, The Netherlands: IEEE, 2012, p. 9, doi: 10.1007/s10291-013-0311-2.

[Simsky et al., 2008a] Simsky, A. et al., 2008a, Multipath and Tracking Performance of Galileo Ranging Signals Transmitted by GIOVE-A. *International Journal of Navigation and Observation*, 2008, p. 13.

[Soloviev & Gibbons, 2012] Soloviev, A. & Gibbons, G., 2012, Challenges in GNSS /INS Integration. *Inside GNSS*, 7(1), pp. 30–31.

[Springer et al., 2013] Springer, T. et al., GNSS analysis in a multi-GNSS and multi-signal environnement. In *AGU*, San Francisco: ESA, 2013, p. 25.

[Steigneberger & Hauschild, 2015] Steigneberger, P. & Hauschild, A., 2015, First Galileo FOC satellite on the air. *GPS World*, 26(1), pp. 8–12.

[Steigneberger et al., 2013] Steigneberger, P. et al., 2013, First demonstration of Galileo-only positioning. *GPS World*, 24(2), pp. 14–15.

[Subarina et al., 2013] Subarina, J. S. et al., *GNSS data processing*, vol. 1. Noordwijk: European Space Agency, 2013.

[Tawk et al., 2012] Tawk, Y. et al., 2012, Analysis of Galileo E5 and E5ab code tracking. *GPS Solutions*, 16(2), pp. 243–258, doi:10.1007/s10291-011-0226-8.

[Tiberius et al., 2002] Tiberius, C. et al., 2002, 0.99999999 confidence ambiguity resolution with GPS and Galileo. *GPS Solutions*, 6(1-2), pp. 96–99, doi:10.1007/s10291-002-0022-6.

[Tiberius et al., 2009] Tiberius, C. C. J. M. et al., Geometry-free Analysis of GIOVE-A/B E1 - E5a, and GPS L1 - L5 Measurements. In *Proceedings of ION GNSS*, Savannah International Convention Center, 2009, vol. 56, pp. 2911–2925.

[Warnant, 2013] Warnant, R., 2013, GNSS : théorie et applications, course notes.

Appendix

A Zero baseline

A.1 Trimble receivers

	GPS				
PDOP values	GPS L1	GPS L2	GPS L5		
Mean	0.749	1.102	3.094		
Min	0.736	1.001	2.760		
Max	0.770	1.070	3.432		
PDOP values (limited to 4 sat.)	GPS L1	GPS L2	GPS L5		
Mean	2.838	3.466	4.140		
Min	2.296	3.256	3.587		
Max	3.011	3.586	4.609		
	Galileo				
PDOP values	E1	E5a	E5b	E5	E1(incl. E20)
Mean	5.858	5.616	5.719	2.458	2.775
Min	3.256	3.075	3.165	1.176	1.809
Max	7.576	7.155	7.366	4.140	6.379

A.2 Septentrio receivers

	GPS				
PDOP values	GPS L1	GPS L2	GPS L5		
Mean	0.765	0.979	2.261		
Min	0.743	0.951	1.752		
Max	0.777	0.995	2.569		
PDOP values (limited to 4 sat.)	GPS L1	GPS L2	GPS L5		
Mean	2.968	3.399	3.356		
Min	2.700	3.020	2.271		
Max	3.134	3.623	4.267		
	Galileo				
PDOP values	E1	E5a	E5b	E5	E1(incl. E20)
Mean	5.846	5.553	5.730	2.696	4.258
Min	4.640	4.379	4.511	1.674	3.161
Max	7.786	7.595	7.688	6.422	5.551

B Short baselines

B.1 Trimble receivers

	GPS			
PDOP values	GPS L1	GPS L2	GPS L5	
Mean	0.735	0.991	1.745	
Min	0.727	0.976	1.675	
Max	0.759	1.021	2.188	
PDOP values (limited to 4 sat.)	GPS L1	GPS L2	GPS L5	
Mean	3.075	3.473	3.006	
Min	2.749	3.250	2.483	
Max	3.437	3.857	4.000	
	Galileo			
PDOP values	E1	E5a	E5b	E5
Mean	3.941	3.765	3.867	1.483
Min	2.373	2.273	2.327	0.859
Max	5.574	5.263	5.418	2.174

B.2 Septentrio receivers

	GPS			
PDOP values	GPS L1	GPS L2	GPS L5	
Mean	0.755	0.970	1.723	
Min	0.737	0.950	1.679	
Max	0.780	1.000	1.789	
PDOP values (limited to 4 sat.)	GPS L1	GPS L2	GPS L5	
Mean	3.007	3.533	3.048	
Min	2.874	3.335	2.713	
Max	3.177	3.733	3.321	
	Galileo			
PDOP values	E1	E5a	E5b	E5
Mean	5.263	5.012	5.176	1.962
Min	3.380	3.342	3.238	1.338
Max	9.389	8.867	9.149	3.398

C Medium baselines

C.1 Waremme

	GPS			
PDOP values	GPS L1	GPS L2	GPS L5	
Mean	0.768	0.984	2.837	
Min	0.762	0.977	2.721	
Max	0.777	0.995	2.958	
PDOP values (limited to 4 sat.)	GPS L1	GPS L2	GPS L5	
Mean	3.104	3.640	3.268	
Min	2.933	3.444	3.116	
Max	3.376	3.964	3.416	
	Galileo			
PDOP values	E1	E5a	E5b	E5
Mean	3.808	3.777	3.703	1.376
Min	3.089	3.056	3.004	1.116
Max	4.213	4.192	4.096	1.524

C.2 Brussels

	GPS			
PDOP values	GPS L1	GPS L2	GPS L5	
Mean	0.755	0.970	1.723	
Min	0.737	0.950	1.679	
Max	0.780	1.000	1.789	
	Galileo			
PDOP values	E1	E5a	E5b	E5
Mean	5.782	5.461	5.623	2.088
Min	2.594	2.454	2.530	0.937
Max	9.375	8.854	9.114	3.385